

PROGRESS REPORT  
 NASA Grant No. Y-NGR-50-002-051  
 "Skeletal Status and Soft Tissue  
 Composition of Astronauts"  
 June 15, 1971



N71-33223

FACILITY FORM 602	(ACCESSION NUMBER)	-	(THRU)
	177		03
	(PAGES)		(CODE)
	CR 121415		04
	(NASA CR OR TMX OR AD NUMBER)		(CATEGORY)

Reproduced by  
**NATIONAL TECHNICAL  
 INFORMATION SERVICE**  
 U.S. Department of Commerce  
 Springfield, VA 22151

PROGRESS REPORT

AEC Grant No. AT-(11-1)-1422

"Determination of Body Composition In Vivo"

NASA Grant No. Y-NGR-50-002-051

"Skeletal Status and Soft Tissue  
Composition of Astronauts"

June 15, 1971

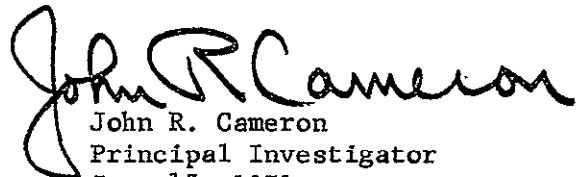
John R. Cameron, Ph.D.  
Principal Investigator  
Department of Radiology  
University of Wisconsin Medical Center  
Madison, Wisconsin 53706

## PREFACE

This Progress Report is a summary of research and instrument development in the area of bone mineral content and body composition measurement in vivo. This report covers work at the University of Wisconsin from June 15, 1970 through June 15, 1971. Research support for the Bone Measurement Laboratory comes from a variety of sources; these are the United States Atomic Energy Commission through Contract AT-(11-1)-1422, the National Aeronautics and Space Administration through Grant Y-NGR-50-002-051 and the University of Wisconsin. This work represents primarily the efforts of the following: Dr. Richard B. Mazess, Dr. John M. Jurist, Dr. Mark Mueller, Dr. James A. Sorenson, Dr. Philip F. Judy, Robert M. Witt, Michael G. Ort, Warren E. Mather, Charles R. Wilson, Clifford Vought, John Sandrik, Kianpour Kianian, Dr. Everett L. Smith, Mrs. Joyce Fischer, Mrs. Sue Kennedy. I wish to express my appreciation for their efforts.

I would also like to thank Miss Laurie Edson, Mrs. Janet Ort, Miss Joyce Reilly, and Mrs. Linda Robbins for their secretarial help in preparing this report.

Certain parts of this report represent work in progress which will be reported in more detail in next year's progress report.

  
John R. Cameron  
Principal Investigator  
June 15, 1971

## ANNUAL PROGRESS REPORT ON AEC CONTRACT AT-(11-1)-1422

TABLE OF CONTENTS

1. C00-1422-87      Determining Body Composition by Radiation Absorption Spectrometry  
.....R.B. Mazess, J.R. Cameron and J.A. Sorenson.
2. C00-1422-88      Skeletal Growth in School Children: Maturation and Bone Mass. Am. J. Phys. Anthropol. (in press).  
.....R.B. Mazess and J.R. Cameron.
3. C00-1422-89      Methods for Quantitating Radioactivity In Vivo by External Counting Measurements. Ph.D. Thesis in Radiological Sciences (abstract only; thesis available upon request).  
.....J.A. Sorenson.
4. C00-1422-90      A Dichromatic Attenuation Technique for the In Vivo Determination of Bone Mineral Content. Ph.D. Thesis in Radiological Sciences (abstract only; thesis available upon request).  
.....P.F. Judy.
5. C00-1422-91      The Relationship of Photon Absorption Measurements of Bone Mineral Content to Bone Strengths. Ph.D. Thesis in Radiological Sciences (abstract only; thesis available upon request).  
.....C.R. Wilson.
6. C00-1422-92      Effects of Physical Activity on Bone Loss. Ph.D. Thesis in Physical Education (abstract only; thesis available upon request).  
.....E.L. Smith.
7. C00-1422-93      Estimation of Bone and Skeletal Weight by Direct Photon Absorptiometry. Invest. Radiol. 6(1): 52-60, 1971 (abstract only; article available upon request).  
.....R.B. Mazess.
8. C00-1422-94      Review of Body Composition in Animals and Man. Human Biology 42: 138-140 (1970).  
.....R.B. Mazess.
9. C00-1422-95      Bone Mineral Determination in Vitro by Radiographic Photodensitometry and Direct Photon Absorptiometry (abstract only; article available upon request).  
.....C. Colbert, R.B. Mazess, and P.B. Schmidt.
10. C00-1422-96      Rectilinear Scanner for Determination of Bone Mineral Content  
.....J.M. Sandrik, R.B. Mazess, C.E. Vought, and J.R. Cameron.

11. COO-1422-97 Developments in the Dichromatic Attenuation Technique for the Determination of Bone Mineral Content In Vivo  
.....P.F. Judy, M.G. Ort, K. Kianian, and R.B. Mazess.
12. COO-1422-98 Preliminary Report on a Dual Photon Bone Mineral Measuring Instrument  
.....J.C. Sitzman, C.E. Vought, and R.B. Mazess.
13. COO-1422-99 Spectral Difference in Commercial  $^{125}\text{I}$  Photon Sources  
.....R.M. Witt, R.B. Mazess, and J.R. Cameron.
14. COO-1422-100 A Direct Digital Readout System for Measurement of Bone Mineral Content Using Photon Absorptiometry  
.....R.B. Mazess, J.R. Cameron, and H. Miller.
15. COO-1422-101 Bone Mineral in Elderly Women Treated with Fluorides: Preliminary Report  
.....R.B. Mazess, J.M. Jurist, and H. Hickey.
16. COO-1422-102 Preliminary Report on a Caliper for Measuring Tissue Composition by Radionuclide Absorption  
.....R.B. Mazess and J.R. Cameron.
17. COO-1422-103 Bone Mineral Content of the Eskimos of Point Hope and Barrow: Preliminary Report  
.....W.E. Mather and R.B. Mazess.
18. COO-1422-104 ~~Three~~ models of Vibrating Long Bones  
.....J.M. Jurist and K. Kianian.
19. COO-1422-105 Experience with a Computer Based Clinical Data Retrieval System  
.....J.M. Jurist and K. Kianian.
20. COO-1422-106 Measurement of Tibial Resonant Frequency: A Preliminary Report  
.....J.W. Raasoch and J.M. Jurist.
21. COO-1422-107 Femoral Trabecular Patterns and Bone Mineral Content  
.....D.H. Kranendonk and J.M. Jurist.
22. COO-1422-108 Skeletal Status in Rheumatoid Arthritis: A Preliminary Report  
.....M.N. Mueller and J.M. Jurist.
23. COO-1422-109 Effects of Sodium Fluoride on Ulnar Resonant Frequency in Elderly Women  
.....J.M. Jurist and C.H. Hickey.
24. COO-1422-110 Quantitation of Radioactivity In Vivo by External Counting Measurements (submitted for publication).  
.....J.A. Sorenson.

DETERMINING BODY COMPOSITION BY RADIATION ABSORPTION SPECTROMETRY

by

Richard B. Mazess, John R. Cameron and James A. Sorenson  
 Department of Radiology  
 University of Wisconsin Medical Center  
 Madison, Wisconsin 53706

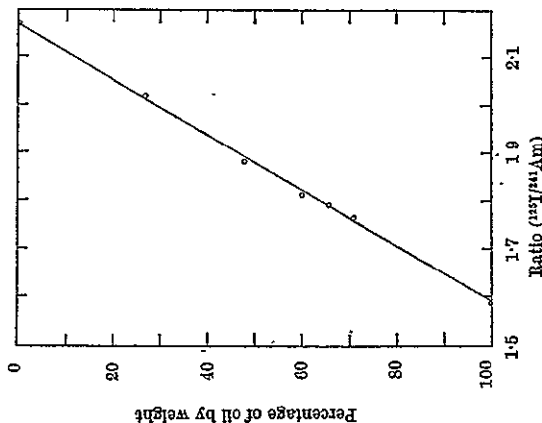


Fig. 1. Relationship between actual composition of a vegetable oil-water mixture and our measure of composition (R); accuracy of composition by absorptiometry is typically 1-2 per cent.  $r=0.996$ , s.e.c. = 1.27 per cent.

The accuracy of this new method was high. In soft tissue phantoms (polyethylene and sodium acetate; vegetable oil and water; paraffin and water) absorptiometry indicated fractional composition with a standard error of estimate (s.e.e.) of less than 0.02 (Fig. 1) and with high correlations ( $r \approx 0.99$ ). Other workers using <sup>137</sup>Cs reported high accuracy with phantoms<sup>14</sup>. In meat samples (fat content by lipid extraction) the measured  $R$  for 100 per cent fat was 1.52 (s.e. = 0.026) while for 100 per cent lean the value was 2.09 (s.e. = 0.016); the s.e.e. in predicting the composition of seven meat samples was 0.03. The measured values of  $R$  in the different mixtures tested corresponded closely to values derived from published absorption coefficients<sup>15</sup>.

Initially we measured tissue composition *in vivo* at single points on human limbs. Reproducibility over several days was usually high (0.5 per cent uncertainty for  $R$ ), but composition changed with small position changes. A scanning method was developed which largely eliminated this problem. A photon source (100-200 mCi of <sup>125</sup>I, or 125 mCi of <sup>241</sup>Am) and detector are mechanically linked and passed several times at uniform speed across an accessible area, usually the middle upper arm<sup>12</sup>. Scanning facilitates both relocation and comparisons among subjects and sites; the total tissue mass varies along the limb but relative composition of the soft tissue in different

(Reprinted from Nature, Vol. 228, No. 5273, pp. 771-772, November 21, 1970)

Determining Body Composition by Radiation Absorption Spectrometry

The fractional composition of a multi-component absorber can be determined from the attenuation of  $\gamma$ -radiation at several energies<sup>1-4</sup>. This technique has been used to measure the amount of bone *in vivo*<sup>5-11</sup>. We now show that absorption measurements at two energies accurately indicate the relative lean-fat composition of soft tissue, and we have developed a scanning method of determining fat, lean cellular and bone mineral mass *in vivo*.

The attenuation of monoenergetic radiation in a single absorber is given by

$$I = I_0 \exp(-\mu x) \text{ or } \ln I_0 - \ln I = \mu x \quad (1)$$

where  $I$  is the beam intensity after it has passed through the absorber,  $I_0$  is the initial unattenuated beam intensity,  $\mu$  is the mass absorption coefficient (cm<sup>2</sup>/g) of the absorber, and  $x$  is the mass per unit area (g/cm<sup>2</sup>) of the absorber in the beam. For a complex absorber the total absorption coefficient ( $\mu_t$ ) at any single energy is the sum of the fractional absorption contributions of the absorber components

$$\mu_t = \mu_a f_a + \mu_b f_b + \dots + \mu_n f_n \quad (2)$$

where  $\mu_a$  is the mass absorption coefficient of component  $a$ , and  $f_a$  is the fractional contribution of  $a$  to the total mass, and so on. For a material composed of  $n$  components the fractional composition is obtained from  $n$  simultaneous equations of the form of equation (1), each incorporating equation (2). In practice, measurement at more than two energies is difficult because of cumulative uncertainties. This and the scarcity of monoenergetic sources in the useful energy range (20-100 keV) generally limit composition analysis to simple mixtures.

We have used <sup>241</sup>Am (59.6 keV) and tin-filtered <sup>125</sup>I (27.4 keV) sources with a conventional detector and a single channel analyser<sup>12,13</sup>. Instead of solving simultaneous equations for each set of observations we used the ratio ( $R$ ) of <sup>125</sup>I absorbance to that with <sup>241</sup>Am as a direct index by establishing a calibration curve relating  $R$  to composition. In soft tissue  $R \approx 2.1$  for 100 per cent lean cellular component and  $R \approx 1.5$  for 100 per cent fat. Because absorption coefficients of fat and lean are nearly equal with <sup>241</sup>Am  $\gamma$ -rays the relationship between the ratio and relative composition of a mixture is linear. Measurements of soft tissue composition by differential absorption spectrometry require high precision and accuracy because of the relatively small differences among the absorption coefficients of low  $Z$  materials at these energies.

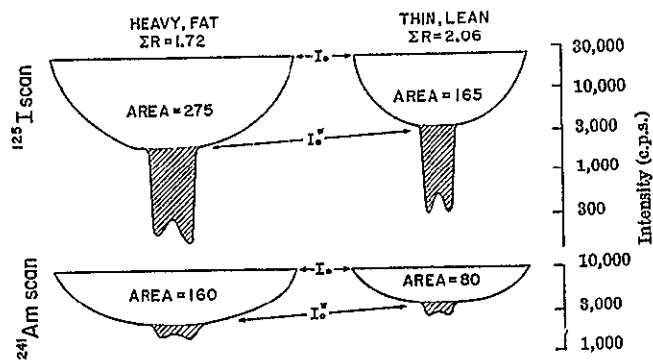


Fig. 2. Absorption scans of the upper arm in a heavy, fat person (left) and a thin, lean person (right).  $I_0$  is the count rate level in air and  $I_0^*$  is the level adjacent to the bone. The shaded area represents absorption by bone mineral. The mineral is usually sharply demarcated in the scan and the baseline ( $I_0^*$ ) is readily determined. The fat person has relatively lower tissue absorption with  $^{125}\text{I}$ . The arm of the thin person contained about 7 per cent fat, while that of the heavy person had 65 per cent; these are the extremes of upperarm composition.

segments is fairly uniform. More important, scanning permits measurement of the mass of the components as well as their proportions, and bone mineral can be measured as well.

Theoretically, a third energy is needed for absorption spectrometry of bone mineral together with soft tissue; but the mass absorption coefficient of the mineral is so much greater than that of soft tissue ( $\times 2$  at 59.6 keV, and  $\times 7$  at 27.4 keV) that the mineral absorption is sharply demarcated in the typical scan (Fig. 2), making it unnecessary in practice. The shaded area in Fig. 2 below the  $I_0^*$  baseline shows the bone mineral absorption, and is directly proportional to the mineral mass<sup>12</sup>. The accuracy of measurement is 1–3 per cent from studies on ashed sections of bone<sup>13</sup>. The unshaded area in the scan represents soft tissue absorbance and is approximately proportional to the soft tissue mass in the scan path. The ratio of  $^{125}\text{I}$  to  $^{241}\text{Am}$  soft tissue scan areas gives an integrated value ( $\Sigma R$ ) indicating relative tissue composition in the scan path. The dose from such scans is about 10 mrad and is confined to a narrow (5 mm) area across the limb.

Immediate reproducibility in replicate upperarm scans ( $n=63$ ) was within about 0.5 per cent for soft tissue scan area, and 1–2 per cent for bone mineral using either nuclide. Long term precision was examined in replicate scans on nine subjects after a 6 month interval; the uncertainty for scan areas with either nuclide was about 4 per cent while the uncertainty in  $\Sigma R$  was only about

Table 1. FIVE REPEAT MEASUREMENTS IN TWO SUBJECTS OVER 9 MONTHS

Subject	$^{241}\text{Am}$ tissue scan		$^{125}\text{I}$ tissue scan		$\Sigma R$	
	1	2	1	2	1	2
Mean	69.6	104.5	144.2	214.2	2.070	2.045
s.d.	1.95	3.07	3.72	8.32	0.006	0.026
c.v. (per cent)	2.80	2.94	2.58	3.88	0.27	1.28

1.6 per cent. Repeated measurements on two subjects over a 9 month period, as well as results on phantoms, showed even higher precision (Table 1). Part of this uncertainty in soft tissue scan areas may reflect actual changes of tissue mass, including those arising from repositioning. In spite of these variations in tissue mass the  $\Sigma R$  was determined with only a 1 per cent error; this typically introduces an uncertainty of about 0.03–0.04 in fractional composition. Such an error is moderately high relative to the usual range in fat fraction (0.10–0.40).

Our measurements were highly correlated with some indirect measures of composition. In nineteen young adults the correlation between tissue absorbance and upperarm circumference was 0.98, while the correlation with triceps skinfold (Lange caliper) was  $-0.91$ . Upperarm composition in these subjects was about 16 per cent fat, 81 per cent lean tissue and 3 per cent bone mineral.

This work was supported by the US Atomic Energy Commission, the US National Aeronautics and Space Administration and the US National Institutes of Health.

RICHARD B. MAZESS  
JOHN R. CAMERON  
JAMES A. SORENSON

Medical Physics Section,  
Department of Radiology,  
University of Wisconsin Hospitals,  
Madison, Wisconsin 53706.

Received November 8, 1969; revised January 15, 1970.

- Lofker, R., *Tech. Rep.*, 2457 (US Army Electronics R and D Labs., Monmouth, New Jersey, 1964).
- Engstrom, A., *Acta Radiol. Suppl.*, 63 (1946).
- Engstrom, A., and Welln, S., *Acta Radiol.*, 31, 483 (1949).
- Jacobson, B., *Science*, 128, 1346 (1958).
- Jacobson, B., *Acta Radiol.*, 39, 437 (1953).
- Omnell, K. A., *Acta Radiol. Suppl.*, 148 (1957).
- Edholm, P., and Jacobson, B., *Acta Radiol.*, 52, 337 (1959).
- Jacobson, B., *Amer. J. Roentgen. Rad. Therap. Nucl. Med.*, 19, 202 (1964).
- Mackay, R. S., *Science*, 128, 1622 (1958).
- Mackay, R. S., *IRE Trans. Med. Electron. ME*, 7, 77 (1960).
- Roy, O. Z., Belique, R. A., and Ombrain, D., *IRE Trans. Med. Electron. ME*, 9, 50 (1963).
- Cameron, J. R., and Sorenson, J. A., *Science*, 142, 230 (1963).
- Sorenson, J. A., and Cameron, J. R., *Proc. Symp. Low Energy X and  $\gamma$  Sources and Applications* (Illinois Institute of Technology, Chicago, 1964).
- Preuss, L. E., and Kosnik, L. T., *J. Nucl. Med.*, 10, 366 (1969).
- McGlinnes, R. T., *Bull. US Nat. Bureau of Standards*, Suppl., 583 (1950).
- Cameron, J. R., Mazess, R. B., and Sorenson, J. A., *Invert. Radiol.*, 3, 141 (1968).

SKELETAL GROWTH IN SCHOOL CHILDREN:  
MATURATION AND BONE MASS

by

Richard B. Mazess and John R. Cameron  
Department of Radiology  
University of Wisconsin Medical Center  
Madison, Wisconsin 53706

ABSTRACT

Skeletal growth and development was evaluated in 322 white children (age 6 to 14 years) using three different methods: (1) I-125 photon absorptiometry, (2) compact bone measures on radiographs, and (3) Greulich-Pyle skeletal age from hand-wrist radiographs. Bone mineral content, measured by photon absorptiometry, increased at an incremental rate of about 8.5% each year. Radiographic measures of compact bone were imprecise, and did not accurately reflect bone mineral content. The error in predicting mineral content from compact bone area was about 12%, or 50% larger than the annual increment of bone. Skeletal age was an equally poor predictor of skeletal status (14% error), and did not decrease the predictive error substantially more than did chronological age. Gross morphology (height and weight) was in fact a better predictor of bone mineral content than were skeletal age, chronological age, and radiographic morphometry. Skeletal age deviations were correlated with deviations in body size. A bone mineral index was devised which was independent of body size and this index was also independent of skeletal age.

The large imprecision (5 to 10%) and inaccuracy (15%) of radiographic morphometry limit its use in assessing skeletal status, especially in growing children. Skeletal age also is imprecise (3 to 6 months error) and the range of variation in normal children (13 months) overlaps the maturational delay of the malnourished and diseased. The difficulties in using skeletal maturation are discussed, and it is suggested that particular maturational indices be used which better indicate skeletal growth than does a composite skeletal age. Both radiographic morphometry and skeletal maturation may be of limited utility in evaluating growth unless validated by more direct measures.

---

\* Paper presented at the Symposium on Assessment of Skeletal Maturity, Am. Assoc. Phys. Anthrop. meeting, April 1971 in Boston.

## INTRODUCTION

Traditionally osseous growth and development has been assessed using the linear dimensions of anthropometry, but these measures have been supplemented, and even supplanted, by indicators of skeletal maturation and determinations of skeletal status (i.e., the amount the distribution of bone, strength, modulus of elasticity, and skeletal dynamics). The ossification patterns used for assessment of skeletal maturation have been shown to have some relationship to linear growth of bones, and in fact can be used to predict stature increments and adult stature. However, stature, and even bone lengths, are only moderately associated with skeletal status, and skeletal maturation therefore might be expected to demonstrate an even lower degree of association. If the latter hypothesis is in fact demonstrable then skeletal maturation would be of little utility as an indicator of skeletal status in either abnormal or normal children, nor would it be of primary use in assessing the influences of environmental variables such as disease, nutrition, activity levels, and stress on the skeleton.

The chief difficulty in testing the above hypothesis is the difficulty in finding acceptable criteria of skeletal status. The amount of bone itself is unacceptable since individuals will vary widely in size depending on their genetic background. This difficulty can be overcome in part by referencing the amount of bone to either the size of the skeleton or to overall body size. The amount of bone can be measured by several non-destructive methods. We have used the measurement of compact bone on radiographs and scanning with radioisotope photon absorptiometry since these are the most commonly used and practical methods.

## METHODS

Measurements were made in 1967 and 1968 on 322 white school age children (age 6 to 14 years) in Middleton, Wisconsin. The age and sex distribution is given in Table 2. The direct photon absorption method (Cameron and Sorenson, 1963; Cameron, Mazess, and Sorenson, 1968; Cameron, 1970; Sorenson and Cameron, 1967) was used to measure bone mineral content. The monoenergetic photon source was I-125 (27.4 keV). Linear scans were made across the distal third of the radius and across the mid-humerus on all subjects, and across the distal third of the ulna on 128 subjects. In addition to mineral content, the bone width was determined from the width of the absorptiometric scan and the mineral-width ratio was calculated as an indicator of the mineral content per unit bone width. The precision and accuracy of this method have been demonstrated to be very high (less than 2% error), and the absorptiometric scan is related not only to local mineral content but to the weight of individual long bones and to total skeletal weight (Mazess, 1971).

Measurements of the bone image on a radiograph (Barnett and Nordin, 1960; Meema, 1963; Virtama and Helela, 1969) have been widely used in clinical settings and in surveys of skeletal growth and development. The thickness of the total bone and of the medullary canal were measured with

Helios callipers on a standard radiograph (36-inch FFD); the site measured was the same as for the absorptiometric scan on the distal radius. Compact bone thickness was derived. In addition, the total cross-sectional area and the area of the compact bone were calculated assuming a circular model (Frisancho, Garn and Ascoli, 1970). The ratio of compact to total bone thickness and area were also calculated as these ratios are commonly used indices of skeletal status.

The remeasurement error (n=113 cases) for both total and medullary thickness was about 0.12 mm; similar values were noted in a series of radiographs in adults (Mazess, Cameron, and Sorenson, 1970). This measurement error amounted to about 1% of the total width and 2 to 3% of the medullary canal width; this resulted in about a 4% error in compact bone thickness and area. In adults when repeat measurements were done on repeat films rather than the same film the magnitude of the errors increased two- or three-fold. The inter-observer errors are given in Table 1.

Table 1. Between Observer Errors of Radiographic Morphometry on the Radius Shaft in School Children (n = 308) and in Adults (n = 240; Mazess et al., 1970.)

		ERRORS		PERCENT ERRORS	
		CHILDREN	ADULTS	CHILDREN	ADULTS
<u>THICKNESS</u>	TOTAL	0.19	0.11	1.80%	0.83%
	MEDULLARY	0.27	0.25	5.58%	2.93%
	COMPACT	0.32	0.26	5.44%	5.03%
<u>AREA</u>	TOTAL	3.25	2.60	3.52%	1.65%
	COMPACT	3.72	4.45	5.16%	4.82%
<u>COMPACT/ TOTAL</u>	THICKNESS	2.59	1.72	4.72%	4.57%
	AREA	2.32	2.24	2.93%	3.74%

The magnitude of the absolute errors was about the same in children as had been observed in adults (about 0.3 mm in compact bone thickness and 4 mm in compact bone area); the adults, due to their larger bones, showed a slightly smaller relative error for some variables. Still there was about a 5% error for both compact bone thickness and area in both children and adults. This analysis indicated that the relatively

high precision of caliper measurement was deceptive since there were substantial difficulties both by the same observer and by different observers in locating the margins of the medullary canal. This led to subsequent errors in derivative measurements such as compact bone thickness and area; these errors might be even greater with refilming. Even though the overall error of individual radiographic measurements may be high, the precision in the present series was lowered by using the average of values from two observers.

Skeletal age determinations were done from hand-wrist radiographs using the atlas of Greulich and Pyle (1959). A variety of weighting formulae and other schemes have been advocated by various investigators, and, in using the Greulich-Pyle method we have simply selected a common method, the success and failure of which is probably fairly representative of analogous techniques.

Two observers were trained to do skeletal age assessments. The error (RMS) in repeat measurements ( $n=141$ ) by the same observer was 5.23 months (4.64%). For the 316 films on which determinations were possible the between observer error (RMS) was 5.17 months (4.41%). Both observers systematically scored skeletal ages about 3.7 months below chronological ages (girls -2.1 months and boys -5.3 months).

## RESULTS

### A. Age Changes in Morphology and the Skeleton.

Age and sex specific values for the morphological variables are given in Table 2, while the corresponding values for bone mineral measurements and for radiographic morphometry are given in Tables 3 and 4. Skeletal age in each age group of females closely approximated the chronological age, but in males the skeletal age was markedly below chronological age during the early school years, and also to some extent during adolescence. Skeletal and chronological ages were nevertheless highly correlated ( $r=0.92$  in girls and  $0.88$  in boys), but the error in predicting skeletal age from chronological age was rather large (11.1 months in girls and 14.7 months in boys). Apparently a deviation of  $\pm 1$  year in skeletal age may be observed in supposedly normal children.

Height and weight values were similar to those usually seen in well-nourished American white children, nor were the arm circumferences and skinfolds unusual (McCammon, 1970).

Bone mineral content was moderately correlated with age ( $r=0.74$  to  $0.80$ ), and the increase was fairly linear amounting to an average of about 10.5%/year or an incremental rate of about 8.5% each year (Table 3 and Figure 1). The bone width and mineral-width ratio increased at an average annual rate of 4.5% or an incremental rate of 4% each year. The rate of increase in bone mineral and the mineral-width ratio was slightly greater in females than in males, apparently reflecting the earlier adolescent growth spurt of the females.

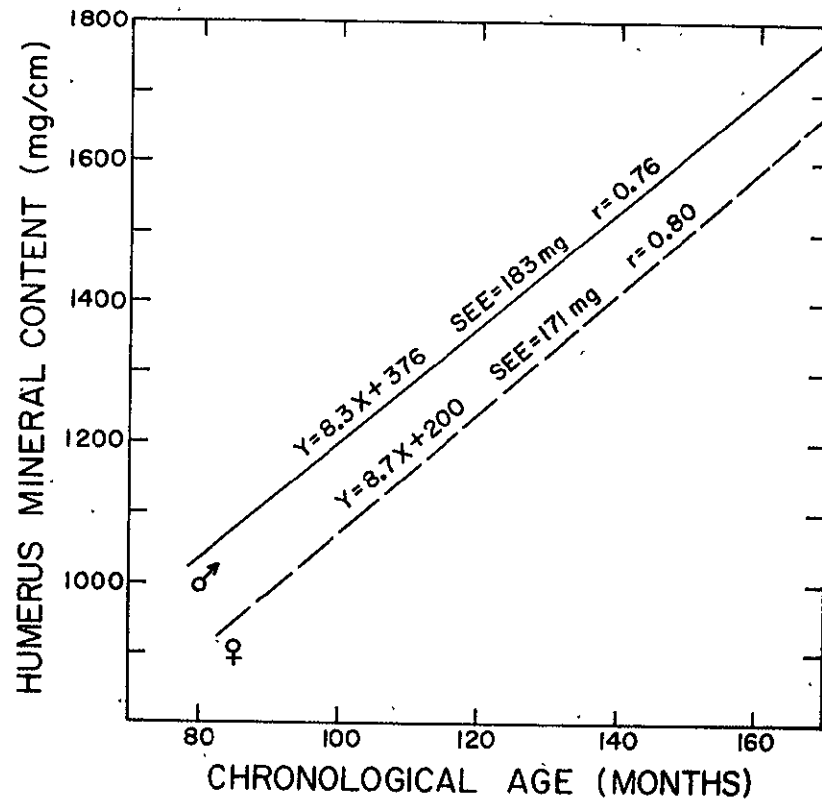
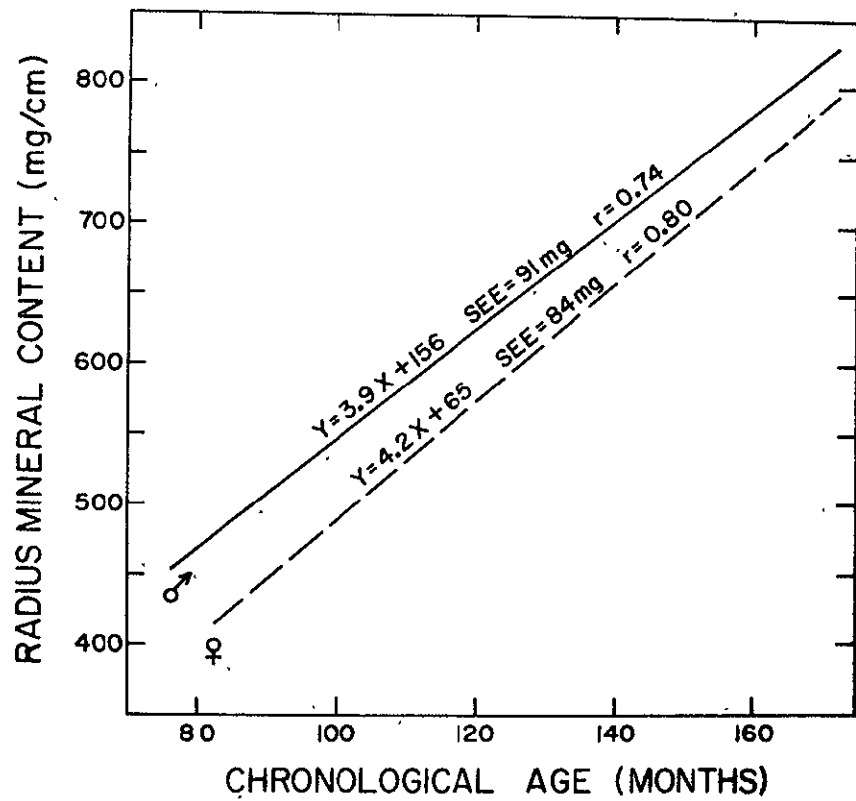


Figure 1. Age changes in the bone mineral content of the radius and the humerus in school children.

Table 2. Means and coefficients of variation for age and morphology in school children

	AGE	NUMBER		AGE (months)		SKELETAL AGE (months)		HEIGHT		WEIGHT		ARM CIRCUM.		TRICEPS SKINFOLD		
		F	M	F	M	F	M	F	M	F	M	F	M	F	M	
MEANS	6	11	16	80	79	79	67	122.8	120.8	22.1	22.2	172	170	11.1	9.2	
	7	19	26	91	90	93	80	128.4	127.3	24.3	25.0	178	181	10.1	10.0	
	8	15	25	103	101	103	98	132.3	134.7	26.6	27.6	193	190	11.1	8.3	
	9	22	25	115	113	111	110	137.6	139.8	30.2	32.0	193	195	12.4	9.4	
	10	29	28	125	126	120	124	141.8	144.6	33.2	35.3	200	204	12.7	9.8	
	11	20	23	137	137	135	133	149.5	148.6	40.5	37.6	216	214	13.8	11.0	
	12	13	19	153	148	152	142	156.8	153.9	42.9	45.7	210	228	11.8	12.6	
	13	15	11	161	161	158	154	158.9	157.6	45.4	49.7	216	235	7.3	8.6	
	14	4	5	172	170	170	163	164.9	163.1	59.7	54.2	249	237	9.7	7.0	
	COEFFICIENTS OF VARIATION	6			3	4	12	28	5	4	19	12	8	8	24	33
		7			3	4	13	18	5	4	16	15	8	10	29	45
		8			3	4	13	18	4	6	14	24	9	13	29	38
		9			3	3	9	16	6	4	21	22	11	12	37	32
		10			3	3	9	12	5	4	19	23	12	13	35	42
11				2	2	8	9	4	3	23	14	17	21	36	48	
12				2	2	9	8	5	6	17	22	8	13	32	52	
13				2	2	9	9	4	6	17	27	10	16	31	61	
14			2	1	5	8	4	4	24	20	16	10	85	23		

Table 3. Means and coefficients of variation for bone mineral measurements of school children, mineral (mg), width (mm) and mineral-width ratio (mg l mm)

AGE	RADIUS						HUMERUS						ULNA					
	Mineral		Width		M/W		Mineral		Width		M/W		Mineral		Width		M/W	
	F	M	F	M	F	M	F	M	F	M	F	M	F	M	F	M	F	M
6	436	466	9.1	9.5	47.5	48.6	943	1018	13.7	14.4	69.2	70.9	354	343	7.6	8.1	46.6	42.1
7	457	510	9.1	10.0	49.9	50.9	1001	1109	14.3	14.7	69.8	75.7	374	411	8.2	8.6	45.9	48.2
8	490	557	9.4	10.2	52.2	54.3	1106	1249	14.9	15.6	74.2	80.2	413	480	8.8	9.1	47.2	52.7
9	542	584	9.7	10.5	55.6	55.4	1216	1276	15.7	15.9	77.3	79.9	481	475	8.4	9.2	57.5	51.6
10	565	633	9.9	11.1	56.6	57.3	1226	1442	15.8	16.8	77.4	85.7	473	554	8.6	9.5	54.6	58.6
11	645	691	10.8	11.3	59.6	61.0	1354	1478	16.5	17.2	81.7	85.9	540	567	9.6	9.8	55.0	58.0
12	716	763	11.3	12.0	63.1	62.9	1533	1662	17.3	19.0	88.1	87.1	-	595	-	10.4	-	57.0
13	742	781	11.5	12.6	64.0	61.6	1627	1624	18.2	18.0	89.4	90.6	-	-	-	-	-	-
14	878	792	12.1	11.9	71.9	66.0	1875	1855	19.1	19.8	98.1	93.2	-	-	-	-	-	-
6	18	11	12	9	10	8	11	12	13	12	10	8	16	10	7	7	15	8
7	12	14	10	8	8	8	11	15	8	14	7	7	14	12	9	13	12	9
8	12	15	9	10	9	9	14	12	9	11	8	7	17	12	9	11	17	11
9	13	12	10	10	6	7	11	13	9	8	7	9	9	15	13	10	7	12
10	17	13	11	10	9	13	12	14	9	10	8	9	16	14	12	7	9	12
11	18	16	11	12	12	8	18	10	11	8	12	8	26	10	12	11	16	9
12	12	16	10	11	8	9	16	13	12	9	9	8	-	10	-	7	-	8
13	13	17	10	12	8	8	12	14	9	11	9	13	-	-	-	-	-	-
14	14	18	14	12	2	10	6	19	6	12	5	12	-	-	-	-	-	-

TABLE 4. Means and coefficients of variation for radiographic morphometry of the radius shaft in school children

	THICKNESS (mm)						AREA (mm <sup>2</sup> )				COMPACT/TOTAL (%)			
	TOTAL		MEDULLARY		COMPACT		TOTAL		COMPACT		THICKNESS		AREA	
	F	M	F	M	F	M	F	M	F	M	F	M	F	M
MEANS														
6	9.4	10.0	4.4	4.6	5.0	5.4	70	79	54	62	54	54	78	79
7	9.7	10.3	4.4	4.8	5.2	5.5	75	84	58	65	54	54	79	78
8	9.6	10.6	4.2	4.9	5.4	5.7	73	89	59	69	56	54	81	78
9	9.9	10.8	4.4	5.2	5.5	5.6	78	93	62	71	56	52	80	77
10	10.3	11.2	4.6	5.0	5.7	6.2	84	101	67	80	56	55	80	80
11	11.2	11.4	4.8	5.2	6.3	6.2	99	103	80	81	56	55	81	79
12	11.5	12.0	5.2	5.7	6.3	6.3	105	113	82	87	55	53	79	77
13	11.6	12.2	4.9	5.5	6.7	6.6	107	117	87	92	58	55	82	79
14	11.7	12.3	4.8	5.5	7.0	6.8	109	120	91	95	60	56	84	80
COEFFICIENTS OF VARIATION														
6	12	10	24	20	15	13	25	20	23	20	15	12	10	7
7	12	8	20	17	10	10	23	15	20	14	9	10	6	7
8	8	10	18	20	12	13	16	20	16	19	11	12	7	8
9	12	9	28	16	9	11	23	18	17	17	14	10	9	6
10	12	11	21	20	12	13	24	22	22	21	11	11	7	7
11	10	9	19	21	15	10	20	19	22	16	12	12	7	7
12	9	9	28	16	11	11	18	17	11	17	17	10	11	6
13	10	9	22	21	12	14	19	18	18	18	12	14	7	9
14	11	13	18	23	7	14	22	26	19	25	6	13	3	8

Radiographic morphometry showed a somewhat similar pattern to bone mineral age changes (Table 4). Total and compact bone thickness increased on the average about 3.8% annually while medullary canal diameter increased only 2.6%. There was some suggestion that medullary canal diameter did not increase at all during early adolescence. The calculated total and compact bone cross-sectional areas increased to a far greater extent (on the average 8% annually) than did the thickness. In contrast, there was virtually no change (0.5% annually) in the ratio of compact to total bone thickness or area.

The age-sex specific coefficients of variation averaged 13.8% for bone mineral content, 10.2% for bone width, and 9.5% for the mineral-width ratio. For total and compact bone thickness the variation was about 11%, while for medullary canal thickness and total and compact bone area it was almost 20%. The ratio of compact to total bone thickness showed a variation of about 11.8% while the area ratio was much less variable - 7.3%.

#### B. Relationship of Radiographic Morphometry and Bone Mineral

Measurements on the radiograph were made at the same spot where photon absorptiometric scans were done, thereby enabling direct evaluation of radiographic morphometry. The radiographic width of the bone was associated with the scan width ( $r=0.88$ ) but it systematically overestimated the actual width by about 2% in both males and females. The mean width from the radiograph was 10.74mm while that from the scan was 10.51mm. The difference of 0.2mm probably represents the magnification due to parallex.

Compact bone thickness was not highly correlated with bone mineral content ( $r=0.73$ ; SEE = 94 mg or 16%). Total bone cross-sectional area was more highly correlated ( $r=0.78$ ) but the error was still too high for useful prediction (SEE = 85 mg or 14%). The best predictor of mineral content was calculated area of the compact bone; the correlation was 0.84 but the predictive error was still fairly large (SEE = 75 mg or 12%).

The regressions of thickness and of area on bone mineral content are shown in Figure 2. There was only a small sex difference over the age range of school children so that a single regression could be used without introducing substantial errors. Such a validation appears necessary wherever radiographic morphometry is used, but this would still limit the validity to grouped data rather than individual cases.

#### C. Association of Chronological and Skeletal Age

The correlations of skeletal and chronological age with morphology, bone mineral and radiographic morphometry are given in Table 5. There was a fairly high association of age with gross morphology, a moderate association with arm circumference, and no association with fatfold. A moderate age association was evident for the bone mineral content of the three bones studied ( $r=0.74$ ) and there was a somewhat lower degree of association with both bone width ( $r=0.59$ ) and mineral-width ratio ( $r=0.65$ ). The correlations of age with radiographic morphometry were

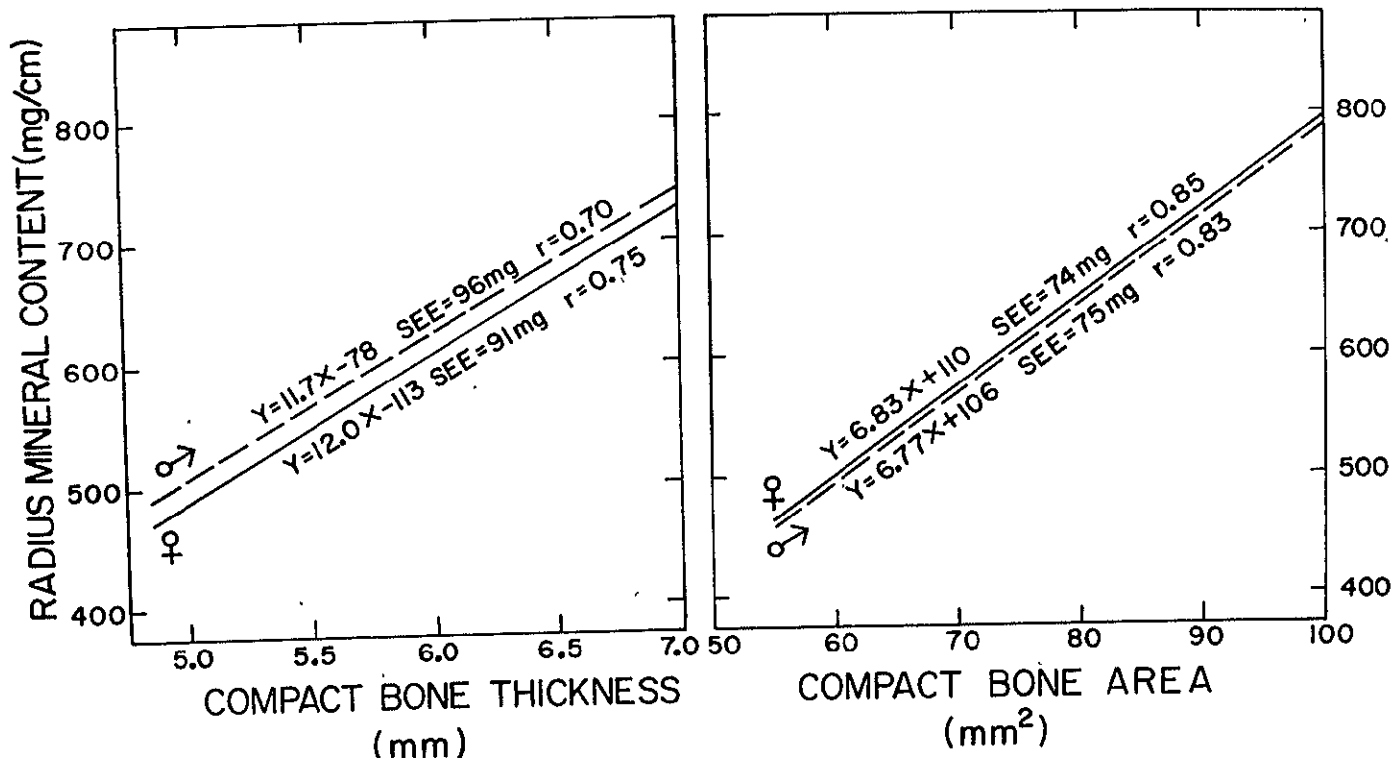


Figure 2. Compact bone thickness and area versus bone mineral content in school children.

Table 5 . Correlations of chronological and skeletal ages with morphology,  
bone mineral measurements, and radiographic morphometry.

		CHRONOLOGICAL AGE	SKELETAL AGE	
<u>MORPHOLOGY</u>	Height	0.88	0.91	
	Weight	0.77	0.82	
	Arm Circumference	0.56	0.64	
	Fatfold	0.04	0.14	
<u>BONE MINERAL</u>	<u>RAD.</u>	Mineral	0.75	0.78
		Width	0.59	0.63
		Mineral/Width	0.71	0.73
	<u>HUM.</u>	Mineral	0.75	0.77
		Width	0.64	0.66
		Mineral/Width	0.65	0.66
	<u>ULNA</u>	Mineral	0.68	0.72
		Width	0.49	0.53
		Mineral/Width	0.57	0.60
<u>RADIOGRAPHIC MORPHOMETRY</u>	<u>THICK.</u>	Total	0.52	0.57
		Medullary	0.23	0.24
		Compact	0.54	0.61
	<u>AREA</u>	Total	0.53	0.58
		Compact	0.58	0.64
	<u>RATIO</u>	Thickness	0.11	0.14
		Area	0.10	0.13

somewhat lower than those with absorptiometry, reflecting the greater errors of the former method. These correlations showed skeletal age to be somewhat more highly associated with morphology and skeletal measurements than was chronological age. However, use of skeletal age increased the correlation coefficient by only a few (0.03) units and increased predictive accuracy by only a few percent.

#### D. Morphology and Bone Mineral Measurements

Increases of body size (height, weight) are associated ( $r=0.81$ ) with increases of bone mineral content, and to a somewhat lesser extent ( $r=0.65$  to  $0.70$ ) with increases in bone width and in the mineral-width ratio (Table 6).

Table 6 . Correlations of morphological features with absorptiometric measurements.

		<u>HEIGHT</u>	<u>WEIGHT</u>	<u>CIRCUM.</u>	<u>FATFOLD</u>
<u>RADIUS</u>	Mineral	0.84	0.83	0.69	0.17
	Width	0.72	0.73	0.62	0.15
	Mineral/Width	0.72	0.68	0.57	0.15
<u>HUMERUS</u>	Mineral	0.82	0.82	0.65	0.12
	Width	0.71	0.73	0.59	0.20
	Mineral/Width	0.69	0.65	0.52	0.00
<u>ULNA</u>	Mineral	0.78	0.78	0.74	0.29
	Width	0.61	0.61	0.56	0.16
	Mineral/Width	0.61	0.59	0.57	0.27

Height was not more closely associated with bone measurements than weight, but both height and weight were more highly associated than was arm circumference. Fatfold thickness was very poorly associated with the bone variables. Standardized regression coefficients and partial correlation coefficients were obtained from multiple regression analysis; these indicated that height and weight were equally important in explaining the variance of the bone measurements.

The correlations of morphological features with radiographic morphology were substantially lower than those with absorptiometry, apparently

reflecting the larger errors of the former measurements.

#### E. Deviant Growth and Development

A closer examination of the associations among skeletal age, morphology, and bone mineral was made by studying the deviation of observed from predicted values (using sex specific regressions derived from this same sample). Height, weight, and bone mineral content (radius and humerus) were predicted for chronological age. A bone mineral index was devised using an average for the radius and humerus of the results from six regressions with the following independent variables:

1. chronological age	r= 0.75
2. height	r= 0.83
3. weight	r= 0.82
4. bone width	r= 0.86
5. bone width, and age	r= 0.91
6. age, height, and weight	r= 0.85

The difference between predicted values were expressed relative to the observed values to get percent deviations. The associations among these deviations are shown in Table 7. Height and weight deviations were moderately associated reflecting the concomitant growth in both parameters. Skeletal age deviations were associated with height and weight ( $r= 0.4$  to  $0.6$ ), and also to some extent with bone mineral content ( $r= 0.38$ ). There was only a very low degree of association, however, between bone mineral index and height, weight, or skeletal age deviations. It therefore appeared that deviations of skeletal age were associated to some extent with body size, and that the association with bone mineral content was secondary to this morphological relationship. The lack of association between bone mineral index and either skeletal age or morphological deviations indicated the dominant influence of body size and skeletal size on bone mineral content; when these factors were taken into account the associations with morphology and skeletal age deviations dropped appreciably.

The relative deviations in children with delayed (more than  $-10\%$ ), normal ( $\pm 9\%$ ), and advanced (more than  $+10\%$ ) skeletal ages are given in Table 8. As is often the case more males than females were delayed. Height, weight, and bone mineral predicted for age tended to be distributed with skeletal age; delayed children, both male and female, had smaller body size and less than usual bone mineral while the reverse was the case for children with advanced skeletal age. This tendency was not evident at all in the bone mineral content predicted for body size or for skeletal size, and this was evidenced clearly by the distribution of the bone mineral index in the normal and deviant groups.

Table 7. Associations among relative deviations (%) of observed from predicted values in school children.

<u>VARIABLE 1</u>	<u>VARIABLE 2</u>	<u>CORRELATIONS</u>	
		<u>FEMALES (n=144)</u>	<u>MALES (n=178)</u>
HEIGHT: for age	WEIGHT: for age	0.66	0.68
Skeletal - Chron. Age	HEIGHT: for age	0.52	0.62
Skeletal - Chron. Age	WEIGHT: for age	0.51	0.43
Skeletal - Chron. Age	BONE MINERAL: for age	0.37	0.39
Skeletal - Chron. Age	BONE MINERAL INDEX	0.16	0.22
HEIGHT: for age	BONE MINERAL INDEX	0.09	0.26
WEIGHT: for age	BONE MINERAL INDEX	0.23	0.24

Table 8. Relative deviations (%) of observed from predicted values in children with delayed (more than -10%), normal ( $\pm 9\%$ ), and advanced (more than 10%) skeletal ages.

	n=	<u>FEMALES</u>			<u>MALES</u>		
		<u>Delayed</u>	<u>Normal</u>	<u>Advanced</u>	<u>Delayed</u>	<u>Normal</u>	<u>Advanced</u>
Skeletal - Chron. Age	$\bar{X}$	-14.0	-1.6	17.5	-20.5	0.3	20.9
	SD	4.2	5.0	8.7	9.7	4.8	10.7
HEIGHT: for age	$\bar{X}$	-4.1	0.2	4.1	-2.9	0.8	5.5
	SD	3.9	3.5	3.2	3.8	3.1	4.0
WEIGHT: for age	$\bar{X}$	-20.1	-1.9	11.4	-11.5	-1.2	19.8
	SD	18.1	16.6	10.6	14.8	16.0	16.3
BONE MINERAL: for age	$\bar{X}$	-7.9	-1.8	7.2	-8.0	-0.3	11.8
	SD	12.2	13.7	10.1	12.6	13.0	9.1
BONE MINERAL INDEX	$\bar{X}$	-0.6	-1.6	1.9	-3.2	-0.3	1.7
	SD	5.8	8.5	6.2	7.2	7.9	5.1

## DISCUSSION

### A. Radiographic Morphometry

Radiographic morphometry has been widely used in assessing skeletal status but the present data suggest that its utility in measurement of children is even less than demonstrated (Mazess et al, 1970) in adults. The errors for repeat measurement of a fixed diameter are rather small, but definition of the medullary canal width is extremely difficult. This leads to large (4 to 6%) errors for both intra- and inter-observer comparisons. The errors would be even larger with refilming and re-positioning. Errors of 5 to 10% have been reported by various workers (Adams, Davies, and Sweetnam, 1969; Anderson, Shimmins, and Smith, 1966; Garn, Feutz, Colbert, and Wagner, 1966; Morgan, Spiers, Pulvertaft, and Fourman, 1967; Mazess, Cameron, and Sorenson, 1970; Saville, 1967).

Such errors of precision in fact limit the accuracy of determinations, but even with repeat measurements by two observers the accuracy (15% error) in predicting mineral content is not high (Mazess et al, 1970). Such large errors virtually preclude use of radiographic morphometry for individual assessment and in particular for assessment of increments where the error may be several times the magnitude of the actual increment. In school age children with an annual increment of only 8 to 10% in bone mineral these errors are substantial and would effectively prohibit evaluation of changes occurring over periods under two or three years in duration.

There are other limitations as well. Some regression adjustment of morphometric results is necessary to render an interpretation in terms of skeletal changes. For example, between the ages of 85 and 165 months males and females increased mineral content by 64% and 80% respectively; compact bone thickness increased by only 22% and 33%, while compact bone area increased by only 46% and 64%. Use of compact bone measurements directly underestimated the magnitude of the age changes, and also exaggerated the extent of male-female differences during this period. A further complication arises since in adults there are differences between bones, and even among locations on the same bone, with regard to the magnitude of the errors, and to regression relationship with mineral content (Mazess et al, 1970); in growing children these factors could lead to even greater variability and uncertainties. Consequently, radiographic morphometry can be used only when steps are taken to minimize errors of precision and when validation of the measurement in terms of mineral content has been accomplished. The resultant measurements would be of use in population studies though not for individual assessments, except where the magnitude of individual differences are very large (for example, protein-calorie malnutrition or several years of growth). However, since stature and weight are more highly correlated with bone mineral than is radiographic morphometry there seems little reason to use the latter method.

## B. Skeletal maturation

There is no need to concern ourselves here with the various investigations of the optimal techniques for assessing maturation, weighting of different bone centers, selection of optimal bones or groups of bones, or comparisons among overall methods. Whatever the procedures used there seems to be substantial errors of about equal magnitude for both intra- and inter-observer reliability (Acheson, Fowler, Fry, James, Urbano, and Van der Werff ten Bosch, 1963; Acheson, Vicinus, and Fowler, 1964, 1966; House, 1950; Johnston and Jahina, 1965; Mainland, 1953, 1954; Moed, Wight, and Vandergrift, 1962; Roche 1963; Roche and French, 1970; Roche, Davila, Pasternack and Walton, 1970; Roche, Rohmann, French and Davila, 1970). Errors as low as one month and as high as 12 months have been reported; the most typical value is about 5 months, or about the same as noted in the present study, though some claim routine errors to decline to 3 months with experience. The fairly large magnitude of these errors has suggested to several workers that a series of repeat determinations should be made by each of several observers so that the error associated with each assessment is minimized. One result of the high imprecision may be a diminution of the apparent degree of communality among bones of an area or among different areas, and an obfuscation of the associations between maturation and growth indicators. It is important to examine the degree to which poor communality of skeletal maturation, and poor association of maturation with growth indicators, contribute to the prevailing vague notions (Falkner, 1958) of the functional import of skeletal maturation.

There is only a moderate degree of communality in ossification timing ( $r = 0.3$  to  $0.5$ ) and rate of maturation ( $r = 0.7$  to  $0.8$ ) in bones of a limited area, and an even lower communality ( $r = 0.3$ ) among bones of different body areas (Garn and Rohmann, 1959, 1966; Garn, Rohmann, Blumenthal, and Kaplan, 1966; Garn, Rohmann, Blumenthal, and Silverman, 1967; Garn, Silverman, and Rohmann, 1964; Roche, 1970; Roche and French, 1970). Several workers have suggested the obvious possibility of selecting bones with a high degree of communality as a more practical and representative skeletal reference than such commonly used composites as hand-wrist skeletal age. It is doubtful that poor precision is responsible for the low communality although it may contribute to it, and hence the variation must reflect wide differences among bones in susceptibility to environmental influences, in the expression of genetic influences (Garn, Rohmann, and Davis, 1963), and in environment-gene interactions (Garn and Rohmann, 1966). Given variation of this nature maturation indices derived by averaging could not reflect clear environmental or genetic influences; a composite skeletal age in no way clarifies this complex interaction of forces.

There have been some indications that populations subject to nutritional deprivation, environmental stress, or diseases have a maturational delay compared to more advantaged groups, but the magnitude of the delay is variable and there is not a close association between the degree of biological stress and maturation. For example, in frank nutritional failure there is some increase in epiphyseal "anomalies" but

skeletal age is delayed by only about 13 months compared to controls (Snodgrasse, Dreizen, Currie, Parker and Spies, 1955; Dreizen, Snodgrasse, Webb-Peploe, and Spies, 1958). In these same studies many normal children were delayed and had anomalies, while some of the undernourished children showed no maturational delay or anomalies. Cahn and Roche (1961) found no correlation between maturation and either calcium intake or disease history in normal Australian children. Sontag and Lipford (1943) actually found a higher incidence of disease among fast-growing children, and showed that illness did not cause delay of centers or alteration of sequence. Garn, Rohmann, and Guzman (1966) showed that Central American children with protein-calorie malnutrition were no more retarded in ossification than the healthy village controls though both the affected and control groups fell below U.S. White standards. The affected children had significantly less compact bone than the controls. During up to a year or more of recovery the increment in ossification of hospitalized children was no greater than expected. The effects of illness or undernutrition on maturation therefore appear quite variable though in all cases the effects on growth are quite marked.

The poor association of growth indicators and skeletal maturation is even more evident in normal children than in those subject to stress. Various investigators have found low or non-existent associations between skeletal maturation and growth variables (Garn, Rohmann, and Robinow, 1961; Johnston, 1964; Moss and Noback, 1958; Noback, Moss and Leszczynska, 1960; Olura, 1956). Even the associations between maturation and growth of the same bones is rather low (Roche and Davila, 1970). Moreover, the overall pattern of discordance may vary with age. For example, Frisancho, Garn and Ascoli (1970) have shown that delays in skeletal maturity in several populations are much less marked in adolescence than childhood although the greatest retardation of growth in these populations occurred in adolescence. The present study indicated that skeletal maturation was only a slightly better indicator of skeletal status than was chronological age, and in fact was, like radiographic morphometry, a poorer indicator than either bone or body size.

Now, just as there is a "rational" approach to selection of bones on the basis of comminality (Garn et al, 1964) so can bones be selected on the basis of their association with growth variables. Johnston (1964) pointed out that maturation is not a unitary process reflecting a single underlying physiological mechanism, and suggested that the utility of a scale of skeletal maturation would be dependent on the ability to select the appropriate maturation indicator for the growth variable being studied. Our data suggest that a composite skeletal age was not an appropriate scale for bone mineral growth in normal children; this might be remedied by selecting a set of interrelated bones which is also highly associated with bone mineralization. It seems, however, that the purpose of a maturation index is not in this diagnostic domain. Instead we suggest that certain bones be selected for their value in predicting the future growth ("growth potential") of a particular parameter, such as bone mineral, under various defined conditions. For example, one may select a set of bones which best predicts the potential

for bone mineral growth during recovery from protein-calorie malnutrition, and these bones could quite conceivably differ from those which best predict the potential elongation of a bone during either normal growth or growth during chronic caloric shortage.

There seems little value in use of even exact observations of skeletal maturation as an indicator of status since: (a) ossification timing, duration, rate, and sequence are quite variable, (b) there is a low degree of communality in maturation, (c) maturation at different areas is variably affected by different environmental influences, (d) there is a complex gene-environment interaction in expression of maturation, and (e) maturation is neither highly nor uniformly associated with growth indicators. On the other hand the ability of skeletal maturation in selected areas to serve as an index of growth potential of specific parameters under specific conditions remains to be investigated.

### C. Skeletal status

It is quite possible to obtain inconclusive assessment of skeletal status if error-prone methods are used to evaluate growth and development (Williams, McDonald, and Pyle, 1964). Anthropometric observations are inexact and indirect indicators of actual bone changes; further of the total growth of bone (10%/year) the dominant process is cross-sectional remodelling (8.5%/year) rather than elongation (5%/year). The discussion of radiographic methods showed them also to be inadequate. Skeletal maturation is associated with large uncertainties in measurement and interpretation, and there is in fact only modest conceptual or practical basis in using this as an adjunct to, or even worse as a substitute for, an indicator of growth status. The measurement of bone mineral content by photon absorptiometry is one of several convenient alternatives which provide a more direct and error-free assessment of skeletal growth than the above methods. Absorptiometry has been used for diagnosis, and for evaluation of treatment, in childhood diseases (unpublished observations; Schuster, Reiss, and Kramer, 1970). The present study suggested several ways to increase the diagnostic sensitivity of this method for both individual and population comparisons.

One approach, which has been used in our laboratory and by most investigators (Cameron, 1970), references the bone mineral content to the bone width in order to eliminate the effects of skeletal size. In the present work we took the additional step of referencing mineral content to age, height and weight in order to provide indices independent of body size. This was necessary as bone mineral content was highly correlated with both bone width ( $r = 0.85$ ), and height and weight ( $r = 0.83$ ). The partial correlations of both age and skeletal age with bone mineral content dropped from  $r = -0.75$  to less than  $r = 0.10$  when body size was held constant. Use of skeletal size and body size references has aided in more specific evaluation of children with bone disorders (unpublished observations), and will aid in differentiating such children from those with uniform retardation of body and skeletal size.

The analysis of deviations from predicted values (section E) demonstrated that the bone mineral content referenced to body size and skeletal

size was in fact independent of not only body size but of skeletal age. This may merely reflect the sporadic occurrence of aberrant mineralization patterns in this normal population. However, about 5% of the children had a bone mineral index two standard deviations or more (mean of 20%, or about 2.5 standard deviations) below normal; even in these children skeletal age averaged only 6% (7 months) below chronological age, and there was no association between degree of demineralization and maturational delay. These findings suggest that skeletal age relates primarily to body size and not to skeletal status. If this is the case one may ask, as did Faulkner (1958), if maturation and body size are associated, and if maturation does not provide information on skeletal growth independent of body size, then why measure maturation? The answer depends on the supposed ability of skeletal maturation to predict the subsequent course of growth and development. As yet, however, the ability of skeletal maturation to provide enhanced prediction of bone mineralization and actual skeletal growth under specific environmental influences has not been demonstrated, and consequently the ability of maturational measures to materially enhance either individual or populational comparisons of growth status remains in doubt.

## REFERENCES

1. Acheson, R.M., Fowler, G., Fry, E.I., Janes, M., Urbano, P., and Van der Werff Ten Bosch, J.J. Studies in the reliability of assessing skeletal maturity from x-rays. I. Gruelich-Pyle Atlas. Hum. Biol. 35: 317-349 (1963).
2. Acheson, R.M., Vicinus, J.H., and Fowler, G.B. Studies in the reliability of assessing skeletal maturity from x-rays. II. The bone-specific approach. Hum. Biol. 36: 211-228 (1964).
3. Acheson, R.M., Vicinus, J.H., and Fowler, G.B. Studies in the reliability of assessing skeletal maturity from x-rays. III. Gruelich-Pyle atlas and Tanner-Whitehouse method contrasted. Hum. Biol. 38: 204-218 (1966).
4. Adams, P., Davies, G.T., and Sweetnam, P.M. Observer error and measurements of the metacarpal. Brit. J. Radiol. 42: 192-197 (1969).
5. Anderson, J.B., Shimmins, J., and Smith, D.A. A new technique for measurement of metacarpal density. Brit. J. Radiol. 39: 443-450 (1966).
6. Barnett, E. and Nordin, B.E.C. The radiological diagnosis of osteoporosis: a new approach. Clin. Radiol. 11: 166-174 (1960).
7. Cahn, A. and Roche, A.F. The influence of illness and calcium intake on the rate of skeletal maturation in children. Brit. J. Nutr. 14: 411-417 (1961).
8. Cameron, J.R. (ed). Proceedings of Bone Measurement Conference. U.S. Atomic Energy Commission Conf-700515; U.S. Dept. of Commerce, Springfield, Va. (1970).
9. Cameron, J.R. and Sorenson, J. Measurement of bone mineral in vivo: an improved method. Science 142: 230-232 (1963).
10. Cameron, J.R., Mazess, R.B., and Sorenson, J.A. Precision and accuracy of bone mineral determination by direct photon absorptiometry. Invest. Radiol. 3: 141-150 (1968).
11. Dreizen, S., Snodgrass, R.M., Webb-Peploe, H., and Spies, T.D. The retarding effect of protracted undernutrition on the appearance of the postnatal ossification centers in the hand and wrist. Hum. Biol. 30: 253-264 (1958).
12. Falkner, F. Skeletal maturation: an appraisal of concept and method. Am. J. Phys. Anthropol. 16: 381-396 (1958).
13. Frisancho, A.R., Garn, S.M., and Ascoli, W. Childhood retardation resulting in reduction of adult body size due to lesser adolescent skeletal delay. Am. J. Phys. Anthropol. 33: 325-336 (1970).

14. Garn, S.M. and Rohmann, C.G. Communalities of the ossification centers of the hand and wrist. Am. J. Phys. Anthrop. 17: 319-323 (1959).
15. Garn, S.M. and Rohmann, C.G. "Communalities" in the ossification timing of the growing foot. Am. J. Phys. Anthrop. 24: 45-50 (1966a).
16. Garn, S.M. and Rohmann, C.G. Interaction of nutrition and genetics in the timing of growth and development. Pediatrics Clinics of N.A. 13: 353-379 (1966b).
17. Garn, S.M., Feutz, E., Colbert, C., and Wagner, B. Comparison of cortical thickness and radiographic microdensitometry in the measurement of bone loss. In: G.D. Whedon, W.F. Neumann, and D.W. Jenkins (eds) - Progress in Development of Methods in Bone Densitometry, NASA-SP-64. Washington, D.C., 65-77 (1966).
18. Garn, S.M., Rohmann, C.G., Blumenthal, T., and Kaplan, C.S. Developmental communalities of homologous and non-homologous body joints. Am. J. Phys. Anthrop. 25: 147-152 (1966).
19. Garn, S.M., Rohmann, C.G., Blumenthal, T., and Silverman, F.N. Ossification communalities of the hand and other body parts; their implication to skeletal assessment. Am. J. Phys. Anthrop. 27: 75-82 (1967).
20. Garn, S.M., Rohmann, C.G., and Davis, A.A. Genetics of hand-wrist ossification. Am. J. Phys. Anthrop. 21: 33-40 (1963).
21. Garn, S.M., Rohmann, C.G., and Guzman, M.A. Malnutrition and skeletal development in the pre-school child. In: Pre-School Child Malnutrition. Nat'l Acad. Svi. - Nat'l Research Council, Washington, D.C. (1966).
22. Garn, S.M., Rohmann, C.G., and Robinow, M. Increments in hand-wrist ossification. Am. J. Phys. Anthrop. 19: 45-53 (1961).
23. Garn, S.M., Silverman, F.N., and Rohmann, C.G. A rational approach to the assessment of skeletal maturation. Ann. Radiol. 7: 297-307 (1964).
24. Greulich, W.W. and Pyle, S.I. Radiographic Atlas of Skeletal Development of Hand and Wrist (2nd Ed), Stanford Univ. Press, Stanford, Calif. (1959).
25. House, R.W. A summary of forty nine radiologists' opinions of the skeletal age limits of apparently normal six-year old children. Am. J. Roentg. 64: 442-445 (1950).
26. Johnston, F.E. The relationship of certain growth variables to chronological and skeletal age. Hum. Biol. 36: 16-27 (1964).
27. Johnston, F.E. and Jahina, S.B. The contribution of the carpal bone to the assessment of skeletal age. Am. J. Phys. Anthrop. 23: 349-354 (1965).

28. Mainland, D. Evaluation of the skeletal age method of estimating children's development. I. Systematic errors in the assessment of roentgenograms. Pediatrics 12: 114-129 (1953).
29. Mainland, D. Evaluation of the skeletal age method of estimating children's development. II. Variable errors in the assessment of roentgenograms. Pediatrics 13: 165-173 (1954).
30. Mazess, R.B. Estimation of bone and skeletal weight by direct photon absorptiometry. Invest. Radiol. 6: 52-60 (1971).
31. Mazess, R.B., Cameron, J.R., and Sorenson, J.A. A comparison of radiological methods for determining bone mineral content. In: G.D. Whedon and J.R. Cameron (eds) - Progress in Methods of Bone Mineral Measurement; U.S. Dept. Health, Educ. and Welfare, Supt. of Documents, Washington, D.C., 455-479 (1970).
32. McCammon, R.W. Human Growth and Development. C.C. Thomas, Springfield, (1970).
33. Meema, H.E. Cortical bone atrophy and osteoporosis as a manifestation of aging. Am. J. Roentgen. 89: 1287-1295 (1963).
34. Moed, G., Wight, B.W., and Vandergrift, H.N. Studies of physical disability: reliability of measurement of skeletal age from hand films. Child Development 33: 37-41 (1962).
35. Morgan, D.B., Spiers, F.W., Pulvertaft, C.N., and Fourman, P. The amount of bone in the metacarpal and the phalanx according to age and sex. Clin. Radiol. 18: 101-108 (1967).
36. Moss, M.L. and Noback, C.R. A longitudinal study of digital epiphyseal fusion in adolescence. Anat. Record 131: 19-32 (1958).
37. Noback, C.R., Moss, M.L., and Leszczynska, E. Digital epiphyseal fusion of the hand in adolescence - a longitudinal study. Am. J. Phys. Anthrop. 18: 13-18 (1960).
38. Olura, K. A study on the standard of evaluating physical maturation degree through measurement of carpal bones radiograph and the validity of this standard. Jap. J. Educ. Psychol. 4: 1-12 (1956).
39. Roche, A.F. Lateral comparisons of the skeletal maturity of the human hand and wrists. Am. J. Roentgen. 89: 1272-1280 (1963).
40. Roche, A.F. Associations between the rates of maturation of the bones of the hand-wrist. Am. J. Phys. Anthrop. 33: 341-348 (1970).
41. Roche, A.F. and Davila, G.H. Associations between the rates of maturation and growth in the short bones of the hand. Am. J. Phys. Anthrop. 33: 349-356 (1970).
42. Roche, A.F. and French, N.Y. Differences in skeletal maturity levels between the knee and hand. Am. J. Roentgen. 109: 307-312 (1970).

43. Roche, A.F., Davila, G.H., Pasternack, B.A., and Walton, M.J. Some factors influencing the replicability of assessments of skeletal maturity (Greulich-Pyle). Am. J. Roentgen. 109: 299-306 (1970).
44. Roche, A.F., Rohmann, C.G., French, N.Y., and Davila, G.H. Effect of training on replicability of assessments of skeletal maturity (Greulich-Pyle). Am. J. Roentgen. 108: 511-515 (1970).
45. Saville, P.D. A quantitative approach to simple radiographic diagnosis of osteoporosis; its application to the osteoporosis of rheumatoid arthritis. Arthr. Rheumat. 10: 416-422 (1967).
46. Schuster, W., Reiss, H., and Kramer, K. The objective assessment of disorders of bone mineralization in congenital and acquired skeletal diseases in childhood. Ann. Radiol. 8: 255-265 (1970).
47. Snodgrasse, R.M., Dreizen, S., Currie, C., Parker, G.S., and Spies, T.D. The association between anomalous ossification centers in the hand skeleton, nutritional status, and the rate of skeletal maturation in children five to fourteen years of age. Am. J. Roentgen. 74: 1037-1048 (1955).
48. Sontag, L.W. and Lipford, J. The effect of illness and other factors on the appearance pattern of skeletal epiphyses. J. Pediatrics 23: 391-409 (1943).
49. Sorenson, J.A. and Cameron, J.R. A reliable in vivo measurement of bone mineral content. J. Bone Jt. Surg. 49A: 481-497 (1967).
50. Virtama, P. and Helela, T. Radiographic Measurements of Cortical Bone. Acta Radiologica Suppl. 293 (1969).
51. Williams, D.E., McDonald, B.B. and Pyle, S.I. Bone density and skeletal maturation as indexes of mineral status in children. Am. J. Clin. Nutr. 14: 91-97 (1964).

#### ACKNOWLEDGEMENTS

Supported by AEC grant AT-(11-1)-1422 and NASA grant Y-NGR-50-002-051. During part of this time RBM was supported through an NIH postdoctoral fellowship. The staff and students of St. Bernards school aided our studies. Substantial help was given by Mrs. J.R. Cameron, Bob Witt, Joyce Fischer, Sue Kennedy, Ellie Sosne, Barbara Binns, Bob Jones, Monica Jaehnig and the staff of the Cosmic Medicine Laboratory.

METHODS FOR QUANTITATING RADIOACTIVITY \*  
IN VIVO BY EXTERNAL COUNTING MEASUREMENTS

by

James A. Sorenson

Under the Supervision of Professor John R. Cameron  
Department of Radiology  
University of Wisconsin Medical Center  
Madison, Wisconsin 53706

Three methods for quantitatively estimating radioactivity in patients by external  $\gamma$ -ray counting measurements were investigated. These were the combined transmission-emission method, ratioing of Compton to photopeak counts, (C/P), and the dual-isotope methods. A general mathematical description of quantitative measurements was obtained, which was then used to assess the possible sources of error in each method. It was found that of all parameters involved, source depth within the patient has the greatest effect, but that this effect can be accounted for by each of the methods studied. Source thickness and uniformity were found to have relatively small effects ( $\leq 10\%$ ), particularly in the (C/P) ratio and dual-isotope methods. Source thickness effects could be accounted for with reasonable accuracy in the transmission-emission method by modification of the equations derived for point sources. In the (C/P) and dual-isotope methods these effects were small enough that they could be ignored, and point source equations could be used. The mathematical analysis was tested in a series of studies involving various radionuclides in water phantoms measured on a linear scanning device. Good agreement between theory and experimental results was obtained over a wide range of photon energies and in several counting geometries. The combined transmission-emission method and (C/P) method were used to study the distribution and total body content of radioactivity in a series of patients injected with Fe-59 and Tc-99m sulfur colloid. Both methods were found to improve accuracy in total body counting (absolute error  $\leq 10\%$ ). The transmission-emission method also gave an apparent improvement in accuracy for determining distribution, and reduced overall random errors in total body counting to about 5% (S.D.), as opposed to 13% for uncorrected data. Distributional accuracy and random error were not found to be improved by the (C/P) method.

\* Ph.D. Thesis Abstract, 1971; thesis available upon request.

A DICHROMATIC ATTENUATION TECHNIQUE FOR THE IN VIVO  
DETERMINATION OF BONE MINERAL CONTENT \*

by

Philip F. Judy

Under the Supervision of Professor John R. Cameron  
Department of Radiology  
University of Wisconsin Medical Center  
Madison, Wisconsin 53706

The determination of the composition of a two component substance by gamma-ray and x-ray attenuation has been studied. The particular application investigated was the measurement of human limbs, which were assumed to contain a bone mineral component and a soft tissue component. Radionuclides (I-125, Am-241, and Gd-153) have been used as sources of nearly mono-energetic photon beams. The attenuation was measured by securely and reproducibly holding the limb or other objects between a collimated NaI(Tl) scintillation detector and a source position. The collimated photon sources were mounted on a wheel, which permitted each source to be sequentially and reproducibly placed in the source position.

The formulas used in the dichromatic attenuation technique (DAT) were derived from simple exponential attenuation theory. The difficulties of such attenuation measurements were (a) the deviation of the attenuation of the photon beams from the exponential formulas, (b) the variation of the composition of the human tissues, and (c) the problems of repositioning the body from measurement to measurement.

Deviation from exponential attenuation was related to the size of the photon beams, monochromaticity of the photon beams, and the scattered radiation detected. Of these factors the photon beam size had the most effect. The size of the photon beams, and the effects of size, were estimated from experimentally determined beam profiles. The size of the I-125 beams (28 keV) ranged from 1.5 mm to 3 mm in diameter, and the size of the Am-241 beams (60 keV) ranged from 2.5 mm to 4 mm. Using these beams the DAT estimate of the bone mineral component deviated from an accurate value by as much as 30% near the edge of the bone, and a 10% deviation was typical.

The scattered radiation was measured by examining the transmission of the photon beam as a function of detector aperture size. The scattered radiation constituted 5% to 15% of the detected photons for the I-125 and Am-241 beams and for thicknesses of tissue of the limbs, but the exponential characteristic of the attenuation was not altered.

---

\* Ph.D. Thesis Abstract, 1971; thesis available upon request.

Deviation of the beams from monochromaticity was evaluated from the spectrum of the photon beams. The hardening of the I-125 beam caused a  $3 \text{ mg/cm}^2$  decrease in the estimated bone mineral content (BMC) per  $\text{g/cm}^2$  of soft tissue cover. Compensation for this small deviation was possible.

The effect of the variation in the composition of soft tissue and bone mineral was investigated. The lipid content of soft tissue was found to decrease the estimate of BMC  $0.06 \text{ g/cm}^2$  per  $\text{gm/cm}^2$  of lipid. This effect was essentially independent of the photon energies used. The variation of the composition of bone mineral had less than a 1% effect on the estimate of BMC.

The effects of the repositioning error could be large, especially for irregular distributions of BMC in the bone. Using casts of the body area measured, the repositioning error for measurements in vivo was minimized.

The BMC of the proximal phalanx was determined with the DAT on five patients undergoing chronic hemodialysis for the treatment of chronic renal failure, one normal subject, and a phantom. The I-125 beam was 2 mm in diameter, and the Am-241 beam was 3 mm in diameter. These beam sizes result in a less accurate measurement than is possible with smaller beams, but also reduce the repositioning error. The precision of the measurements in vivo was 1.4% (coefficient of variation) and of the phantom was 0.5%. The precision in vivo was limited by the ability to reposition the subject from measurement to measurement. The accuracy was affected by the size of the photon beams and the uncertainty of the actual soft tissue composition of the patients. Each effect resulted in a 10% deviation of the estimated BMC of the proximal phalanx from the accurate value and were independent of each other. No changes of BMC of the patients undergoing chronic hemodialysis was observed. The precision of the measurements was 3% per year with a 95% confidence.

#### ACKNOWLEDGEMENT

This work is supported in part by the National Aeronautics and Space Administration through Grant Y-NCR-50-002-051.

THE RELATIONSHIP OF PHOTON ABSORPTION MEASUREMENTS  
OF BONE MINERAL CONTENT TO BONE STRENGTHS \*

by

Charles R. Wilson\*\*

Under the Supervision of Professor John R. Cameron  
Department of Radiology  
University of Wisconsin Medical Center  
Madison, Wisconsin 53706

The importance of bones' structural and physio-chemical functions to the health and physical well being of the individual is well known. This dissertation deals with the structural characteristics of bone and its relation to bone mineral content. During aging bone decreases in total mass with the most obvious decrease occurring in the axial skeleton. There is also an apparently corresponding decrease in the structural integrity of the skeleton as seen by the increased incidence of fracture with age. These changes occur normally but to a greater extent in osteoporosis. The sites of greatest importance, the spine and the femoral neck, which are mainly cancellous bone, are also the most inaccessible for the accurate measurement of bone mineral content. Both sites show increased incidence of fracture and definite changes in trabecular bone patterns with age. Whether the amount of bone in the appendicular skeleton is representative of the axial skeleton, and whether the former could be used to predict the latter is unclear. The use of appendicular bone mineral content, measured by the direct photon absorptiometric technique, has been investigated as a means for the evaluation of skeletal status; that is, the bone mineral content and strength of the axial skeleton and other inaccessible sites.

The mineral content and the maximum compressive strength of bone from the axial and appendicular skeletons of 24 cadavers have been measured. It was found that the mineral content of different sites on the same bone are highly interrelated ( $r \sim 0.95$  or better). The correlations between sites on different long bones or between the mineral content of different vertebral bodies were moderate ( $r \sim 0.85$ ). The mineral content of sites on the long bones were related to the mineral content of the axial skeleton to a lesser degree ( $r \sim 0.65$ ), and the associations were not sufficient to accurately predict the axial mineral. There was a high degree of correlation between the mineral content of the femoral neck and the axial skeleton ( $r \sim 0.88$ ). The maximum compressive strength and the mineral content were moderately associated for both compact and cancellous bone but there was no significant relationship between the mineral content of the long bones and the strength of the axial skeleton. The mineral content per unit volume of the appendicular and axial skeleton decreased with age after the third decade. Similarly the compressive strength of bone from both areas decreased with age however the rate of decrease of the strength was greater than the rate of decrease of bone mineral mass.

---

\* Ph.D. Thesis Abstract, 1971; thesis available upon request.

\*\* Supported by NIH Training Grant No. 144-9684.

Although the absorptiometric method determines the mineral content both accurately and precisely the predictability of these measurements is of limited value in quantitative evaluation of bone strength, but may be useful for the qualitative descriptions. The reasons for this are discussed.

#### ACKNOWLEDGEMENT

This work is supported in part by the U.S. Atomic Energy Commission through Contract AT-(11-1)-1422.

EFFECTS OF PHYSICAL ACTIVITY  
ON BONE LOSS \*

by

Everett L. Smith  
Department of Radiology  
University of Wisconsin Medical Center  
Madison, Wisconsin 53706

EFFECTS OF PHYSICAL ACTIVITY ON BONE LOSS

The purpose of this investigation was to study the effects of physical activity in slowing the normal process of osteoporosis and/or increasing bone mineral in the aged. Thirty-nine subjects were involved and included both sexes age fifty-five to ninety-four. The subjects were classified into three groups: twenty-one in a control group, twelve in a physical activity group, and six in a physical therapy group, for an eight month study. The physical activity group participated in an exercise program forty-five minutes, three times a week for eight months. The physical therapy group received supervised physical therapy for medical indications during the study. The control group participated in no formal physical activity.

The mid-shaft of the radius of all subjects was measured by absorptiometry three times during the eight months: September 1968 (T<sub>1</sub>), March 1969 (T<sub>2</sub>) and May 1969 (T<sub>3</sub>). Comparisons were made between the initial bone mineral (T<sub>1</sub>) and the final bone mineral (T<sub>2</sub>) values within the groups and between the groups.

OSTEOPOROSIS IN AGED WOMEN

The purpose of this phase of the investigation was to define the degree of demineralization that occurs with age in the normal process of bone loss and clinical osteoporosis. One hundred aged female subjects were involved in the study. Fifty subjects in a control group were age matched with fifty clinically osteoporotic females. The mid-shaft of the radius of all the subjects was measured by absorptiometry. Bone mineral values were compared between the groups.

OXYGEN CONSUMPTION (VO<sub>2</sub>) FOR PHYSICAL ACTIVITY

Four different subjects were involved in the analysis of oxygen consumption of ten physical activities used in the physical activity phase of this study. Each of the ten activities were completed three times by the four subjects. Energy expenditure was estimated by measurement of the oxygen consumption. Expired gases were collected and immediately analyzed on a Beckman gas analyzer. The average oxygen consumption for each activity was obtained.

---

\* Ph.D. Thesis Abstract, 1971; thesis available upon request.

## CONCLUSIONS

### A. Effects of Physical Activity on Bone Loss

Physical activity slowed and in some cases seemed to reverse the normal process of osteoporosis.

1. Bone Mineral - The physical activity group demonstrated a significant ( $P < .05$ ) bone mineral increase of 2.6 per cent during the eight month study, while the control group demonstrated no bone mineral change. The physical therapy group demonstrated a significant ( $P < .05$ ) bone mineral increase of 7.8 per cent. The bone mineral change difference between the control group and the physical activity group was not significant at the .05 level. The bone mineral change difference between the control group and the physical therapy group was significant at the ( $P < .05$ ) level.
2. Bone Mineral Divided by Bone Width - The bone mineral divided by bone width change in the control group of .5 per cent and physical therapy group of 1.7 per cent demonstrated no significant difference between  $T_1$  and  $T_2$ . The physical therapy group demonstrated a significant ( $P < .05$ ) bone mineral divided by bone width increase of 7.8 per cent between  $T_1$  and  $T_3$ . The bone mineral divided by bone width change between the control group and the physical activity group was not significant. The bone mineral divided by bone width of the physical therapy group was significantly ( $P < .05$ ) different than both the control and the physical activity group.
- 3 Width - Bone width of the three groups remained constant throughout the eight months study.

### B. Osteoporosis in the Aged Women

The normal aging process of osteoporosis can be separated from clinical osteoporotic.

1. Bone Mineral - The mean bone mineral content of the clinical osteoporotic group was significantly ( $P < .001$ ) lower than the control group. A bone mineral discriminant value of 0.68 g/cm separated seventy-six per cent of the normal subjects from the clinical osteoporotics.
2. Bone Mineral Divided by Bone Width - The mean bone mineral divided by bone width was significantly ( $P < .01$ ) lower than the control group. A bone mineral divided by bone width discriminant value of 0.55 g/cm<sup>2</sup> separated seventy-three per cent of the normal subjects from the clinical osteoporotics.
3. Bone Width - The bone width of the two groups were not significantly different.

The absorptiometry system was not able to determine subjects who were hypermineralized due to osteocyte death and therefore more

prone to bone fracture.

#### ACKNOWLEDGEMENT

This work is supported in part by the National Institute of Health under Grant AM10623.

ESTIMATION OF BONE AND SKELETAL WEIGHT  
BY DIRECT PHOTON ABSORPTIOMETRY \*

by

Richard B. Mazess  
Department of Radiology  
University of Wisconsin Medical Center  
Madison, Wisconsin 53706

The direct photon (I-125) absorptiometric method for radiologic measurement of bone was used to examine the intercorrelations among determinations at various sites on the human ulna, radius, humerus and femur. The relationships of local mineral content, determined by this scanning method, with the weights of individual bones and of the total skeleton were also examined. Scans on the different bones were highly intercorrelated ( $r = 0.80$  to  $0.90$ ), and correlation coefficients were even higher ( $r = 0.90$  to  $0.95$ ) for different locations on the same bone. The relative uniformity of local mineral content was not sufficiently high, however, to allow specific extrapolation from single scan sites. Absorptiometric scans were also highly correlated with the weights of the bones on which they were made ( $r = 0.94$ ) and with the weights of other bones ( $\bar{r} = 0.90$ ) or of the total skeleton ( $r = 0.90$ ). The weights of individual bones or of the entire skeleton were estimated with only a 5 to 10 per cent error; scans at several sites improved the accuracy. In contrast, linear measurements on the bones were only moderately correlated with local mineral content or bone weights.

Printed in: Invest. Radiol. 6(1): 52-60, 1971.

\* Abstract only; article available upon request.

## REVIEW OF BODY COMPOSITION IN ANIMALS AND MAN \* \*\*

by

Richard B. Mazess  
 Department of Radiology  
 University of Wisconsin Medical Center  
 Madison, Wisconsin 53706

This volume, like many symposia, is of uneven caliber. It is remarkable, however, that the contributions are largely devoid of the broad biological and methodological perspective seen in composition symposia of the past decade. The apparent focus of the May 1967 conference at the University of Missouri was on methods of composition analysis, both direct and indirect, as applied principally to livestock and only marginally to man. Aside from this dominant concern with meat animals there is little basically new in the book.

The first section provides a general introduction to biological results. Reid et al., and Pitts and Bullard, provide interesting interspecific comparisons, while Widdowson, and also Forbes, discuss growth. Baily and Zobriskey present a most valuable review of specific protein changes and cellular differentiation during growth in several species as well as outlining protein distribution in the body.

A brief section on statistics gives the usual admonitions, and in particular cautions against misuse of the correlation coefficient; unfortunately most of the authors did not heed these caveats.

There is little on the once popular topic of densitometry. Pearson et al. review volume methods, particularly gas displacement while Garrett reports on validation studies in sheep, cattle and pigs. Unfortunately, it is only Behnke, in his all too brief commentary, who notes the large errors associated with varying contribution of water and mineral to the fat free body.

The major portion of the book is devoted to whole body counting of K-40. Several authors examine technical problems of measurement, such as precision, calibration, and efficiency of counters; analytic errors can be high (10%) if extreme care is not taken. The accuracy of the method, and biological interpretations, are discussed in other sections. For example, in the succeeding section on dilution methods Remenchik et al. astutely note that both K-40 and exchangeable K-42 are poor predictors of body composition although these measures may be of some use in examining potassium stores in disease. The rest of the section on dilution contains little new material and generally is less adequate than previous review articles. Panaretto deals with hydrogen isotopes and Doornenbal looks at blood volume, but there is no systematic analysis of fluid compartments, or even of extracellular fluid.

\* viii + 521 pp. National Academy of Sciences (U.S.A.) Publication 1598.  
 Washington, D.C. 1968. \$13.00.

\*\* In: Human Biology 42: 138-140 (1970).

The last section consists of comparisons of miscellaneous methods. Several authors try to validate K-40 measurement and other indirect measures in livestock without much success. Besadoun et al. find that antipyrine and creatinine aid in composition analysis of sheep, while Fries and Lynch seem to find K-42 and Na-24 of marginal utility. Flynn et al. used deuterium oxide and thiocyanate space in children and pigs, and finally there is a report on composition measures used for U.S. Army nutrition surveys.

This volume did not come up to my initial expectations. First, there is a lack of clarity, poor exposition, limited outlook, and downright obfuscation exhibited throughout. Moreover some of the authors seemed bent on displaying the maximum amount of incoherent tabular material possible, together with an uncritical dependency on the correlation coefficient. Despite these drawbacks some useful information can be obtained with careful reading.

Second, there was a wholly untoward emphasis on measuring body potassium to predict composition. The technical articles on whole body counters are satisfactory, but would be more appropriate in another context. Most reports indicated that there are large analytic errors in measuring body potassium, and even if perfectly measured by K-40 or K-42 (which is not the case) the biological variation in K concentration is large enough to prohibit predicting composition. The organizers of this meeting can be blamed for the gross excess of reports on such a dubious, albeit elegant and costly method.

Third, inadequate treatment was given to dilution and densitometric techniques, nor were fluid compartments covered. Other techniques (radiography, metrical, ultrasonic, activation analysis, and radiation absorptiometry) are not touched on, although these probably would be of greater use to livestock specialists.

There are also persistent minor irritations such as the use of the term "fat" for adipose tissue, or of "bone" or "skeletal" without specifying the chemical condition (ashed, dried, or wet). It is unfortunate that this symposium did not cover the complete range of useful methods and provided inadequate treatment even for those covered. The animal scientists have contributed much through carcass analysis to the field of body composition, but this volume does not elaborate on those contributions and instead mainly depicts explorations in the application of indirect methods to livestock. These trails and deadends have been covered in greater detail in previous symposia. Nevertheless the volume is a major addition to the growing literature on composition and will be purchased by all workers in the field, although it will be of only modest value to human biologists, or even for the animal scientists for whom it was intended.

BONE MINERAL DETERMINATION IN VITRO  
BY RADIOGRAPHIC PHOTODENSITOMETRY  
AND DIRECT PHOTON ABSORPTIOMETRY \*

by

Charles Colbert<sup>^^</sup>, Richard B. Mazess<sup>\*\*\*</sup>,  
and Peter B. Schmidt<sup>\*\*</sup>

For the first time, the accuracies of two radiologic methods for determining bone mineral content were compared under the same test conditions. Direct photon absorptiometry at the University of Wisconsin uses a monoenergetic radionuclide source (I-125 at 27.4 keV) with a scintillation-detector/pulse-height analyzer system. The source and detector are passed across the bone and changes in beam intensity are proportional to the mineral content. Radiographic photodensitometry at Fels Research Institute uses optical density measurements of the bone image on a standard radiograph. A microdensitometer/computer system is used for these radiographic measurements, while the radiograph itself is made with an ordinary x-ray machine. The error in predicting ash weight using Wisconsin absorptiometry was 3% while the error using the Fels method of photodensitometry was 6%. The accuracy of the Fels method was superior to that reported by other workers who do not correct for background film density.

Printed in: Invest. Radiol. 5(5): 336-340, 1970.

- \* Abstract only; article available upon request.
- \*\* Fels Research Institute
- \*\*\* Department of Radiology; University of Wisconsin Medical Center; Madison, Wisconsin 53706

RECTILINEAR SCANNER FOR DETERMINATION  
OF BONE MINERAL CONTENT

by

John M. Sandrik, Richard B. Mazess,  
Clifford E. Vought, and John R. Cameron  
Department of Radiology  
University of Wisconsin Medical Center  
Madison, Wisconsin 53706

## INTRODUCTION

A rectilinear scanner and the associated electronic control apparatus (Fig. 1) have been built for use in the photon absorptiometric determination of bone mineral content in vivo. Rectilinear scanning has the advantage of minimizing repositioning errors as compared to a single point determination or a single linear scan. It has been shown (1) that the reproducibility of measurements of bone mineral content of irregularly shaped bones, eg. the distal radius, can be improved from 5% to 2% by averaging three measurements at 3 mm intervals along the bone. The above experiments showed that it is apparently simpler to relocate an area rather than a single line when making measurements on irregularly shaped bones.

This rectilinear scanner was designed to scan a 15 cm x 15 cm area in a raster pattern with a continuous scanning speed of 2 mm/sec in the "y"-direction and variable stepping increments in the "x"-direction. The system has been built on an aluminum base 25 cm square and has a height of about 40 cm. Its weight is approximately 25 pounds including the table for limb support.

The electronic control apparatus includes an electronic timer, relays, and power supplies. This equipment is enclosed in a metal chassis with dimensions 10 in. x 6 in. x 3.5 in. deep. Interconnections between the control box and the scanner are made through a cable which plugs into a socket on the scanner base.

## LINEAR SCANNING MECHANISM

The reversible, synchronous motor (see Parts List [P.L.] #1) used for scanning has an output shaft speed of 1 rpm and a torque of 100 in-oz. It is equipped with a planetary type clutch actuated by a 115 VAC relay. When the clutch is de-energized, the output shaft is free to rotate, permitting the scanner to be moved manually to any desired position.

The platform to which the source and detector holders are attached, the guide rods and their end supports, and the base plate to which these supports and the scanning motor are mounted will be termed the linear scanning system. Power is transmitted to the

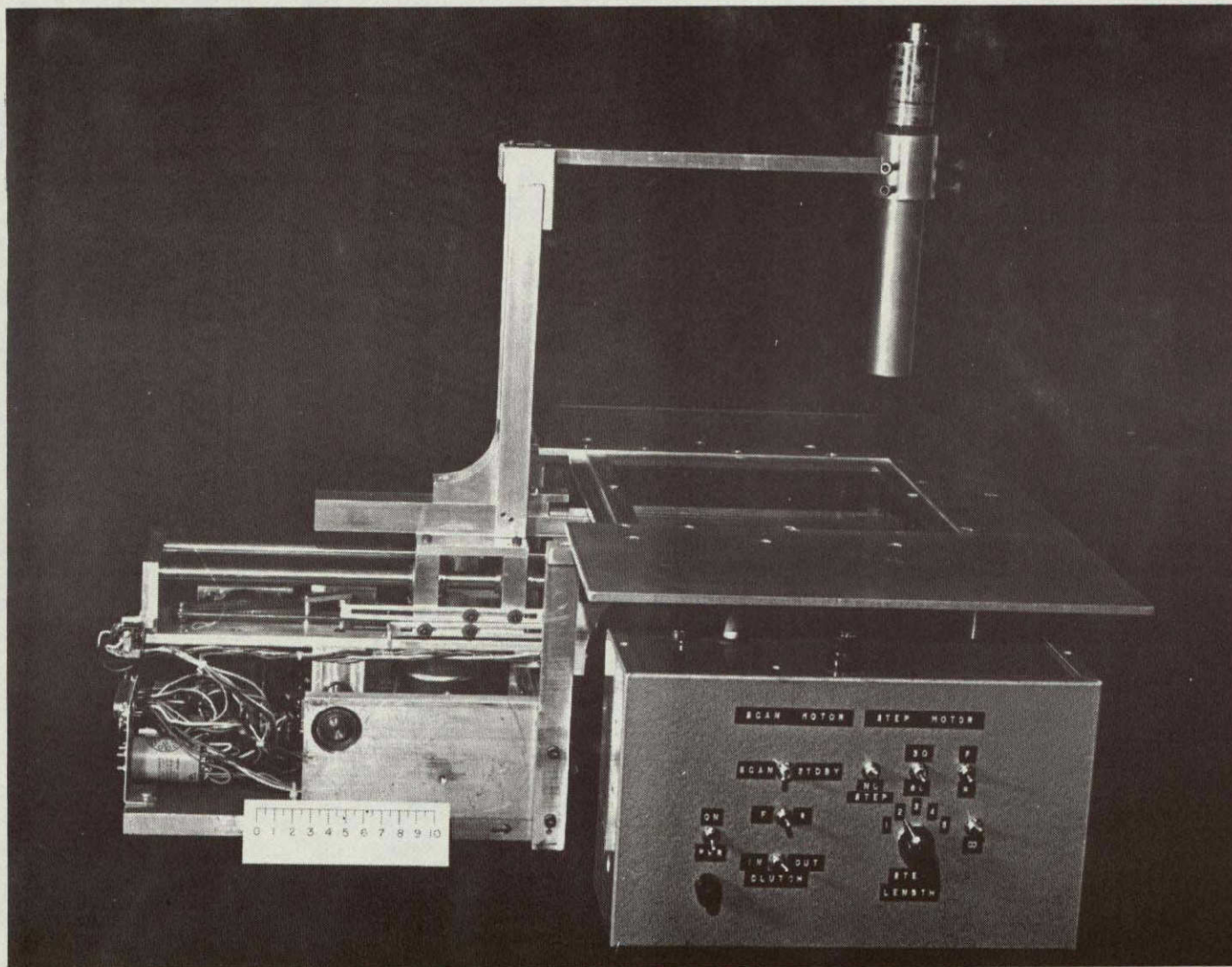


Fig. 1. Photograph of the rectilinear scanner and the control box. The end of scan bumpers on the source and detector platform and the limit switches on the guide-rod end supports can be seen (scale in cm.).

platform carrying the source and detector via a toothed belt attached to the platform and a geared pulley (P.L. #2). The platform, supported by ball bushings, travels along a parallel pair of hardened, stainless steel guide rods (P.L. #3) (Fig. 2). The geared pulley has a pitch diameter of 1.500 in. yielding a theoretical belt speed of 1.995 mm/sec. Measurements of the time elapsed in scanning a 10.00 cm (SD = .06 cm) path yielded scanning speeds of 1.997 mm/sec (SD = .012 mm/sec) in the forward direction and 2.002 mm/sec (SD = .013 mm/sec) in the reverse direction.

The limits of the scan are set at the desired end points by adjusting a pair of bumpers attached to the source and detector platform. These bumpers activate a set of limit switches fastened to the guide-rod end supports (Fig. 1). Depending on the settings selected on the control panel, either the direction of the scanning motor is reversed at the end of the path and the scanner moves back along the same line in the opposite direction or dynamic braking is applied to the scanning motor and the stepping sequence is initiated.

#### STEPPING MECHANISM

With the scanning motor stopped, power is applied to the stepping motor: a reversible, synchronous motor with 30 in-oz of torque and output shaft speeds of 30 or 60 rpm (P.L. #4). The stepping motor remains "on" for a time interval, set on the control panel, ranging from 1.1 to 17.1 seconds. Power is transmitted to a lead screw of 1.25 mm pitch via a toothed belt and a pair of geared pulleys (P.L. #5) (Fig. 3). The lead screw is threaded through a pair of bronze lead nuts attached to the base plate of the linear scanning system (Fig. 2). The rotation of the screw thus indexes the linear scanner by the pre-set distance. The scanning system is supported by the lead screw and a parallel, hardened, stainless steel shaft. The system is borne on the shaft by a ball bushing (P.L. #6). At the completion of the step, dynamic braking is applied to the stepping motor and removed from the scanning motor. The scanner then resumes its motion in the opposite direction.

#### ELECTRONIC CONTROLS

The "on" time of the stepping motor is determined by an electronic timer. A 60 Hz sinusoidal signal is fed to a Schmitt trigger which outputs a 60 Hz square wave. This signal is inputted to the clock of the first of eleven J-K flip-flops (P.L. #7). The Q output of this flip-flop is connected to the clock of the second and so on. Each of the flip-flops outputs a square wave with a period twice that of its input. The outputs of the last five flip-flops yield "on" times of 1.1, 2.1, 4.3, 8.5, and 17.1 seconds. The amplified output operates a relay which disconnects the power from the stepping motor. Dynamic braking is then applied to this motor thereby insuring that the

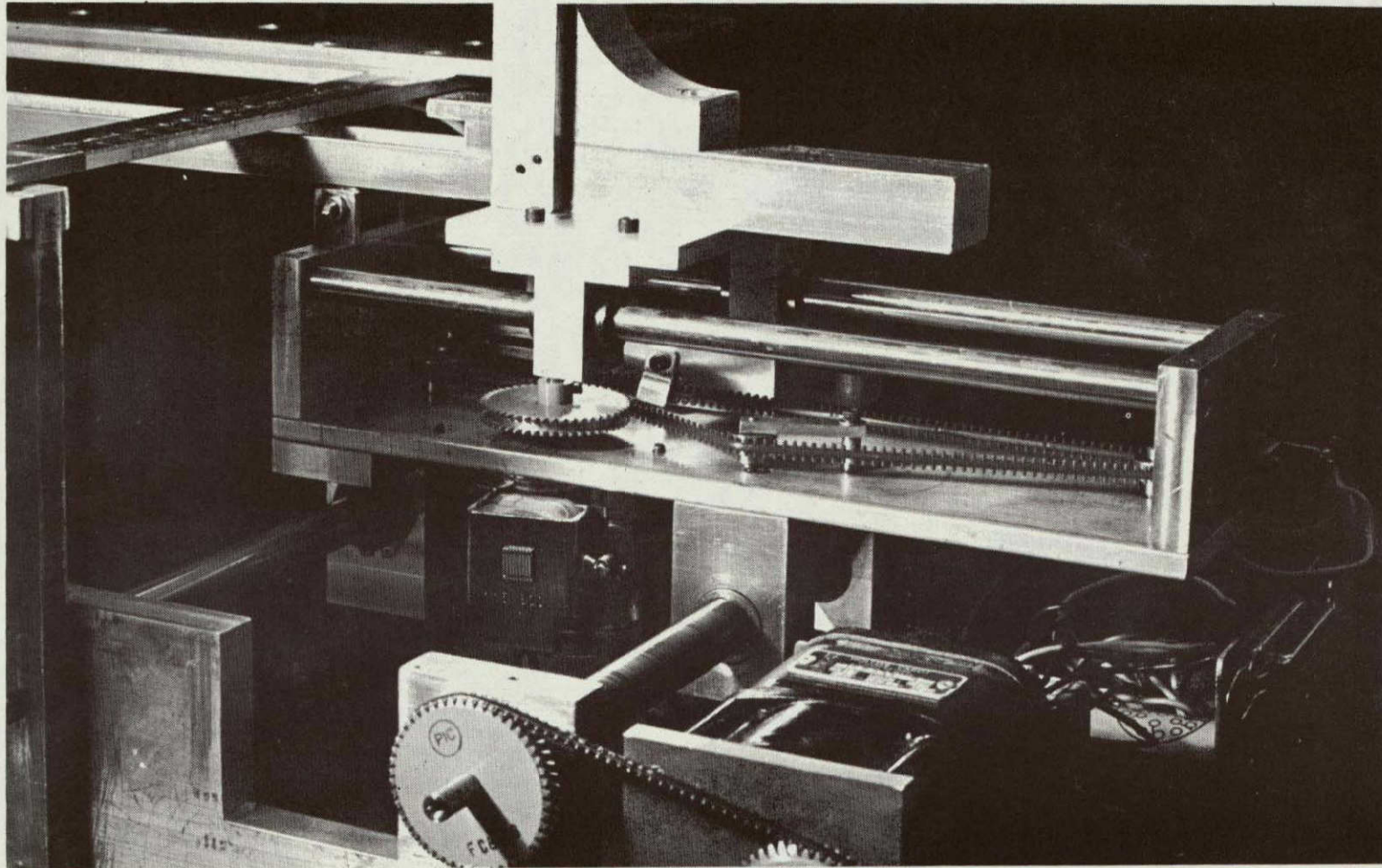


Fig. 2. Photograph of the linear scanning system showing the toothed belt, geared pulley, and guide rods. Also shown are the lead screw and nut used for the stepping motion.

*Gilbert Bond*

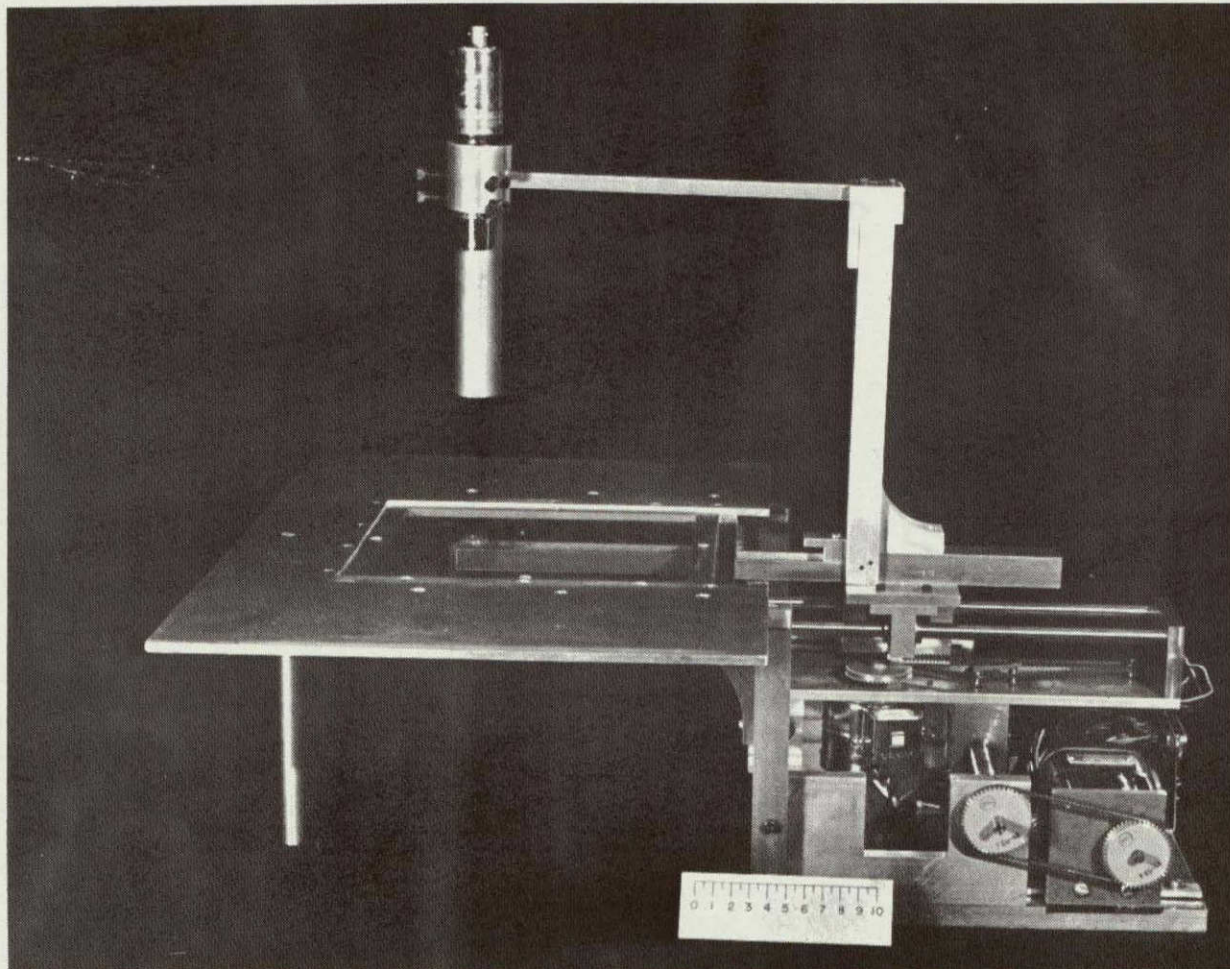


Fig. 3. Shown here are the belt and geared pulleys for transmitting power to the lead and the aluminum table for limb support (scale in cm.).

step terminates without coasting. Stepping can be done in either direction with negligible difference between the length of steps for the two directions (see Table 1). Stepping is done at the 30 rpm speed. The 60 rpm speed is available for slewing to a desired starting position.

The control panel (Fig. 4) is divided into two sections plus the main power switch and neon pilot light. The section labelled "Scan Motor" includes three switches: scan-standby; forward reverse; and clutch, in-out. The "Scan-St'dby" switch supplies either 115 VAC, for scanning, or D.C., for braking, to the scanning motor. With the switch in the "St'dby" position the scanner is rigidly locked in place by the dynamic braking applied to the motor. The "F-R" switch operates a relay for reversing the direction of the scanning motor at any time during a scan. The "Clutch, In-Out" switch controls the relay on the scan motor which operates the clutch on its output shaft. With the clutch out the source and detector platform can be moved manually for easy positioning.

The controls for the step motor include the "No-Step" switch which de-activates the stepping electronics. With this switch in the "No-Step" position, the scanner will reverse at the end of each linear scan without stepping. The "30-60" switch controls a relay which selects either the 30 or 60 rpm speed of the stepping motor. There is also an "F-R" switch for reversing the direction of stepping. Limit switches attached to the linear scanner will also do this automatically when it comes to the end of the lead screw. The switch labelled " $\infty$ " is used to put the stepping motor into the slewing mode for arriving quickly at the desired starting position. Finally, a rotary switch labelled "Step-Length - 1, 2, 3, 4, 5" selects the length of step that the scanner will make at the end of a linear scan. The lengths of the steps are those given in Table 1.

#### PROPOSALS AND CONCLUSIONS

In contrast to the linear scanners made at Wisconsin (2,3) for which the scan path is within the guide-rod end supports the scan path of the rectilinear scanner is totally outside of the scanner mechanism. An aluminum table, 30 cm x 50 cm, has been attached to the scanner for supporting a subject's limb during the scan (Fig. 3). A section of the table-top somewhat greater than the maximum scanning area has been removed and the opening is surrounded by a one half inch wide shelf. It is intended that special holders for scanning the forearm, humerus, or os calcis, etc. will be designed to sit on this shelf and be fastened to the table, thus obviating the need for several special purpose scanners.

We eventually hope to obtain position information by installing linear potentiometers coupled to the scanning and stepping systems. Also suitable logic circuits can be designed to use this information to provide precise electronic settings for the limits of a scan.

Table 1.

<u>Step Number</u>	<u>Theoretical Step Length (mm)</u>	<u>Measured Forward Step Length (mm) <math>\pm</math> S.D.</u>	<u>Measured Reverse Step Length (mm) <math>\pm</math> S.D.</u>
1	0.669	0.715 $\pm$ .069	0.712 $\pm$ .062
2	1.331	1.377 $\pm$ .052	1.378 $\pm$ .051
3	2.669	2.714 $\pm$ .047	2.715 $\pm$ .052
4	5.331	5.37 $\pm$ .10	5.380 $\pm$ .083
5	10.669	10.728 $\pm$ .029	10.739 $\pm$ .037

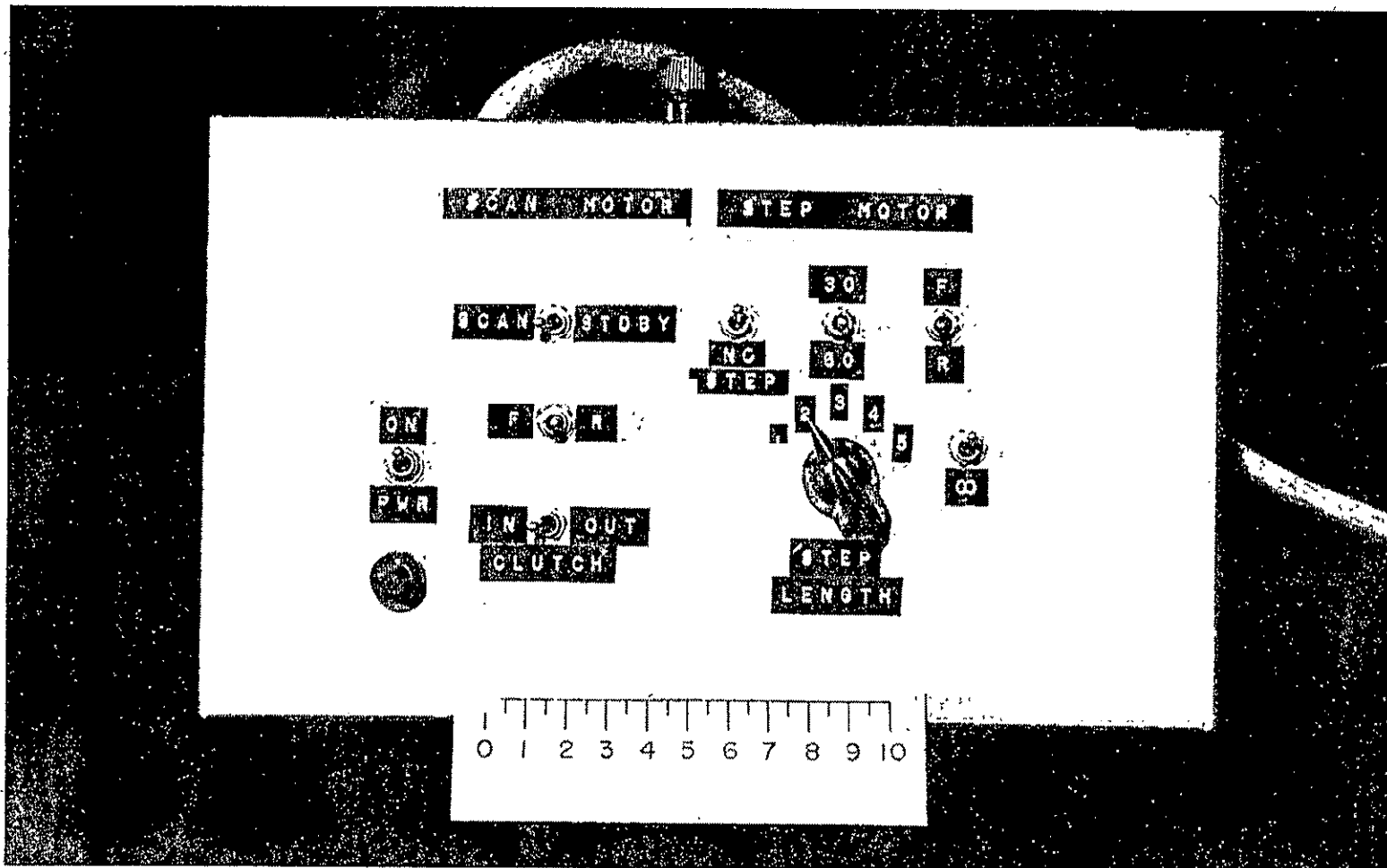


Fig. 4. The control panel used to operate the scanner (scale in cm.).

Because this unit was designed to be versatile it is necessarily larger and heavier than a similar unit which might be designed for a specific application. Considerable savings in weight could be made by replacing the stepping motor with a manually activated stepping device. Various structural components could possibly be made of thinner material, or channeled and tubular elements could be used. A side-on photomultiplier tube and a radiation source mounted on a telescoping, hydraulically activated linear scanner could offer considerable size and weight savings. .

## PARTS LIST

1. Hurst Model AR-DA; 100 in.-oz. @ 1 rpm; Hurst Manufacturing Corp., Princeton, Indiana 47570.
2. Pic No. FA-189 "No-Slip" Positive Drive Belt and No. FC4-48 "No-Slip" Geared Pulley; Pic Design Corporation, P.O. Box 335, Benrus Center, Ridgefield, Conn. 06877.
3. Thomson Solid Stainless Steel 60 Case Hardened and Ground Shafts, 3/8 in. dia. x 10 in. long; and three of Thomson Precision Series A Ball Bushings, 3/8 in. bore, No. A-61014; Thomson Industries Inc., Manhasset, New York 11030.
4. Holtzer-Cabot Ser. No. MF 3810-1; Holtzer-Cabot Corp., Tri-Boro Industrial Park, North Attleboro, Mass. 02760.
5. Pic No. FA-95 "No-Slip" Positive Drive Belt and two of No. FC6-48 "No-Slip" Geared Pulleys (see #2).
6. Thomson Solid Stainless Steel 60 Case Hardened and Ground Shaft, 1/2 in. dia. x 10 in. long; and Thomson Precision Series A Ball Bushing No. A-81420, 1/2 in. bore (see #3).
7. Motorola Integrated Circuit No. MC 723 P; Motorola Inc., Chicago, Ill.

## REFERENCES

1. Sorenson, J.A. and Cameron, J.R. A Reliable In Vivo Measurement of Bone-Mineral Content. The Journal of Bone and Joint Surgery 49: 481 (1967).
2. Judy, P.F., Sadrzadeh-Raffii, A., Cameron, J.R. and Sorenson, J.A. New Bone Mineral Scanners. U.S. Atomic Energy Commission Report COO-1422-10 (August, 1967).
3. Witt, R.M., Sorenson, J.A. and Cameron, J.R. An Improved Linear Bone Mineral Scanner. U.S. Atomic Energy Commission Report COO-1422-40 (August, 1968).

## ACKNOWLEDGEMENT

This work is supported in part by the U.S. Atomic Energy Commission through Contract AT-(11-1)-1422.

DEVELOPMENTS IN THE DICHROMATIC ATTENUATION TECHNIQUE FOR THE  
DETERMINATION OF BONE MINERAL CONTENT IN VIVO

by

Philip F. Judy, Michael G. Ort,  
Kianpour Kianian, and Richard B. Mazess  
Department of Radiology  
University of Wisconsin Medical Center  
Madison, Wisconsin 53706

INTRODUCTION

The modular electronic components used to process and record the data for the dichromatic attenuation technique (DAT) are described in this report. Also, the use of these components in the scanning mode of the DAT is described. Factors affecting the DAT measurement of vertebral bone mineral content are also described. The principles of the DAT were previously reported (Judy and Cameron, 1969; Ort and Cameron, 1970; and Judy, 1971).

EQUIPMENT

The electronic components, listed below, used to collect and process the DAT information are shown in the block diagram of Figure 1. In this figure they have been connected to form a dual channel analyzer. The first seven components of the list were manufactured to Nuclear Instrument Module (NIM) standards.

1. High Voltage Supply  
(ND-537, Nuclear Data<sup>1</sup>)
2. Amplifier  
(ND-520, Nuclear Data<sup>1</sup>)
3. Two Single Channel Analyzers  
(Model 1431, Canberra Industries<sup>2</sup>)
4. Two Scalers with buffers  
(NS-30A, The Harshaw Chemical Company<sup>3</sup>)
5. Timer  
(NT-29, The Harshaw Chemical Company<sup>3</sup>)
6. Parametric Data Module  
(NY-20, The Harshaw Chemical Company<sup>3</sup>)
7. Modular Magnetic Tape Interface  
(NE-25, The Harshaw Chemical Company<sup>3</sup>)

---

1) 100 West Golf Road, Palatine, Ill. 60067

2) 45 Gracey Avenue, Meriden, Connecticut 06450

3) 6801 Cochran Road, Solon, Ohio 44139

8. Magnetic Tape Unit  
(Model 1337-200, Digi-Data Corp.<sup>4</sup>)

9. Bin/Power Supply  
(Model 140D, Canberra Industries<sup>2</sup>)

The computer programs which were used for the point DAT (Ort and Cameron, 1970) and the single photon technique (Sorenson and Cameron, 1967) have been modified to accept magnetic tape input. Figure 2 illustrates this equipment in use.

#### USE OF THE EQUIPMENT IN THE SCANNING MODE OF THE DAT

Gadolinium-153 was used as a source of dichromatic photons. The NaI(Tl) scintillation detector had sufficient energy resolution to separate two photopeaks of the Gd-153 spectrum at 43 keV and 100 keV. The output of the amplifier was fed into both single channel analyzers. In the scanning mode of the DAT the counts of each channel are collected at regular time intervals as the source and detector move at a constant rate over the material of interest. The lower level setting for the 43 keV photopeak was 27 keV and for the 100 keV photopeak was 82 keV. The window for both analyzers was 28 keV. The attenuation of these "beams" has been shown to be sufficiently exponential to be useful for the DAT (Mazess et al., 1970).

The output of each single channel analyzer was fed into a buffered scaler. Both scalers were controlled by a single timer. The counts from the scalers were outputted every 0.6 sec as the scanner moved across the limb or phantom. The scanner used has been described (Witt et al., 1968). Other digital information was put on the magnetic tape by setting the thumb switches of the parametric recorder. Because this system collects data from both channels simultaneously, the radiation dose to the patient is half that which was received using the older system (Ort and Cameron, 1970) which alternated between the two channels.

The results of measurements on a bone phantom constructed of methyl methacrylate and a saturated solution of dipotassium hydrogen phosphate (a solution which closely resembles bone in its attenuation of x-rays, Witt and Cameron, 1969) are shown in Figure 3. The cross section and orientation of the phantom are also indicated. The precision of the sum of individual point measurements across the scan was 3%. The intensity of the Gd-153 was low and these measurements were made at a scan speed slower than is practical for human studies. The preliminary measurements were encouraging and indicated the measurement of bone mineral content of the limbs could be made with this technique, using a source of Gd-153 with an activity greater than 40 mCi.

#### MEASUREMENT OF VERTEBRAL BONE MINERAL CONTENT USING <sup>153</sup>Gd

Dichromatic attenuation measurements of phantoms and excised bones and vertebral bodies in vivo were made. The equipment used for these measurements was described in detail by Ort and Cameron (1970). A specially adapted multi-channel analyzer contained a single channel

---

4) 4315 Baltimore Avenue, Bladensburg, Md. 20710

analyzer whose lower level and window were alternately set, electronically, for the 43 keV photopeak and 100 keV photopeak of Gd-153. The memory of the multi-channel analyzer served as a buffer from which the data was punched into paper tape. The data was then processed by computer.

The mass attenuation coefficients of water, a saturated solution of dipotassium hydrogen phosphate, soybean oil, pressed board and aluminum were determined for the two photopeaks of Gd-153 and are tabulated in Table 1. The mass attenuation coefficients were measured for two beam sizes, 1 x 3 cm and 1 x 1.5 cm (beam size at the level of the attenuators). Within the limits of the experiment, the coefficients measured for each beam size were the same. This suggests that for this range of beam size, there is little variation in these coefficients with beam size.

These materials were used to construct phantoms to evaluate the effects of the position of the bone and the variation of the composition of soft tissue on the determined bone mineral content. Using a phantom of aluminum and pressed board, the dichromatic attenuation determination of the mass of each component was found to be independent of the order in which the sheets of aluminum and pressed board were stacked. DAT point measurements were made on a three component phantom: soybean oil, saturated solution of dipotassium hydrogen phosphate, and water. The amount of soybean oil was varied to simulate the variation of the lipid content of soft tissue. Our results were in agreement with those previously reported by Jacobson (1970). The error introduced by a uniform layer of lipid can be corrected (Roos et al., 1970), however, there is no simple correction for the lipid in the lumen of the bone (Sorenson and Mazess, 1970).

The bone and soft tissue mass of an excised human femur in 6 cm of water were determined using the DAT with Gd-153. In Figure 4 the results of the point by point measurements are shown. The bone mineral content determined differed by 2.5% from results obtained using the scanning monochromatic technique (Sorenson and Cameron, 1967). The vertebral bone mineral mass of two human subjects was measured. The results were encouraging, but because of the low activity of the Gd-153 ( $\sim 30$  mCi) source, and consequently long counting times, only a few points were measured. Using a more active source\* of Gd-153 (200 mCi) and the dual channel analyzer, we hope to make either point by point or continuous scans on human patients in a practical amount of time.

\* On loan from Oak Ridge National Laboratory

## REFERENCES

1. Jacobson, B. Bone Salt Determination by X-ray Spectrophotometry. In: Proceedings of Bone Measurement Conference, J.R. Cameron (Ed.), CONF-700515, USAEC, Division of Technical Information, p. 237, Oak Ridge, Tennessee (1970).
2. Judy, P.F. and Cameron, J.R. A Dichromatic Absorption Method for the Measurement of Bone Mineral Content In Vivo. USAEC Progress Report COO-1422-60 (1969).
3. Judy, P.F. A Dichromatic Attenuation Technique for the In Vivo Determination of Bone Mineral Content. Ph.D. Thesis, University of Wisconsin-Madison, Madison, Wisconsin (1971).
4. Mazess, R.M., Ort, M.G., Judy, P.F., and Mather, W.E. Absorptiometric Bone Mineral Determination Using Gd-153. In: Proceedings of Bone Measurement Conference, J.R. Cameron (Ed.), CONF-700515, USAEC, Division of Technical Information, p. 308, Oak Ridge, Tennessee (1970).
5. Nuclear Instrument Module (NIM) Standards, USAEC Report TID-20893 (Rev).
6. Ort, M.G. and Cameron, J.R. Determination of Vertebral Bone Mineral In Vivo. USAEC Progress Report COO-1422-79 (1970).
7. Roos, B., Rosengren, B., and Sköldbörn, H. Determination of Bone Mineral Content in Lumbar Vertebrae by a Double Gamma-ray Technique. In: Proceedings of Bone Measurement Conference, J.R. Cameron (Ed.), CONF-700515, USAEC, Division of Technical Information, p. 243, Oak Ridge, Tennessee (1970).
8. Sorenson, J.A. and Cameron, J.R. A Reliable In Vivo Measurement of Bone Mineral Content. J. Bone Joint Surg. 49A: 481 (1967).
9. Sorenson, J.A. and Mazess, R.M. Effects of Fat on Bone Mineral Measurements. In: Proceedings of Bone Measurement Conference, J.R. Cameron (Ed.), CONF-700515, USAEC, Division of Technical Information, p. 255, Oak Ridge, Tennessee (1970).
10. Witt, R.M., Sorenson, J.A., and Cameron, J.R. An Improved Bone Mineral Scanner. USAEC Progress Report COO-1422-40 (1968).
11. Witt, R.M. and Cameron, J.R. Bone Standards. USAEC Progress Report COO-1422-42 (1969).

## ACKNOWLEDGEMENT

This work is supported in part by the U.S. Atomic Energy Commission under Contract AT-(11-1)-1422.

Table 1. Experimentally determined mass attenuation coefficients ( $\text{cm}^2/\text{gm}$ ) for Gd-153.

	Low Energy Peak ( $\sim 43\text{keV}$ )	High Energy Peak ( $\sim 100\text{keV}$ )
Water	$0.233 \pm .003$	$0.166 \pm .003$
Pressed board	$0.220 \pm .002$	$0.160 \pm .001$
Saturated Dipotassium Hydrogen Phosphate Solution	$0.530 \pm .005$	$0.176 \pm .003$
Soybean Oil	$0.211 \pm .001$	$0.166 \pm .001$
Aluminum	$0.490 \pm .002$	$0.169 \pm .002$

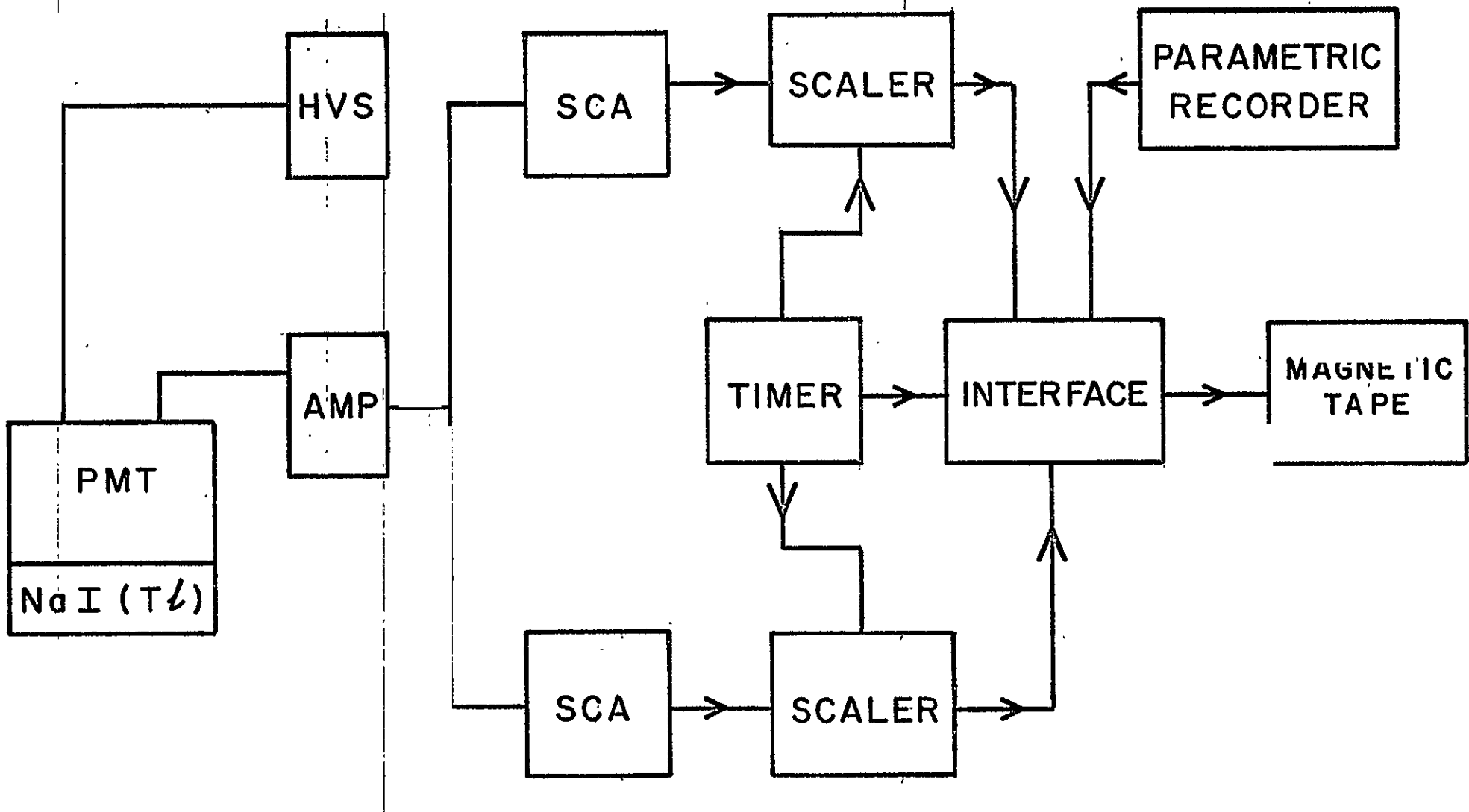


Figure 1. Schematic of the electronic components used for the DAT measurements.

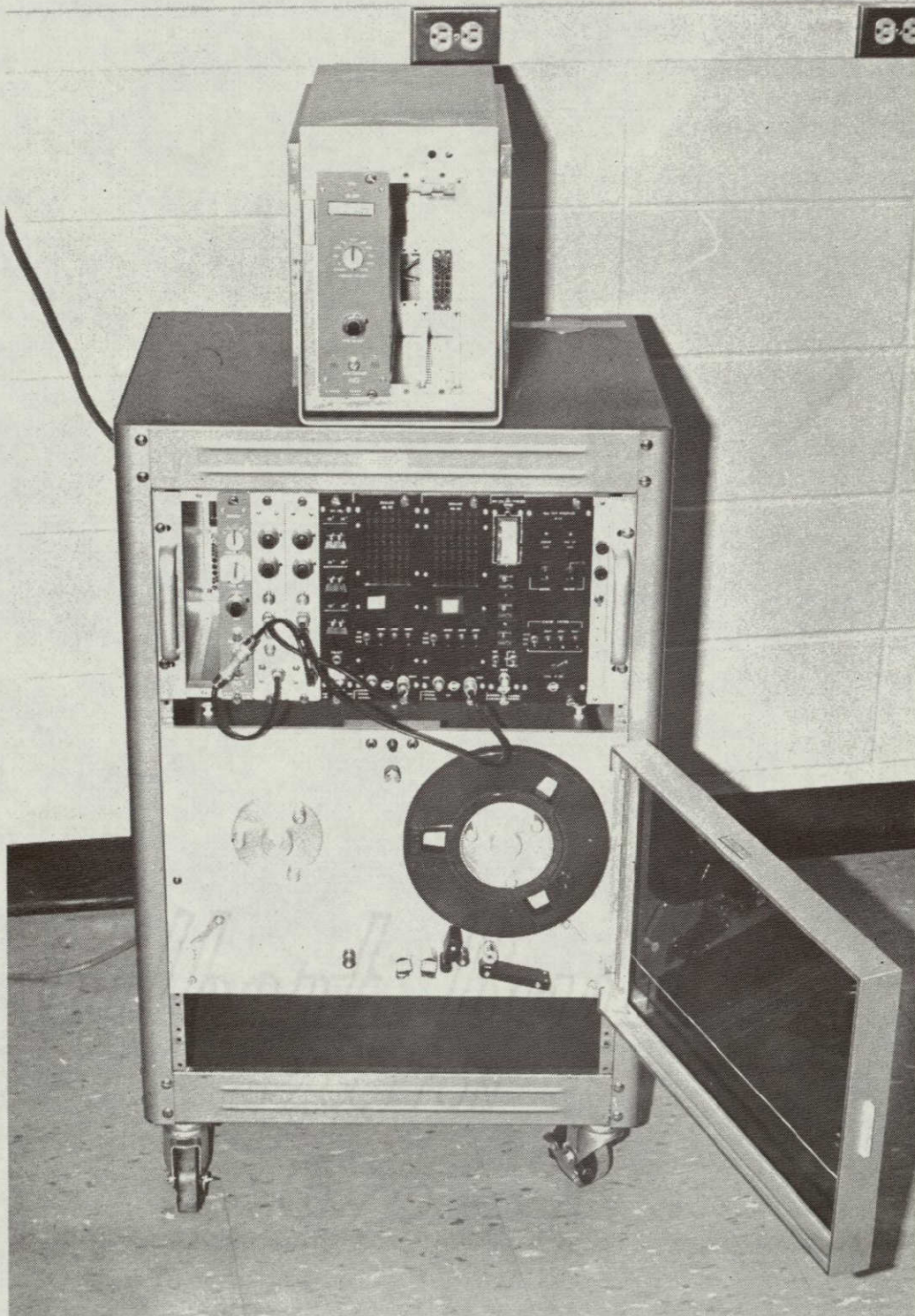


Figure 2. The modular electronic components and the incremental magnetic tape unit of the DAT.

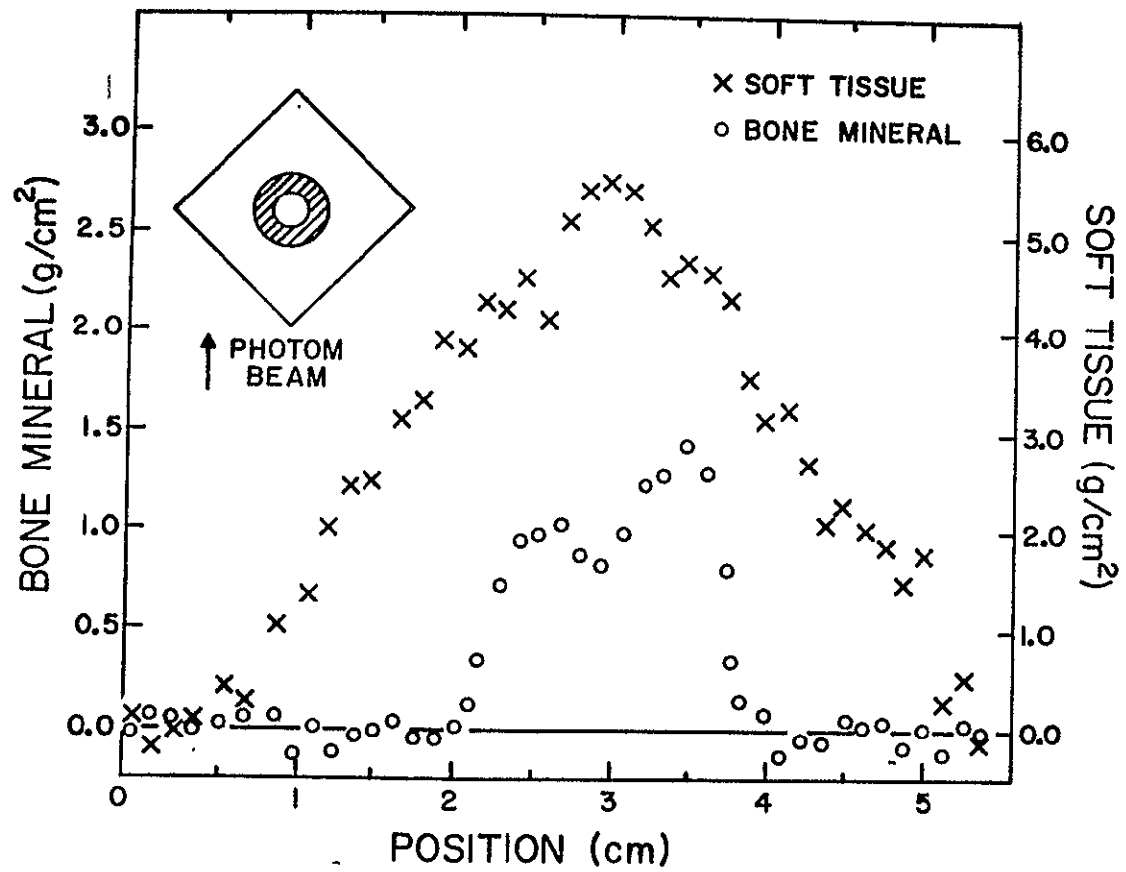


Figure 3. Results of a DAT scan of a phantom with <sup>153</sup>Gd.

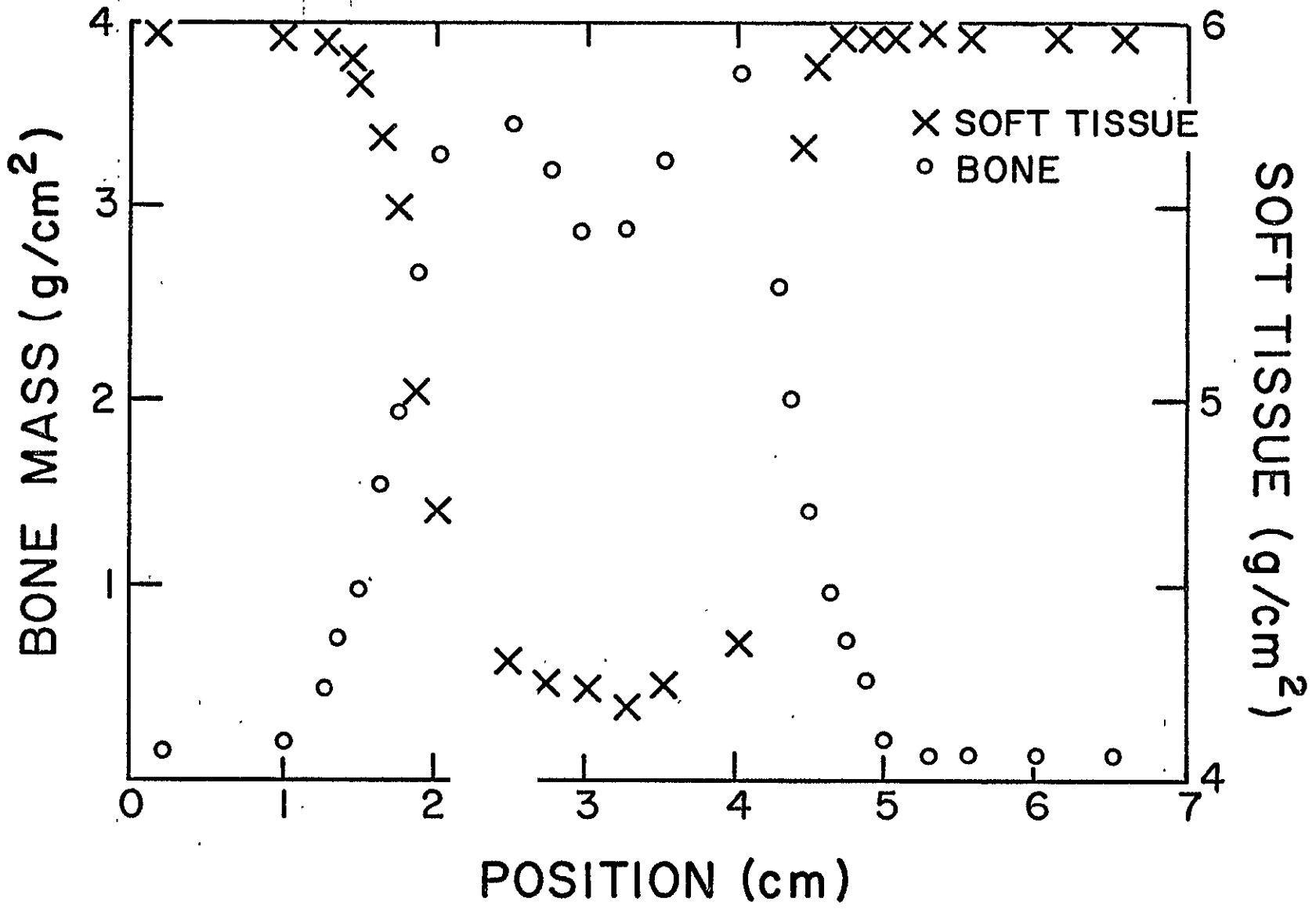


Figure 4. DAT scan using <sup>153</sup>Gd of midshaft of an excised human femur in 6 cm of water.

PRELIMINARY REPORT ON A DUAL PHOTON  
BONE MINERAL MEASURING INSTRUMENT

by

Jerry C. Sitzman\*, Clifford Vought\*\*,  
and Richard B. Mazess\*\*

## SCOPE

This report describes the work accomplished in developing an operating breadboard of a two-channel pulse-height analyzer. This breadboard is to serve as a portion of a demonstration model of a proposed Bone Mineral Measuring Instrument system.

## TECHNICAL DESCRIPTION

The analyzer is very similar to the technical concept originally outlined. The major functional units are a charge amplifier, two level discriminators, and associated 5-decade scalars.

A. Charge Amplifier

The charge amplifier is of conventional design, consisting of a charge loop, single RC-CR pulse shaping network with pole-zero cancellation, and variable gain voltage amplifier. Power required for the charge amplifier is obtained from a  $\pm 12$  v supply.

B. Charge Loop

The loop amplifier is a LM201 linear IC operational amplifier, compensated for stable operation, at zero input stray capacitance, with a 12 pf compensating capacitor. The feedback network provides a loop charge sensitivity of 0.25 v/pc with a 100  $\mu$ s decay time constant.

C. Pulse Shaping Network

The input circuit to the pulse shaping stage provides a "zero" to cancel the 100  $\mu$ s pole response of the charge loop, and differentiates the effective step function input with a 0.5  $\mu$ s time constant. The integrating feedback network produces the desired 0.5  $\mu$ s, shaped pulse response. The gain element of the pulse shaping network is a high-performance CA3015A operational amplifier.

---

\* Space Science and Engineering Center; University of Wisconsin;  
Madison, Wisconsin 53706

\*\* Department of Radiology; University of Wisconsin Medical Center;  
Madison, Wisconsin 53706

#### D. Voltage Amplifier

The voltage amplifier, also utilizing a CA3015A, provides adjustable gain for an overall amplifier gain range of 8v/pc to 1.3 v/pc.

The output dynamic range of the voltage amplifier is 0 to +7v.

#### E. Discriminator

The discriminator resolves the pulse height of the charge amplifier into two channels, or "bins". The upper and lower thresholds of each bin are separately adjustable. Functionally, the discriminator is divided into two functional blocks: the comparators and the comparator logic.

#### F. Comparator

The comparators are constructed on a separate board which is also powered from the  $\pm$  12 volt supply.

The charge amplifier output signal is AC-coupled to the inverting inputs of four differential comparator IC's. It is compared with a threshold voltage set by a potentiometer and resistor divider which is supplied from a reference zener voltage source. The threshold voltage is adjustable from 0 to +4.25 volts.

A second zener regulates the nominal -6v supply required by the comparator IC's.

#### G. Comparator Logic

The comparator logic operates on the comparator output signals to generate pulse outputs to the two scalers according to the Logic Function Table 1. It is assumed that the comparators A through D are set to successively higher levels, so any output state not shown in Table 1 is "illegal".

Comparator Output	"1" indicates comparator switched "0" indicates comparator not switched				
D	0	0	0	0	1
C	0	0	0	1	1
B	0	0	1	1	1
A	0	1	1	1	1
Logic Output	None	Pulse to low channel scaler	None	Pulse to high channel scaler	None

Table 1. Comparator Logic Function

The comparator logic consists of two functionally identical circuits, one of which operates on the A and B comparator outputs, the second on the C and D outputs.

The leading edge of the signal switches comparator A, which triggers MONO A1 and A2 in sequence. The output of A2 is applied through gating to the scaler input, unless the signal is sufficiently large to trigger comparator B and MONO B. In the latter case, the output of MONO A1 is inhibited by the MONO B output, therefore only those signals with a peak amplitude between the comparator A and B thresholds produce a count input to the low channel scaler. Identical operations are performed on the C and D comparator signals to generate the input to the high channel scaler.

#### H. Scalers

Two five-decade scalers accumulate the pulse outputs from the comparator logic. Separate reset lines are provided for each complete scaler.

#### MECHANICAL LAYOUT

The breadboard is constructed on three separate P-type "Vector" breadboards:

Board #1---Charge Amplifier  
Board #2---Comparators  
Board #3---Comparator Logic and Scalers

To aid in trouble-shooting and signal tracing, all integrated circuits are socket-mounted.

#### PERFORMANCE

The system operates to prescribed specifications.

To assure proper performance of the breadboard when packaged, the charge amplifier, including input and output lines, should be electrostatically shielded from all other circuits and wiring.

One input of the comparator logic output gates should be utilized as a scaler input inhibit to assure that the scaler content is static when transferring data to an output display device.

The 6.5  $\mu$ s processing time will result in approximately 30% dead time at a counting rate of 50 KHz. Depending upon data accuracy requirements, it may be necessary to monitor the dead time or event rate, and apply a dead time correction factor.

#### ACKNOWLEDGEMENT

This work is supported in part by the U.S. Atomic Energy Commission through Contract AT-(11-1)-1422.

SPECTRAL DIFFERENCE IN COMMERCIAL  $^{125}\text{I}$  PHOTON SOURCES

by

Robert M. Witt, Richard B. Mazess,  
and John R. Cameron \*\*

## INTRODUCTION

Several factors may alter the attenuation properties and the apparent spectral composition of the I-125 photon sources used in the absorptiometric determination of bone mineral content (BMC). Some of the more important attenuation and spectral altering factors are the presence of a radionuclide contaminant, induced fluorescence radiation, instrumentation shifts, and variations in the beam filtration.

The presence of the radionuclide contaminant I-126 has been previously observed in I-125 (1). It appears in reactor produced I-125 when a neutron is captured by the I-125. The amount of I-126 present is greatest for batch produced I-125 unless it is "aged", and is small (<0.1%) for continuously produced I-125 used in the current commercial sources. This amount of I-126 appears to have no effect on the BMC determinations.

Fluorescence radiation can be induced by I-125 if high atomic number (Z) material such as silver is part of the source or its container. Previous commercial sources (those provided before April, 1969) had the I-125 electroplated on a silver wire. The I-125 decay photons excited the 22 keV silver K x-ray and gave a low energy contribution to the spectrum. However, when the I-125 is electroplated on low Z materials such as charcoal as in the current sources the fluorescence is completely eliminated. Our earlier ion exchange resin bead sources made with polystyrene beads also had no induced fluorescence radiation.

Since the NaI-PMT detector signal passes through a single channel analyzer (SCA), the detection instrumentation is sensitive to gain variations. These gain variations can be caused by changes in the high voltage supply to the photomultiplier tube and/or by changes in the gain of the pulse amplifier. Either or both gain changes shifts the photopeak relative to the fixed SCA lower level-window settings making the detected spectrum appear to have either a higher or lower effective energy. Previous experiments, in which the BMC was measured as a function of the lower level position with a fixed window determined that the BMC will vary with shifts in the gain (2).

The I-125 decay spectrum is not monoenergetic but contains five different energy photons ranging from 27.5 to 35 keV. At these low energies the photoelectric effect is the dominant attenuation process and the attenuation coefficients are rapidly changing with energy.

---

\* Atomic Energy of Canada Limited, Ottawa, I-125 source type G-236.

\*\* Department of Radiology; University of Wisconsin Medical Center; Madison, Wisconsin 53706.

Placing any material over the emission aperture of the I-125 will alter the energy composition of the emitted beam because for the same thickness of material the different photon energies present will be attenuated by different amounts. In general the lower energy photons are attenuated more than the higher energy photons.

The I-125 sources, used for bone mineral content measurements, are selectively filtered with tin which improves the monochromaticity and decreases the effective energy of the emission spectrum (3). Since we first began assembling our resin bead sources, the source output aperture has been covered with a 0.06 mm thick electrolytically pure tin foil. The tin has its K absorption edge at 29.2 keV and therefore, preferentially absorbs the two Te  $K_{\beta}$  x-rays and the 35 keV gamma present in the I-125 spectrum.

From the equation for bone mineral content, one can see that for the same calibration constants or attenuation coefficients increasing the effective photon energy decreases the ratio of  $I_0^*/I_i$ , thereby decreasing the integrated bone mineral content. Decreasing the effective photon energy would increase the ratio of  $I_0^*/I_i$ ,

$$\text{B.M.C.} = K \log(I_0^*/I_i)$$

thereby increasing the bone mineral content. Since our bone mineral content measurements have been made with a 0.06 mm tin filtered source, any decrease in the filter thickness will result in a decreased bone mineral content. Since the measured bone mineral content depends upon the energy composition of the photon spectrum to obtain long term precision in the mineral content measurements, the tin thickness, hence the effective filtration, must remain constant. Recently we have observed variations in the tin filter thickness of commercial I-125 photon sources by observing a reduction of the bone mineral content of our  $K_2HPO_4$  polymethacrylate block standards (4).

#### METHODS AND RESULTS

These first observations of lower bone mineral content could also have been due to incorrect equipment settings or a constant source of background counts, possibly due to a radionuclide contaminant. Additional intercomparison scans with older sources at constant equipment settings eliminated the possibility of errors in the equipment settings. The lack of any unusually high background count plus the observation that the effect did not change with time eliminated the possibility that the sources contained a radionuclide contaminant. Therefore the decrease in bone mineral content was apparently due to a decrease in the source filtration.

This decrease in effective filtration could have been due to either or both of the following: a "change" in the effective filtration of the aluminum source capsule and/or a decrease in the tin foil thickness. To test possible differences in source capsules a suspected

deviant source capsule was placed in a brass holder from an old source and filtered with the filter from the old source holder. Scans of the  $K_2HPO_4$  standard with this source capsule-holder-filter combination gave results comparable with results obtained with correctly filtered sources (Table 1). The effective capsule filtrations were apparently the same. Next we placed the deviant source capsule in its original brass holder, but replaced its original filter with a filter cut from our tin stock (this is the same tin stock used to filter all our home-built sources). Now the scans of the  $K_2HPO_4$  standard agreed with the long term average values for the standard (Table 1).

To further demonstrate that the problem was due to insufficient tin filtration, the standard was scanned with another underfiltered source where additional amounts of .001-inch tin attenuators were placed between the source and the standard. The bone mineral content of the standard was plotted as a function of the tin thickness (Figure 1).

This source had two company supplied tin filters. The total initial thickness of tin on the source was estimated to be .0012-inch, which was twice the thickness of a single filter. The thickness of a single filter was estimated by assuming the filter was a disc with a cross sectional area,  $A$ , thickness,  $t$ , mass,  $m$ , and density,  $\rho$ . By measuring the mass and cross sectional area, and assuming the density is constant, one can calculate the thickness of the disc.

Adding the extra tin caused the bone mineral content to quickly reach the expected average value. Again when the tin filter was replaced with tin from our stock, the values for the standard agreed with the long term average values.

Since tin changes the spectral composition of the I-125 energy spectrum, sources with less tin filtration should have a different spectral composition which is characterized by a higher effective energy or a lower effective attenuation coefficient.

One way to determine the spectral composition of a radiation source is to precisely measure its attenuation or absorption in some pure material. To test for spectral composition differences between correctly and incorrectly filtered I-125 sources, transmission measurements were made through copper foils .002-inch thick and lead foils .038-mm thick. These measurements were made with our clinical scanning system during the past year for each new source. The source-detector geometry of this system which had a source aperture of 2.3 mm, a detector aperture of 3.2 mm, and a source-to-detector distance of 173 mm could be considered representative for all the measurements. Count rates were either corrected for count loss or else kept below 10,000 per second to minimize count loss errors. The data was not corrected for background which was typically 0.5 counts per second for the 3-mm thick x 0.5-in. diameter NaI(Tl) detector.

The natural logarithms of the ratio of the attenuated and the unattenuated count rates were plotted as a function of the foil

thickness for six different commercial I-125 sources; two sources were attenuated with copper and four were attenuated with lead. The slope of each plot was estimated from a straight-line regression analysis. These estimated slopes which are the effective attenuation coefficients for the different sources are listed in Table 2. For each material and source the slopes were tested by a parallel straight line test to determine if the slopes for the underfiltered sources were significantly different than the slopes for the correctly filtered sources. With copper as the attenuating material, the slopes were not significantly different (Table 3). In fact, further statistical testing demonstrated that the regression lines were identical. However, with lead as the attenuating material, the slopes for the two correctly filtered sources were significantly different from the slopes for each of the two underfiltered sources (Table 3). The two sources which had insufficient tin filtration had a lower effective attenuation coefficient, implying that the beam had a higher effective energy.

#### DISCUSSION

The observations of low bone mineral content of the standard and the significantly lower effective attenuation coefficient for lead both agree with the hypothesis that these sources had insufficient tin filtration. This hypothesis was further confirmed when the B.M.C. of the standard approached its expected value after placing additional tin over the source aperture of an underfiltered source.

Provided that the change in B.M.C. is due only to spectral changes in the photon sources, careful comparison measurements of the  $K_2HPO_4$  standard can detect these differences between sources. Although the observed changes in B.M.C. of the standard can be large ( $\sim 6\%$ ), making judgements about spectral changes from scan measurements alone is still achieved by the process of elimination. One would prefer a more direct determination of the spectrum by spectrometry techniques. Most laboratories (including ours) lack the high resolution detectors (e.g., Si(Li)) necessary to observe these small spectral changes.

An alternative method to determine the energy spectrum of the I-125 sources is the attenuation technique. In general, the data are not precise enough to resolve the attenuation curve into a sum of exponential lines, one for each of the energies present in the beam. However, one can fit the data to a straight line and obtain an effective attenuation coefficient. Even though there are only small spectral differences between a correctly and incorrectly filtered source, small and significant differences in effective attenuation coefficients could be demonstrated for material with a high atomic number,  $Z$ , such as lead ( $Z = 82$ ), while attenuation of the same sources by copper ( $Z = 29$ ) showed no significant differences between the effective attenuation coefficients.

## CONCLUSION

We have observed variations in the thickness of the tin filters in commercially available I-125 photon sources. Discussions with the manufacturer have revealed that the problem appeared due to a misunderstanding about the need for a constant tin filtration of the I-125 beam and inadequate quality control governing the thickness of the tin filter. In order to allow intercomparison of the data from all laboratories performing bone absorptiometric measurements with I-125 photon sources, all sources must have the same spectral characteristics and these spectral characteristics are controlled primarily by the thickness of the tin filter. The company intends to solve the problem by providing all users with a tin filter window which would be placed over the source holder. The separate tin window would be retained by the user and placed on each subsequent new source (5).

## REFERENCES

1. Judy, P.F., Cameron, J.R., and Sorenson, J.A. Effect on the measurement of bone mineral of I-126 contamination of I-125, USAEC Report COO-1422-12 (1966).
2. Cameron, J.R. Factors affecting the measurement of bone mineral content by the direct photon absorption technique, USAEC Report COO-1422-4 (1965).
3. Sorenson, J.A. and Cameron, J.R., A reliable in vivo measurement of bone mineral content. J. Bone Joint Surg. 49-A: 481 (1967).
4. Witt, R.M., Mazess, R.B., and Cameron, J.R. Standardization of bone mineral measurements, USAEC CONF-700515, 303 (1970).
5. Jackson, B.J. Private communication.

## ACKNOWLEDGEMENT

This work is supported in part by the U.S. Atomic Energy Commission through Contract AT-(11-1)-1422.

Table 1. A comparison of the bone mineral content of the  $K_2HPO_4$  standards determined with sources having different capsule-holder-filter source combinations and with the same source filtered with UW tin.

<u>Source-capsule</u>	<u>Source holder</u>	<u>Filter</u>	Ratio $\frac{\text{B.M.C. Test Sources}}{\text{B.M.C. Control (UW filter)}}$
D	D	D	.938
D	F	F	.994
D	D	UW	1.000
C	C	UW	1.009
C	C	UW	1.006

Table 2. The slopes of the attenuation curves estimated from a straight-line regression analysis.

<u>Source</u> <u>Source</u>	<u>Attenuating</u> <u>Material</u>	<u>Slopes (Effective Attenuation Coefficients)</u>		
		$\text{layer}^{-1}$	$\text{cm}^{-1}$	$\text{cm}^2/\text{g}$
A	Pb	1.28	336.2	29.6
B	Pb	1.28	336.1	29.6
C	Pb	1.13	297.6	26.2
D	Pb	1.13	295.4	26.0
E	Cu	0.578	113.7	12.7
F	Cu	0.575	113.2	12.7

Table 3. A comparison of regression lines of the natural logarithm of the fractional transmission verses the number of copper or lead attenuators. Sources A, B, and F correctly filtered. Sources C, D, and E underfiltered.

<u>Sources Compared</u>	<u>Attenuating Material</u>	<u>t value</u>	<u>Significance Level</u>
A, C	Pb	3.99	.002
A, D	Pb	2.47	.05
B, C	Pb	5.83	.002
B, D	Pb	3.12	.01
E, F	Cu	0.273	----

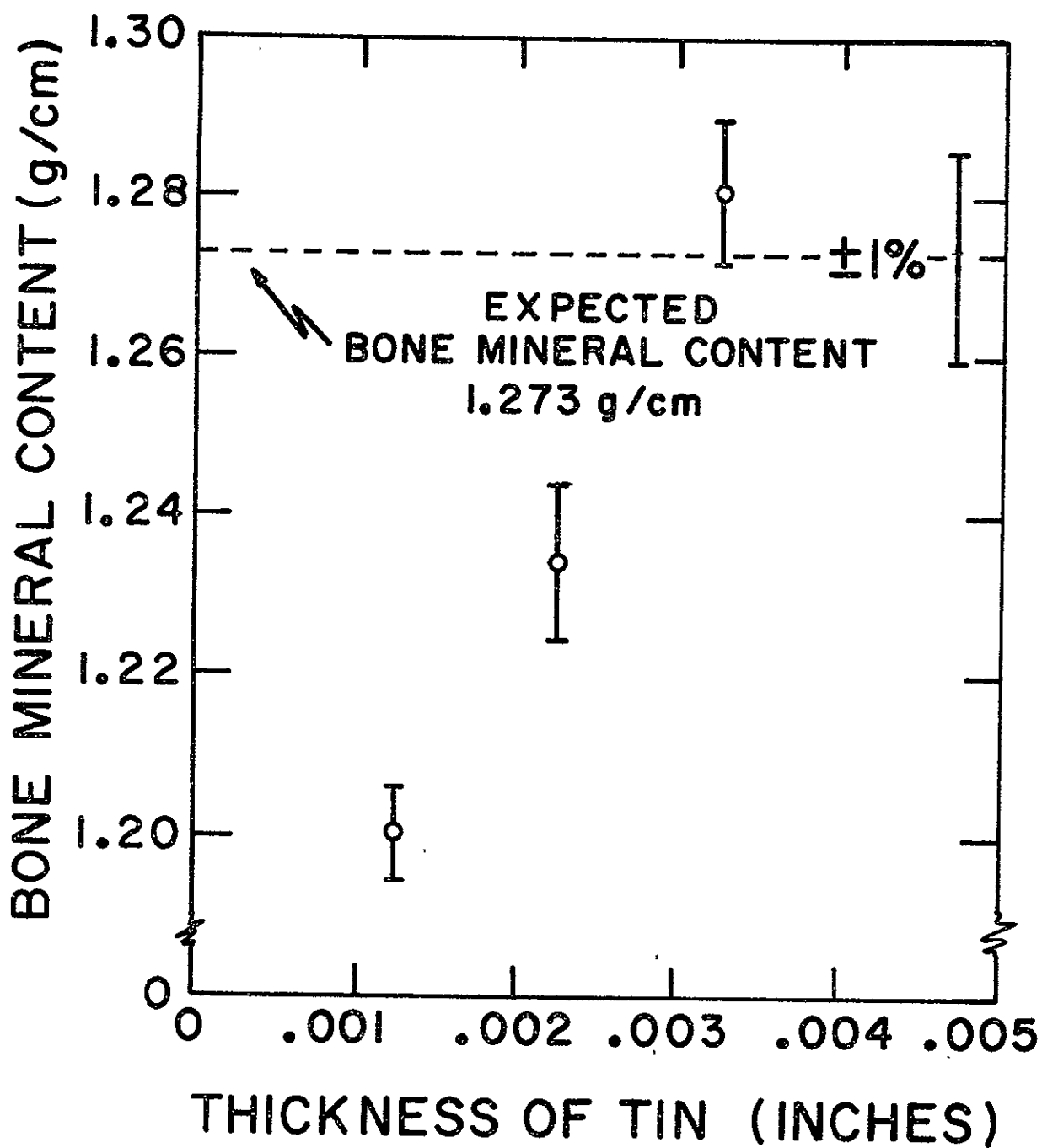


Figure 1. The bone mineral content of the large chamber of the 3-chamber  $K_2HPO_4$  standard as a function of the thickness of the tin filtration on a commercial I-125 photon source. The dashed line indicates the expected value of the bone mineral content for this chamber measured with a correctly filtered source.

A DIRECT DIGITAL READOUT SYSTEM FOR MEASUREMENT OF  
BONE MINERAL CONTENT USING PHOTON ABSORPTIOMETRY

by

Richard B. Mazess\*, John R. Cameron\*,  
and Harry Miller\*\*

Previous reports have described the system developed for giving an immediate direct digital readout of bone mineral and bone width (Mazess and Cameron, 1968, 1969; Mazess et al, 1970). The unit is designed for input from a conventional single channel analyzer, and cost of components and construction is about \$2000. A block diagram (Figure 1) and schematic of this unit are included with this report. One such unit has been in use in our laboratory for research purposes and field studies for the past 30 months. Another unit has been used for clinical measurements for about 9 months. In addition, three units have been constructed for other laboratories. The only difficulties encountered so far with these instruments have been the persistent failures of the commercial digital panel meters (API Instrument Co.) and occasional failures of the commercial power supplies (Analog Devices).

## RESULTS

A. Measurements of Standard

Measurements were made of a standard having three chambers containing dipotassium hydrogen phosphate solution over a five month period with the direct readout device. During this period four different sources of I-125 were used. Generally measurements of the standard were made twice a day: once in the morning and again in the afternoon. The coefficients of variation obtained with four different sources are given in Table 1.

Changing sources had no systematic effect on the mean values of bone mineral and bone width, nor did it affect the coefficients of variation for bone mineral content. There seemed to be some effect on bone width, which suggested that the source may have been loose within its container in some cases. The mean coefficient of variation for bone mineral was between 1 to 2%, and for bone width it was 0.5 to 1%. These results were obtained with an  $I_0^*$  between 1000 and 7000 cps. The variability associated with the sources was on the order of that associated with scanning per se.

---

\* Department of Radiology; University of Wisconsin Medical Center; Madison, Wisconsin 53706.

\*\* Instrumentation Systems Center; Madison, Wisconsin.

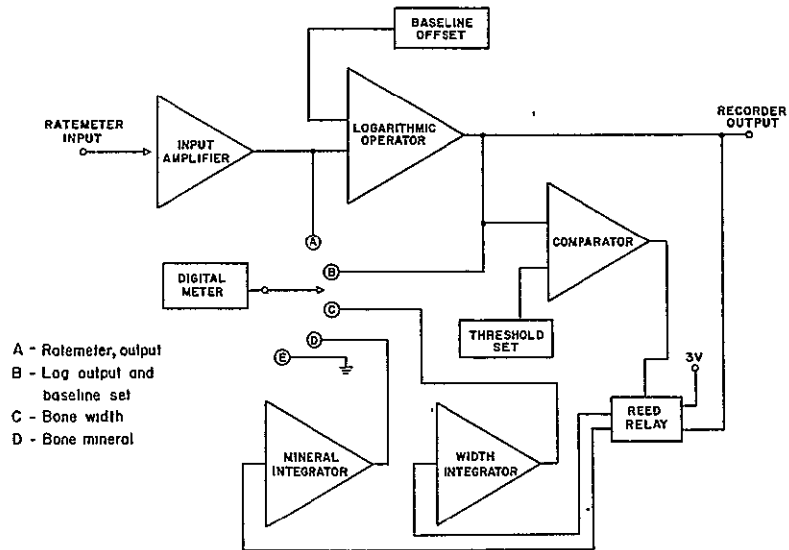


Figure 1a. Block diagram of log converter-integrator device.

Figure 1b. (Following page) Schematic diagram of ratemeter-log converter-integrator unit.



B. Comparison of Direct Readout and Line Printer

Over a period of several months 61 patients were scanned with our clinical bone measuring system and the scan output data was simultaneously recorded by the digital line printer and integrated by the direct readout unit. Each patient was scanned at the mid-shaft and the distal portions of both the radius and the ulna. The bone mineral content was calculated from the digital line printer records of the scaler output and compared to the directly integrated digital readout.

The mean values obtained by the two techniques were virtually identical; there were very high correlations between the techniques and the standard errors of the estimates were low.

Table 2. Comparison of direct readout (DR) and line printer (LP) results on patients.

		RADIUS (n= 102)		ULNA (n= 102)	
		<u>Mineral</u>	<u>Width</u>	<u>Mineral</u>	<u>Width</u>
MEANS	(LP)	.984	1.598	.684	1.052
	(DR)	.978	1.595	.689	1.048
CORRELATION		0.996	0.990	0.997	0.966
S.E.E. (%)		2.8%	3.7%	3.5%	4.7%

The error in predicting bone mineral from one technique to the other was about 3% while the error for predicting bone width was about 4%. It is likely that the error is associated largely with the less reliable line printer technique, and that the direct readout values actually are correct. Our studies on phantoms indicate that the direct readout device has a precision of about 0.5 to 1.0%, and an accuracy of prediction of about 1%.

## REFERENCES

1. Mazess, R.B. and Cameron, J.R. A portable scanning system with direct digital readout for absorptiometric determination of bone mineral content. USAEC Progress Report COO-1422-39 (1968).
2. Mazess, R.B. and Cameron, J.R. A portable unit for determination of bone mineral content by photon absorptiometry. USAEC Progress Report COO-1422-56 (1969).
3. Mazess, R.B., Cameron, J.R., and Miller, H. Preliminary report on a direct digital readout system for absorptiometric determination of bone mineral content. In: J.R. Cameron (ed) - Proc. Bone Measurement Conference, U.S.A.E.C. CONF-700515, CFSTI U.S. Dept. of Commerce, Springfield, Va. (1970) (also USAEC Progress Report COO-1422-69, 1970).

## ACKNOWLEDGEMENT

This work is supported in part by the U.S. Atomic Energy Commission through Contract AT-(11-1)-1422.

COEFFICIENTS OF VARIATION

Source No	STANDARD CHAMBER								
	N	Small BMC	W	N	Medium BMC	W	N	Large BMC	W
97	36	2.0	1.3	71	1.2	1.6	36	0.9	0.5
116	33	1.6	0.9	78	1.2	1.1	33	0.8	0.4
132	15	2.1	0.6	54	1.1	0.6	16	0.9	0.3
153	38	1.1	0.8	132	0.9	0.6	40	0.7	0.5
All	122	2.1	1.1	335	1.2	1.1	125	1.0	0.4
Mean	4	1.7	0.9	4	1.1	0.9	4	0.8	0.4

Table 1. Coefficients of variation for multiple scans of 3-step 3 chamber standard made with 4 different I-125 sources during 5 months from Jan. 1971 to May 1971. The additional scans for the medium size chamber include scans made of the standard after each patient.

BONE MINERAL IN ELDERLY WOMEN  
TREATED WITH FLUORIDES: PRELIMINARY REPORT &

by

Richard B. Mazess\*, John M. Jurist\*\*\*  
and Hugh Hickey\*\*

A group of elderly nuns received 50 mg daily fluoride, in addition to a vitamin supplement, while a control group received the vitamin supplement alone. Bone mineral measurements were made on both the fluoride and control group over a year period. Measurements were made on the radius and ulna, at both midshaft and distal sites. The results are outlined in Tables 1 and 2, showing the ratio of bone mineral in controls vs. fluoride treated.

Table 1. FLUORIDE TREATED NUNS

RATIO: CONTROLS/FLUORIDE for mineral/width

	<u>MIDSHAFT</u>	<u>DISTAL</u>	<u>BOTH</u>
Sept. '69	0.976	1.014	0.995
Jan. '70	0.978	1.050	1.014
June '70	0.948	0.998	0.973
Oct. '70	0.966	1.040	1.003

The average for both sites for the three occasions during treatment was 0.997 vs the original value of 0.995.

Table 2. FLUORIDE TREATED NUNS

RATIO: CONTROLS/FLUORIDE for bone mineral

	<u>MIDSHAFT</u>	<u>DISTAL</u>	<u>BOTH</u>
Sept. '69	0.975	1.005	0.988
Jan. '70	0.970	1.023	0.992
June '70	0.944	1.010	0.972
Oct. '70	0.968	1.002	0.982

There appears to be about a 1.3% greater loss in the control group than in the fluoride treated.

There was no apparent change of bone mineral in the fluoride group relative to the control group over the year period. However, the analysis is as yet incomplete. Many of the nuns included in the "fluoride" group actually terminated treatment due to adverse side effects yet were included in this analysis. Also, the data have not been analyzed in terms of individual changes to ascertain rates of loss in both groups. Following a final measurement in July 1971 a more complete analysis of the data will be done.

---

\* Department of Radiology; University of Wisconsin Medical Center; Madison, Wisconsin 53706.

\*\* Wisconsin Medical College; Department of Orthopedics; Milwaukee, Wisconsin.

\*\*\* Department of Surgery; University of Wisconsin Medical Center; Madison, Wisconsin 53706.

& Supported in part by the U.S. Atomic Energy Commission under Contract AT-(11-1)-1422.

PRELIMINARY REPORT ON A CALIPER  
FOR MEASURING TISSUE COMPOSITION  
BY RADIONUCLIDE ABSORPTION

by

Richard B. Mazess and John R. Cameron  
Department of Radiology  
University of Wisconsin Medical Center  
Madison, Wisconsin 53706

The relative lipid-lean content of subcutaneous adipose tissue, or even the water content of cutaneous tissue, could be determined in vivo by absorption measurements at two discrete energies. If the thickness of the tissue were known, then measurements would be needed at only a single energy since the linear absorption coefficient would change with composition. In order to make such determinations we have modified a Harpenden skinfold caliper; this caliper permits accurate measurements of tissue thickness with a constant tension on the tissue. A pinch of subcutaneous adipose tissue is picked up between the fingers and the caliper applied. A scintillation detector is located on one side of the tissue and a radionuclide source on the other. The signal goes to a single channel analyzer and scaler.

Initially a head-on PM tube (RCA 4516) was used with a right angle scintillation crystal assembly, but a side window tube (RCA 8571) has also been used. The detector assembly is mounted to the fixed arm of the caliper. Our first experiments were done with the source mounted directly on the opposing jaw. However, the problems with geometry and with varying count rate were large. The source is now coupled directly to the fixed arm of the caliper thus minimizing geometric problems (Figure 1). The opposing jaw is slotted, and covered with a thin lucite plate, to allow transmission of the beam. We have done experiments with this system using both single (I-125 at 28 keV) and dual (Cd-109 at 22 and 88 keV) energy sources. Reliability of such measurements is far higher than the reliability of skinfold measurements alone, and the method may be useful in relation to problems of obesity and malnutrition.

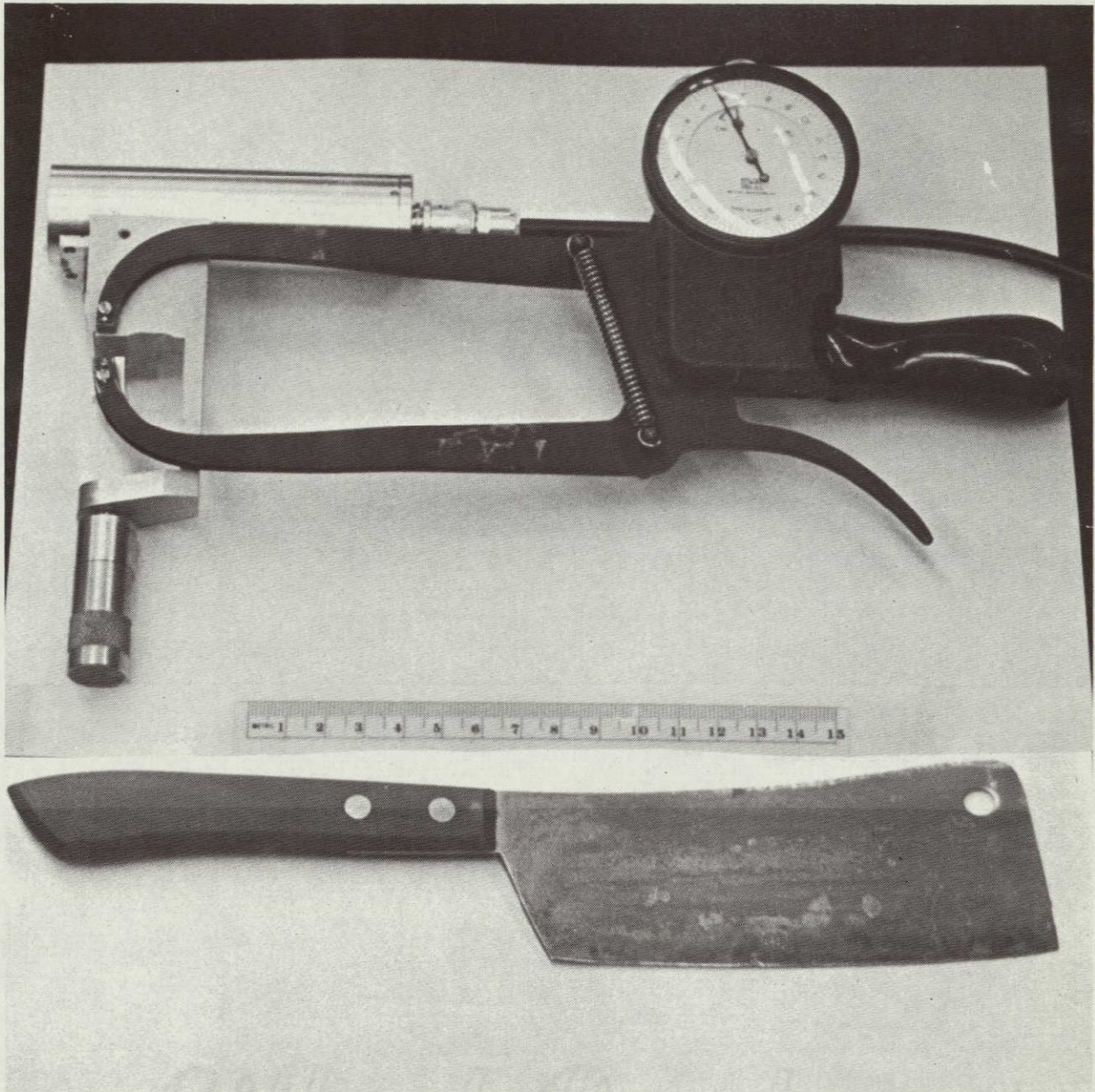


Figure 1. (UPPER)- New caliper for measuring soft tissue composition by absorptiometry, with source at bottom and PM tube at top of the jaws; (LOWER)- Old style device for sampling soft tissue prior to chemical analysis.

BONE MINERAL CONTENT OF THE ESKIMOS  
OF POINT HOPE AND BARROW: PRELIMINARY REPORT

by

Warren E. Mather and Richard B. Mazess  
Department of Radiology  
University of Wisconsin Medical Center  
Madison, Wisconsin 53706

Direct photon absorptiometry was used to determine the bone mineral content of Eskimo natives of the north coast of Alaska during the summers of 1968-1970. This is a preliminary report of measurements of the bone mineral content of the inhabitants of Point Hope and Barrow, Alaska collected in 1970. Measurements made in Wainwright, Alaska have been previously reported (Mazess, 1968; Mazess, 1970).

#### METHODS

Bone mineral content on two sites of both the radius and ulna was determined by the method of direct photon absorptiometry developed at the University of Wisconsin (Cameron and Sorenson, 1963; Cameron et al., 1968; Sorenson and Cameron, 1967). The Point Hope and Barrow measurements were made with a portable system allowing immediate digital readout of bone mineral content and bone width (Mazess and Cameron, 1969). Calibration of absorptiometric scans of the radius and ulna using an I-125 source (28 keV) was made with a 3-chambered bone phantom of saturated dipotassium hydrogen phosphate solution (Witt et al., 1970).

Measurements of 61 elderly subjects were made at Barrow. There were 26 males and 35 females age 40 to 89. At Point Hope a total of 188 subjects were measured: 117 children age 5 to 19, 43 adult females and 28 adult males. As in Wainwright the average of 4 determinations was taken at each site. The coefficient of variation of the determination at each site was 2 to 4%, decreasing with larger bone size and older subjects. A high correlation ( $r \approx 0.80$ ) was found between the coefficient of variation of mineral and width measurements on children indicating systematic variation due to subject movement.

Table 1 gives results of measurements of the 3-chambered bone phantom in Alaska and in Madison. Mean values differed in the field from those obtained in the laboratory, presumably due to the less than reliable line frequency produced by the small village generators. The ratio of bone mineral divided by bone width was identical in Point Hope and in Barrow for all 3 chambers of the phantom, and the Alaska ratios were systematically about 0.02 units higher than the Madison ratios for the 3 chambers. The mean integral values of the bone phantom as measured in each of the villages were used to calculate separate regression equations in order to obtain the bone mineral content in gram/centimeter of the subjects studied. For the scans performed on the bone phantom there was a tendency for the coefficients of variation

of the mineral and width values (coefficient of variation per occasion) to be higher in Alaska than in the Madison laboratory. The coefficients of variation of the mean mineral and width values determined at each occasion (coefficient of variation among occasions) were higher at Barrow than in Madison and 3-6 times larger at Point Hope. This reflected the fluctuation in line frequency: at Barrow measurements were done in the hospital with a generator independent from village use; in Point Hope the generator was more subject to line frequency fluctuation from usage by the entire village.

Measurements of adults (age 20-49) and elderly (age  $\geq 50$ ) from Point Hope and Barrow were pooled after t-tests revealed no significant differences in the bone mineral content, bone width, mineral to width ratio, height, and weight of any of the age and sex groups except the bone mineral content of females 50 to 59.

## RESULTS

Table 2 gives heights and weights of Eskimos measured in Point Hope and Barrow and U.S. whites measured at the University of Wisconsin Bone Mineral Clinic over the past several years (Cameron, 1969). Eskimo children, adults, and elderly of both sexes appeared to have comparable weights but shorter stature. Determinations of bone mineral content, bone width and mineral to width ratio are presented in Table 3.

The bone mineral of Point Hope Eskimo children appeared somewhat reduced from that of whites until about age 20 when they were similar. Adjustment for bone width and stature would make Eskimo children normal with respect to U.S. whites.

At Point Hope male and female Eskimo adults age 20-49 did not demonstrate an increase in bone mineral past age 19 whereas white females and males increased 5 and 10%. However the sample of adult males was rather small and may not be representative; for example, the average weight of this group was 10% less than 17-19 year olds.

Eskimo elderly, both males and females, apparently lost bone mineral at a faster rate than whites. Female Eskimo 60-69 and over 70 had 15 and 28% less mineral than whites of comparable age; 62% of the female Eskimos were below the 0.70 gram/centimeter bone mineral content level associated with a high rate of fracture (Mazess, 1970).

## DISCUSSION AND CONCLUSIONS

The bone mineral content of Eskimos at Point Hope and Barrow showed the same sort of pattern as found earlier at Wainwright. Children followed a course of mineralization similar to whites; adults (with possible errors associated with small sample size) had slightly lower mineral values than whites, and elderly Eskimos, especially females, had a much lower mineral content.

A final evaluation of the skeletal status of the northern Alaskan Eskimo population will be made from an incorporation of all data from Point Hope, Barrow, and Wainwright. We will measure Eskimos of the Canadian Arctic in the fall of 1971 for a comparison of Eskimo populations.

## REFERENCES

1. Cameron, J.R. and Sorenson, J.A. Measurement of bone mineral in vivo: an improved method. Science 142: 230-232 (1963).
2. Cameron, J.R., Mazess, R.B., and Sorenson, J.A. Precision and accuracy of bone mineral determination by direct photon absorptiometry. Invest. Radiol. 3: 141-150 (1968).
3. Cameron, J.R. Summary of data on the bone mineral of radius in normals. USAEC Report COO-1422-41 (1969).
4. Mazess, R.B. Preliminary Report: Bone mineral content of Wainwright Eskimo. USAEC Report COO-1422-65 (1968).
5. Mazess, R.B. and Cameron, J.R. A portable unit for determination of bone mineral content by photon absorptiometry. USAEC Report COO-1422-56 (1969).
6. Mazess, R.B. Bone mineral content in Wainwright Eskimos: preliminary report. Arctic Anthropology 7(1): 114-116 (1970).
7. Sorenson, J.A. and Cameron, J.R. A reliable in vivo measurement of bone mineral content. J. Bone Jt. Surg. 49-A: 491-497 (1967).
8. Witt, R.M., Mazess, R.B., and Cameron, J.R. Standardization of bone mineral measurements. USAEC Report COO-1422-70 (1970).

## ACKNOWLEDGEMENT

This work is supported in part by NASA-Y-NGR-50-051 and by the U.S. Atomic Energy Commission under contract AT-(11-1)-1422. A special thanks is extended to Dr. Fred Milan of the Department of Anthropology, University of Wisconsin, Madison.

Table 1. Averages of measurements on 3-chambered bone phantom in Wisconsin and in Alaska.

		SMALL			MEDIUM			LARGE		
		Barrow	Pt. Hope	Madison	Barrow	Pt. Hope	Madison	Barrow	Pt. Hope	Madison
MINERAL	Mean Integral	.673	.662	.629	1.120	1.106	1.077	2.406	2.375	2.346
	% Coefficient of Variation { among occasions per occasion	1.62	2.92	1.11	1.30	2.63	.86	.81	2.37	.43
		1.88	1.53	1.18	1.53	1.01	1.14	.84	.78	.85
WIDTH	Mean Integral	.694	.683	.664	1.358	1.340	1.335	1.667	1.644	1.642
	% Coefficient of Variation { among occasions per occasion	.92	2.24	.67	.44	2.04	.33	.39	1.98	.29
		1.59	1.07	.71	.92	.68	.56	.67	.54	.51
MINERAL/WIDTH		.970	.969	.947	.825	.825	.807	1.443	1.445	1.428

Table 2. Average heights and weights of Eskimo and White subjects by age.

	AGE	NUMBER		HEIGHT (cm)		WEIGHT (kg)	
		<u>Eskimo</u>	<u>White</u>	<u>Eskimo</u>	<u>White</u>	<u>Eskimo</u>	<u>White</u>
MALES	5-7	14	41	117	125	23.1	24.5
	8-9	9	47	131	138	31.4	31.0
	10-11	14	55	139	147	33.2	37.7
	12-14	13	45	150	160	46.9	52.2
	15-16	6	43	164	175	56.3	68.1
	17-19	7	37	172	182	72.9	74.5
	20-49	14	168	166	178	67.2	77.5
	50-59	10	24	166	176	75.4	77.0
	60-69	18	35	164	175	70.2	75.4
	70+	10	32	162	175	70.2	71.2
FEMALES	5-7	14	32	119	126	25.4	24.3
	8-9	13	36	128	136	29.2	29.4
	10-11	8	43	142	147	37.9	38.0
	12-14	8	46	150	162	53.2	48.6
	15-16	5	37	157	166	59.2	56.2
	17-19	8	62	157	166	59.6	58.3
	20-49	30	121	153	163	61.6	62.5
	50-59	19	37	154	162	64.6	64.9
	60-69	18	43	152	160	65.2	61.5
	70+	11	103	141	160	48.6	57.7

Table 3. Bone mineral content, bone width, and ratio of mineral to width of the radius (1/3 length from distal).

AGE	BONE MINERAL CONTENT (g/cm)		BONE WIDTH (cm)		MINERAL/WIDTH (g/cm <sup>2</sup> )		
	<u>Eskimo</u>	<u>White</u>	<u>Eskimo</u>	<u>White</u>	<u>Eskimo</u>	<u>White</u>	
MALES	5-7	0.46	0.50	0.96	0.98	0.48	0.50
	8-9	0.55	0.57	1.02	1.03	0.54	0.55
	10-11	0.60	0.67	1.09	1.12	0.55	0.60
	12-14	0.72	0.81	1.20	1.25	0.61	0.65
	15-16	0.94	1.08	1.30	1.41	0.73	0.76
	17-19	1.19	1.20	1.43	1.46	0.83	0.82
	20-49	1.20	1.31	1.51	1.49	0.80	0.88
	50-59	1.12	1.33	1.52	1.51	0.74	0.88
	60-69	1.00	1.24	1.48	1.56	0.68	0.79
	70+	1.04	1.23	1.50	1.56	0.69	0.79
FEMALES	5-7	0.44	0.45	0.92	0.92	0.47	0.49
	8-9	0.48	0.52	0.97	0.95	0.49	0.55
	10-11	0.58	0.61	1.00	1.04	0.58	0.59
	12-14	0.71	0.78	1.12	1.16	0.63	0.67
	15-16	0.84	0.87	1.20	1.20	0.70	0.73
	17-19	0.89	0.92	1.21	1.23	0.74	0.75
	20-49	0.89	0.97	1.24	1.27	0.72	0.76
	50-59	0.81	0.86	1.31	1.23	0.62	0.70
	60-69	0.68	0.80	1.28	1.25	0.53	0.63
	70+	0.51	0.71	1.26	1.28	0.40	0.55

### THREE MODELS OF VIBRATING LONG BONES

John Jurist, Ph.D. and Kianpour Kianian, B.S.

Division of Orthopedic Surgery Internal Report  
University of Wisconsin Medical Center  
Madison, Wisconsin 53706

#### MODEL I

##### INTRODUCTION

Previous papers have reported the ulnar resonant frequencies of normal subjects and of various patient populations [5-7,9]. As a conceptual model for these studies, the ulna was treated as a cylindrical tube attached to rigid supports at each end by hinges which simulate the joints. This report evaluates the ability of the model to predict the ulnar resonant frequency of patients for whom the ulnar length was measured and for whom the ulnar mineral content and width was determined at a specific location by the photon absorptiometric method [11].

##### THEORY

The ulna is considered to be a uniform cylindrical tube of length  $L$ , outside diameter  $2a_p$ , and inside diameter  $2a_e$  (Fig. 1).

The tube is attached at each end to rigid supports by hinges which allow deflection in the x-y plane only (Fig. 2). The material of which the tube is composed is treated as a homogeneous, isotropic substance of density  $\rho$  with a Young's modulus of elasticity of  $Y$ .

It can be shown [8] that the transverse deflection  $y$  from the equilibrium position at a location  $x$  along the axis of the vibrating tube is given by

$$(1) \quad y = \cos(\omega t + \phi) [A \cosh(\omega x/v) + B \sinh(\omega x/v) + C \cos(\omega x/v) + D \sin(\omega x/v)]$$

In this equation,  $\omega$  is the angular frequency of vibration,  $t$  is time,  $\phi$  is an arbitrary epoch, and  $v$  is the phase velocity of the transverse wave component with angular frequency  $\omega$  along the length of the tube.  $A$ ,  $B$ ,  $C$ , and  $D$  are arbitrary constants determined from boundary conditions.

The phase velocity is given by

$$(2) \quad v = \sqrt{\omega c K} ,$$

where  $c$  is the speed of longitudinal wave propagation through the

material of the tube and  $K$  is the radius of gyration of the cross section of the tube about the neutral axis. The speed of longitudinal wave propagation is given by

$$(3) \quad c = \sqrt{Y/\rho} ,$$

and the radius of gyration is given by

$$(4) \quad K = 0.5 \sqrt{a_p^2 + a_e^2} .$$

The angular frequency of vibration ( $\omega$ ) is related to the cyclic frequency of vibration ( $f$ ) by

$$(5) \quad \omega = 2\pi f .$$

At each end of the hinged bar, the displacement and internal moment must vanish [8]. Therefore,

$$(6) \quad y = 0 \quad \text{and} \quad (7) \quad \frac{\partial^2 y}{\partial x^2} = 0 \quad \text{at} \quad x = 0 \quad \text{and} \quad x = L .$$

Substitution of Equation 1 into Equations 6 and 7 at  $x = 0$  and simplifying shows that the constants  $A$  and  $C$  vanish. Therefore,

$$(8) \quad y = \cos(\omega t + \phi) [B \sinh(\omega x/v) + D \sin(\omega x/v)] .$$

Substitution of Equation 8 into Equations 6 and 7 at  $x = L$ , eliminating  $\sinh(\omega L/v)$  and simplifying yields

$$(9) \quad \sin(\omega L/v) = 0 .$$

The fundamental nontrivial solution of Equation 9 is

$$(10) \quad \omega_0 L = \pi v ,$$

where  $\omega_0$  is the allowed angular frequency of vibration. If  $f_0$  is defined as the allowed cyclic frequency of vibration,

$$(11) \quad f_0 = \frac{\pi c}{4L^2} \sqrt{a_p^2 + a_e^2}$$

is obtained by combining Equations 2, 4, 5, and 10 and then simplifying. Equation 11 forms the basis for predicting ulnar resonant frequency given  $L$ ,  $M_B$ , and  $W$ .  $M_B$  and  $W$  are the mineral content (expressed in g/cm) and width (expressed in cm) of the ulna at a scan site proximal to the ulnar head by  $0.3L$ . It is assumed that this location provides a representative cross section of the ulna (Fig. 3).

From experimental data relating ash content to density of compact bone [10], one finds that

$$(12) \quad b = 1.1806\rho - 1.1945 ,$$

where  $b$  is the ash or mineral content (expressed in  $\text{g/cm}^3$ ) of fresh cortical bone. If Equation 12 is multiplied by the cross sectional area of the bone, one finds that, since

$$(13) \quad M_B = \pi b(a_p^2 - a_e^2) ,$$

$$(14) \quad M_B = \pi(a_p^2 - a_e^2)(1.1806\rho - 1.1945) .$$

Since the width of the bone at the scan site ( $W$ ) is given by  $2a_p$ , one may solve Equation 14 for  $a_e^2$ , combine the result with Equation 11, substitute the expression for  $W$ , and simplify:

$$(15) \quad f_o = \frac{\pi c}{4L^2} \sqrt{\frac{W^2}{2} - \frac{M_B}{\pi(1.1806\rho - 1.1945)}} .$$

Experimental measurements of  $c$ ,  $\rho$ , and  $Y$  in excised strips of fresh cortical bone [1] allow one to derive (in cgs units)

$$(16) \quad c = 2.1427 \cdot 10^5 + 6.5333 \cdot 10^{-7} Y , \quad \text{and} \quad (17) \quad \rho = 1.2586 + 3.6429 \cdot 10^{-12} Y ,$$

If these equations are substituted into Equation 15 and the result simplified, one obtains

$$(18) \quad f_o = \frac{\pi}{4L^2} (a_1 + b_1 Y) \sqrt{\frac{W^2}{2} - \frac{M_B}{\pi(a_2 + b_2 Y)}} ,$$

where  $a_1 = 2.1427 \cdot 10^5$  ,  $a_2 = 0.2914$  ,  $b_1 = 6.5333 \cdot 10^{-7}$  ,  
and  $b_2 = 4.3008 \cdot 10^{-12}$  . Equation 18 can be used in either of 2 ways. First, it can be used to determine the value of  $f_o$  predicted by the model given  $L$ ,  $M_B$ , and  $W$ . In this case, some accepted mean value of  $Y$  must be used. Then, the predicted value of  $f_o$  can be compared to the measured value of this parameter. Second, Equation 18 can be used to determine the value of  $Y$  predicted by the model given the values of  $f_o$ ,  $L$ ,  $M_B$ , and  $W$ .

#### METHOD AND RESULTS

A group of 118 schoolchildren, ranging in age from 6 to 11 years, was selected for this study. First, assuming a constant Young's

modulus of  $1.6865 \cdot 10^{11}$  [1], and given  $L$ ,  $W$ , and  $M_B$  for each child, Equation 18 was used to predict  $f_0$ . The predicted  $f_0$  values are plotted against the measured values in Fig. 4. Second, Equation 18 was rearranged to obtain a third order polynomial expression for  $Y$ :

$$(19) \quad A_1 Y^3 + A_2 Y^2 + A_3 Y + B = 0 ,$$

$$\text{where } A_1 = \pi^2 W^2 b_1^2 b_2 , \quad A_2 = \pi^2 W^2 b_1^2 a_2 + 2\pi^2 W^2 b_1 b_2 a_1 - 2\pi M_B b_1^2 ,$$

$$A_3 = 2\pi^2 W^2 b_1 a_1 a_2 + \pi^2 W^2 b_2 a_1^2 - 4\pi M_B b_1 a_1 - 32f_0^2 b_2 L^4 , \text{ and}$$

$$B = \pi^2 W^2 a_1^2 a_2 - 2\pi M_B a_1^2 - 32f_0^2 a_2 L^4 .$$

This cubic was solved by a standard formula which yields only the real root(s). The values of  $Y$  which are obtained by solution of Equation 19 are plotted as a function of age for the schoolchildren in Fig. 5. The RMS values (root mean square of the percentage discrepancies of the predicted values in terms of the actual values) of resonant frequency and Young's modulus are rather large. This suggests that either the uncertainty in the experimentally measured quantities caused poor behavior of the model, or the model itself is not applicable.

The calculated value of Young's modulus based on this model was determined for each member of the 6 patient populations described in Table I. Figs. 6-11 show the predicted  $Y$  values as a function of age for these groups.

#### ERROR ANALYSIS

For an analytic function  $y$ , where  $y = y(x_1, x_2, x_3, \dots)$  with uncertainties of  $\Delta x_1$ ,  $\Delta x_2$ ,  $\Delta x_3$ , etc. associated with  $x_1$ ,  $x_2$ ,  $x_3$ , etc., respectively, the uncertainty  $\Delta y$  in  $y$  is given by

$$\Delta y = y \sqrt{\left(\frac{\partial y}{\partial x_1} \frac{\Delta x_1}{y}\right)^2 + \left(\frac{\partial y}{\partial x_2} \frac{\Delta x_2}{y}\right)^2 + \left(\frac{\partial y}{\partial x_3} \frac{\Delta x_3}{y}\right)^2 + \dots .}$$

In order to estimate the uncertainty of  $f_0$  and  $Y$  associated with the model, we calculated  $\Delta f_0$  and  $\Delta Y$  using data for a typical subject:

$$M_B = 0.80 \pm 0.05 \text{ g/cm (uncertainty 6.3%) ,}$$

$$W = 1.00 \pm 0.10 \text{ cm (uncertainty 10.0%) ,}$$

$L = 25 \pm 1$  cm (uncertainty 4.0%) , and  $Y = 1.6865 \cdot 10^{11} \pm 1.6865 \cdot 10^{10}$  dynes/cm<sup>2</sup> (uncertainty 10.0%) . The predicted value of the resonant frequency is then  $f_o = 204 \pm 47$  Hz (uncertainty 23%) . Similarly, the uncertainty in  $Y$  was calculated using the same assumed values and uncertainties for  $M_B$ ,  $W$ , and  $L$ . If the measured  $f_o$  is assumed to be  $204 \pm 10$  Hz (5%), then the calculated value of Young's modulus is found to be  $1.6865 \cdot 10^{11} \pm 1.4323 \cdot 10^{10}$  dynes/cm<sup>2</sup> (8.5%) . These calculations clearly demonstrate that a small uncertainty in Young's modulus introduces a larger uncertainty in the resonant frequency predicted by the model.

## MODEL II

### INTRODUCTION

This model simulates the flexural vibration of a beam which is hinged at each end and is supported along its length by an elastic foundation. This model is similar to Model I except for the addition of the elastic foundation which simulates the elastic properties of the soft tissue (mostly muscle) which surrounds the ulna. Conceptually, this model is a better approximation of the vibrating ulna than is Model I, but it is not satisfactory for several inherent reasons.

### THEORY

Consider the beam shown in Fig. 12. For the first and second mode of vibration, the deflection curve may be approximated by

$$(20) \quad y = \alpha_n \sin(n\pi x/L) , \quad \text{where} \quad (21) \quad \alpha_n = \alpha_o \sin(\omega_n t) .$$

The kinetic ( $E_k$ ) and potential ( $E_p$ ) energy of the vibrating bar may be written as

$$(22) \quad E_k = \frac{M}{2L} \int_0^L \left( \frac{\partial y}{\partial t} \right)^2 dx , \quad \text{and} \quad (23) \quad E_p = \frac{YI}{2} \int_0^L \left( \frac{\partial^2 y}{\partial x^2} \right)^2 dx + \frac{k}{2L} \int_0^L y^2 dx ,$$

respectively. In these equations,  $M$  is the mass of the bar,  $I$  is the moment of inertia of the cross section of the bar, and  $k$  is the spring constant of the foundation (soft tissue). By substitution of the proper derivatives into Equations 22 and 23, one can maximize  $E_k$  and  $E_p$  to obtain

$$(24) \quad E_{k \max} = 0.25 M b_n^2 \alpha_o^2 , \quad \text{and} \quad (25) \quad E_{p \max} = \frac{\alpha_o^2}{4} (k + YI n^4 \pi^4 / L^3) .$$

Equating  $E_{k_{\max}}$  and  $E_{p_{\max}}$  yields the nondimensional equation

$$(26) \quad \omega_n^2 = YI \frac{(n\pi)^4}{ML^3} + \frac{k}{M} .$$

In Equation 26, n has allowed values of 0, 1, or 2. It can be shown that

$$(27) \quad M = M_B L \rho / b , \quad \text{and} \quad (28) \quad I = \frac{M_B}{2b} \left( \frac{W^2}{2} - \frac{M_B}{\pi b} \right) .$$

In order to obtain an estimate of k, the foundation spring constant, we assume that the bone is surrounded by a muscle-like material of thickness 2.5 cm and Young's modulus of 52,000 dynes/cm<sup>2</sup> [3]. With this assumption, one finds that

$$(29) \quad k = 4.15 \cdot 10^4 LW .$$

By substituting Equations 27-29 into Equation 26 for n = 1, one can calculate the allowed frequency of vibration.

### RESULTS

This model was tested with the same data as was used for Model I. In general, the predicted resonant frequencies were larger than for the first model. This is predominantly a result of the term k/M in Equation 26 (representing the foundation or soft tissue elasticity).

There are 2 additional difficulties with this model. First, the approximation that is made for the flexural deflection is not easily justified. Second, using the exact expression of flexural deflection for solving the equations of motion for the model is so difficult as to be impractical.

### MODEL III

#### INTRODUCTION

The previous models were inadequate in some respects. Thus, we evaluated a third model which assumes that the vibrating bar is attached to rigid supports by springs rather than hinges at each end. These springs simulate the elastic properties of the articular cartilage found at each end of the ulna.

#### THEORY

The only difference between this model and Model I is the change in boundary conditions. The force constants of the 2 springs are  $K_e$  and  $K_w$  for the "elbow" and "wrist" respectively. Fig. 13 illustrates this model.

At each end of the bar, the internal moment vanishes. Thus,

$$(30) \quad \frac{\partial^2 y}{\partial x^2} = 0 \quad \text{at } x = 0 \text{ and } x = L .$$

Substitution of Equation 1 into Equation 30 at  $x = 0$  and simplifying shows that

$$(31) \quad A = C .$$

Substitution of Equation 31 into Equation 1 and substitution of the result into Equation 30 at  $x = L$  and simplifying yields

$$(32) \quad D = A \frac{\cosh(\omega L/v) - \cos(\omega L/v)}{\sin(\omega L/v)} + B \frac{\sinh(\omega L/v)}{\sin(\omega L/v)}$$

Therefore,

$$(33) \quad y = \cos(\omega t + \phi) \left[ A \left\{ \cosh(\omega x/v) + \cos(\omega x/v) + \frac{\sin(\omega x/v)}{\sin(\omega L/v)} [\cosh(\omega L/v) - \cos(\omega L/v)] \right\} \right. \\ \left. + B \left\{ \sinh(\omega x/v) + \frac{\sin(\omega x/v)}{\sin(\omega L/v)} \sinh(\omega L/v) \right\} \right]$$

Also, it can be shown that the elastic force [8] is

$$(34) \quad K_e y = \left( a_p^4 - a_e^4 \right) \frac{\pi Y}{4} \frac{\partial^3 y}{\partial x^3} \quad \text{and} \quad (35) \quad K_w y = - \left( a_p^4 - a_e^4 \right) \frac{\pi Y}{4} \frac{\partial^3 y}{\partial x^3}$$

at  $x = 0$  and  $x = L$ , respectively. Substitution of Equation 33 into Equations 34 and 35, combining and simplifying the result yields

$$(36) \quad \frac{8K_w}{\pi Y \alpha_1 X^3} \left( \sinh(XL) - \frac{\alpha_2 \cosh(XL)}{\alpha_3 - \alpha_5} \right) = \cot(XL) \sinh(XL) - \cosh(XL) + \frac{\alpha_2 \alpha_4}{\alpha_3 - \alpha_5}$$

where

$$(37) \quad X = \omega/v ,$$

$$(38) \quad \alpha_1 = a_p^4 - a_e^4 ,$$

$$(39) \quad \alpha_2 = \sin(XL) - \sinh(XL) ,$$

$$(40) \quad \alpha_3 = \cos(XL) - \cosh(XL) ,$$

$$(41) \quad \alpha_4 = \alpha_3 \cot(XL) + \sin(XL) + \sinh(XL) , \text{ and}$$

$$(42) \quad \alpha_5 = 8K_e \sin(XL) / (\pi Y \alpha_1 X^3) .$$

As for the case of Model I, the variables in Equation 36 may be expressed in terms of  $W$ ,  $L$ ,  $M_B$ ,  $Y$ ,  $f_o$ , etc. Young's modulus of

cartilage was derived from the literature [2] ( $3.385 \cdot 10^8$  dynes/cm<sup>2</sup>). Based on the assumption that the articular cartilage is 2 mm thick at both wrist and elbow, and that the bearing surface is 2 cm<sup>2</sup> and 1 cm<sup>2</sup> at the elbow and wrist, respectively,  $K_e$  and  $K_w$  were estimated to have values of

$$(43) \quad K_e = 6.78 \cdot 10^9 \text{ dynes/cm} , \quad \text{and} \quad (44) \quad K_w = 1.69 \cdot 10^9 \text{ dynes/cm} .$$

In order to calculate the resonant frequency of the ulna based on this model, one must solve Equation 36 for  $X$  or  $\omega/v$ . Unfortunately, there is no explicit solution of the function

$$(45) \quad X = X(Y, L, W, M_B, K_e, K_w) .$$

Therefore, one must solve this function numerically with a digital computer. This function was initially solved by Newton's method [4], but the convergence was too slow. We then used  $\Delta^2$ -Aitken's accelerating method. This improved convergence markedly.

A typical plot of Equation 36 is shown in Fig. 14. The resonant frequency predicted by the model can be found from the value of  $X$  where the left hand side (LHS) and right hand side (RHS) of Equation 36 intersect. The fundamental resonance is obtained from the lowest value of  $X$  at intersection if several intersections occur. In Fig. 14, the first intersection occurs at  $X \cong 0.13$ .

## RESULTS

Generally, this model is similar to the hinged-hinged model (see Fig. 15). One expects Models I and III to yield increasingly similar results as the values of  $K_e$  and  $K_w$  increase. Experimentally, this was shown to be the case. The behavior of the model is quite satisfactory for realistic values of  $K_e$  and  $K_w$ . At first, this model was compared to Model I on the basis of the data collected from the schoolchildren. Initially, the RMS of frequency was 10% larger for Model III than for Model I. However, by systematically changing  $W$ ,  $M_B$ ,  $K_e$ , and  $K_w$ , we were able to force a marked improvement in RMS of predicted frequency. Table II summarizes the behavior of Model III as the parameters mentioned above were changed.

From the above, it is apparent that the predicted resonant frequency based on this model is largely dependent on bone width and is not critically dependent on the other parameters. As mentioned earlier, we assumed that  $W$  at the standard 0.3L scan site represented an average width for the ulna. However, this assumption may not be valid.

We found that using  $1.1W$  instead of  $W$  in the model improved the RMS of frequency (Fig. 16).

#### DISCUSSION

Model I and Model III were also compared for several patient populations. Our findings are summarized in Table III. From this table, one can see that the spring-spring model (Model III) more accurately predicts resonant frequency than does the hinge-hinge model (Model I), but this fit is still far from ideal. This by no means implies that the model is invalid, but may be a result of the rather large uncertainty in some of the measured variables. For example, as we have seen previously, the uncertainty in the average width measurement of the ulna introduces a large uncertainty in the predicted frequency of ulnar resonance ( $f_0$  is critically dependent on  $W$ ).

Based on the above analysis, a better model can be proposed that is independent of  $W$ . This model would be essentially a spring-spring model like Model III, but a truncated conical bar or tube would be substituted for the cylindrical bar. This proposed model would more closely approximate the anatomical shape of the ulna, but has the disadvantage that one must know the width of the bone at 2 different scan sites in order to completely define the dimensions of the bar. Theoretically, we can then expect a better resonant frequency approximation to the measured frequency of ulnar resonance.

#### REFERENCES

1. W. Abendschein, G. Hyatt: Clin. Orthop. 69:294, 1970.
2. F. Evans, H. Lissner: p. 4 in The Seventh Stapp Car Crash Conference Proceedings, Springfield, Ill., Thomas, 1965.
3. P. Honcke: Acta Physiol. Scand. Supp. 48, 1947.
4. E. Isaacson, H. Keller: p. 97, 108 in Analysis of Numerical Methods, New York, Wiley, 1966.
5. J. Jurist: Phys. Med. Biol. 15:417, 1970.
6. J. Jurist: Phys. Med. Biol. 15:427, 1970.
7. J. Jurist: p. 68 in Proceedings of Bone Measurement Conference, AEC Conf-700515, 1970.
8. L. Kinsler, A. Frey: p. 64 in Fundamentals of Acoustics, New York, Wiley, 1950.
9. M. Mueller, J. Cameron, J. Jurist: p. 405 in Proceedings of Bone

Measurement Conference, AEC Conf-700515, 1970.

10. R. Robinson: p. 186 in Bone as a Tissue, New York, McGraw-Hill, 1960.
11. J. Sorenson, J. Cameron: J. Bone Jt. Surg. 49A:481, 1967.

TABLE I  
Clinical Groups Evaluated

<u>SEX</u>	<u>CLINICAL DESCRIPTION OF GROUP</u>	<u># IN GROUP</u>
M	Normal	91
F	Normal	97
M	Rheumatoid Arthritis Without Steroids	17
F	Rheumatoid Arthritis Without Steroids	39
M	Rheumatoid Arthritis With Steroids	11
F	Rheumatoid Arthritis With Steroids	34

TABLE II  
Effect of Parameter Variation on Frequency RMS for Schoolchildren

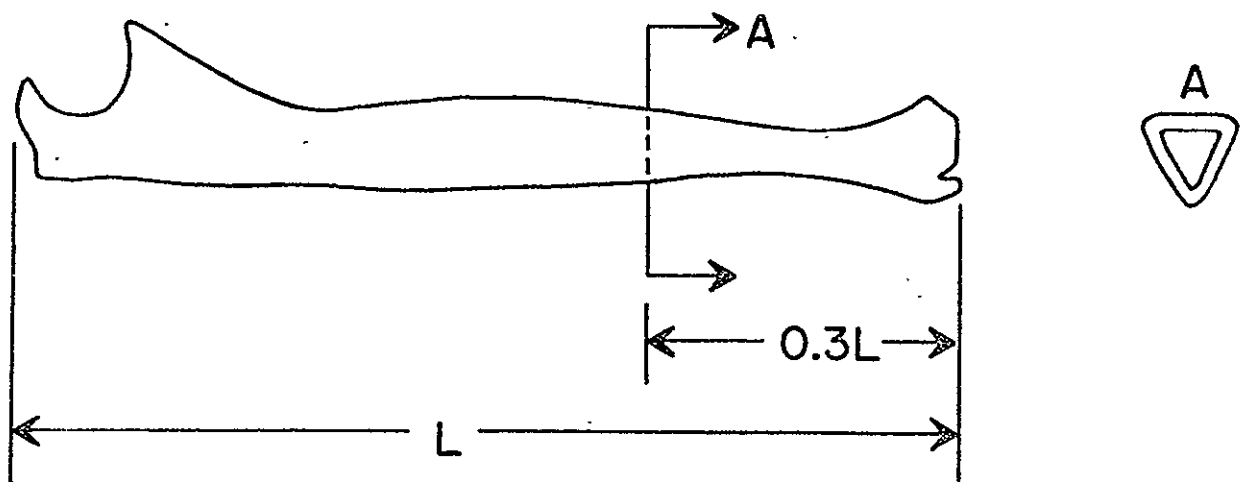
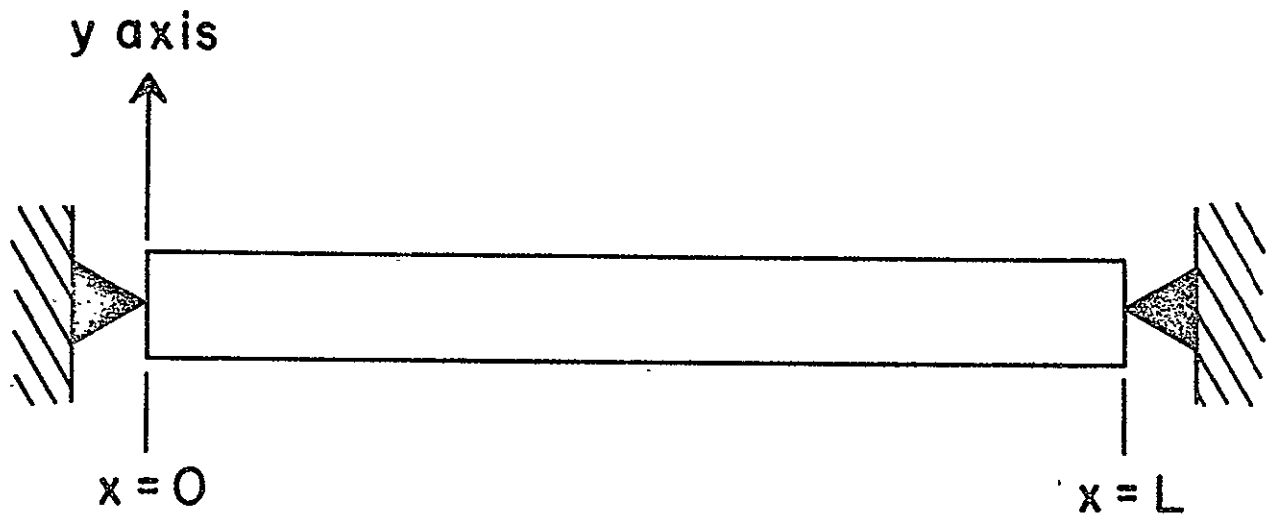
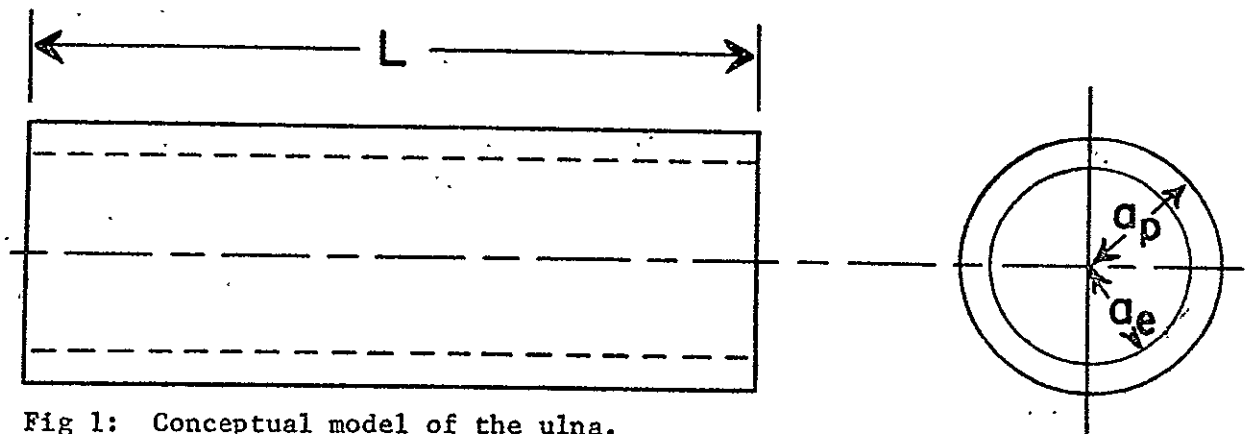
<u>PARAMETER(S)</u>	<u>CHANGE</u>	<u>CHANGE IN RMS</u>
$K_e, K_w$	+13%	-1%
$K_e, K_w$	-20%	+3%
$M_B$	+15%	+9%
W	+10%	-16%
$M_B, W$	+15, 10%	+4%
$M_B, W$	-15, +10%	+1%
W, Y*	+10%	-13%

\*Y corrected for age based on Fig. 5.

TABLE III  
Reliability of Resonant Frequency Prediction

SEX	GROUP	MODEL I				MODEL III*			
		W		1.1W		W		1.1W	
		#	RMS	#	RMS	#	RMS	#	RMS
M+F	Schoolchildren	118	19.249	118	23.300	111	21.368	118	17.700
F	No Rheumatoid Arthritis No Steroids No Osteoporosis	41	28.410	41	35.700	20	19.820	38	29.730
F	Rheumatoid Arthritis No Steroids	39	33.883	39	36.700	18	26.092	31	32.360
F	Rheumatoid Arthritis With Steroids	34	47.299	34	58.300	21	42.090	28	46.900
M	No Rheumatoid Arthritis No Steroids No Osteoporosis	29	25.949	28	26.000	20	29.038	28	20.700
M	Rheumatoid Arthritis No Steroids	17	28.840	17	35.800	13	222.640	17	45.200
M	Rheumatoid Arthritis With Steroids	11	30.782	11	38.800	7	32.628	11	31.100
F	No Rheumatoid Arthritis With Steroids	9	28.440	9	38.700	6	24.737	9	28.700
M	No Rheumatoid Arthritis With Steroids	4	25.153	5	31.600	3	29.683	4	24.500
F	No Rheumatoid Arthritis No Steroids With Osteoporosis	6	33.459	6	49.500	6	25.200	6	34.300

\*When Model III was used for the Schoolchildren with 1.1W and with Y corrected for age, the RMS of the predicted resonant frequency was 15.500%.



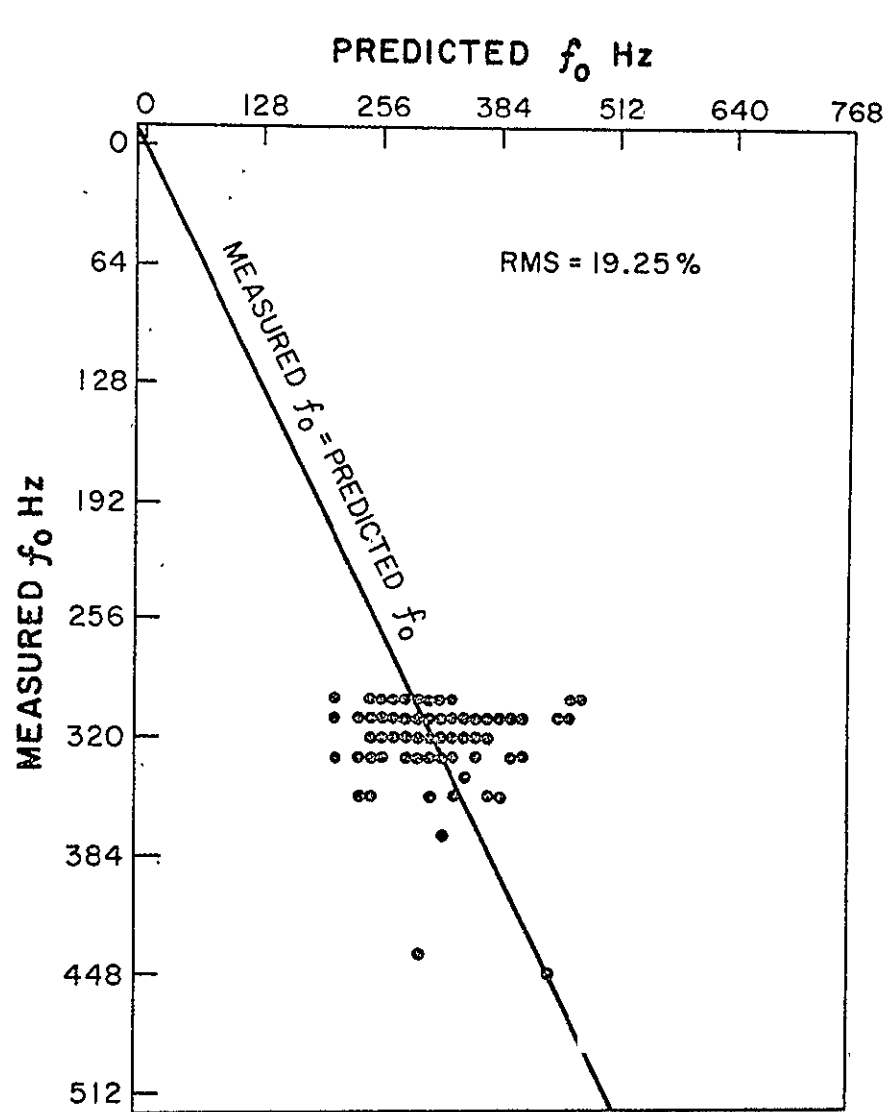


Fig 4: Predicted  $f_0$  vs measured  $f_0$  based on Model I for 118 schoolchildren. The RMS value (root mean square of the percentage discrepancy of predicted  $f_0$  in terms of the measured  $f_0$ ) is 19.25%.

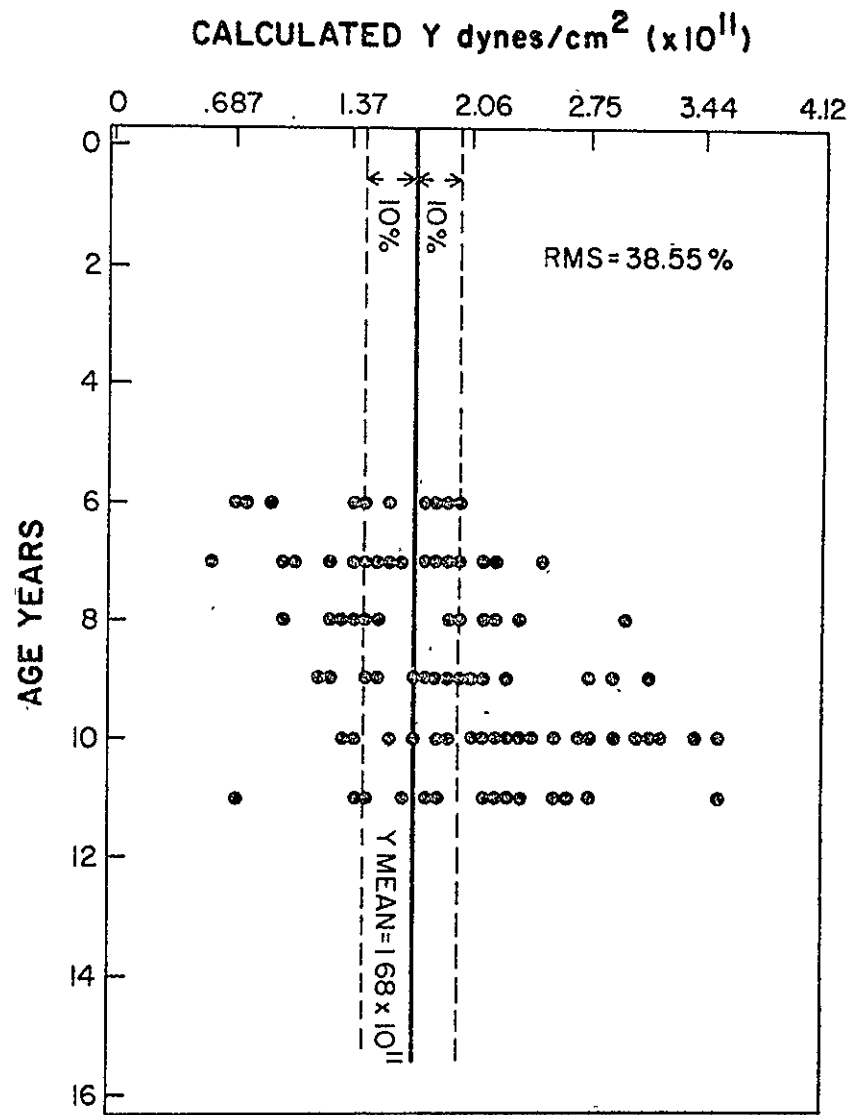


Fig 5: Calculated  $Y$  vs age based on Model I for 118 schoolchildren.

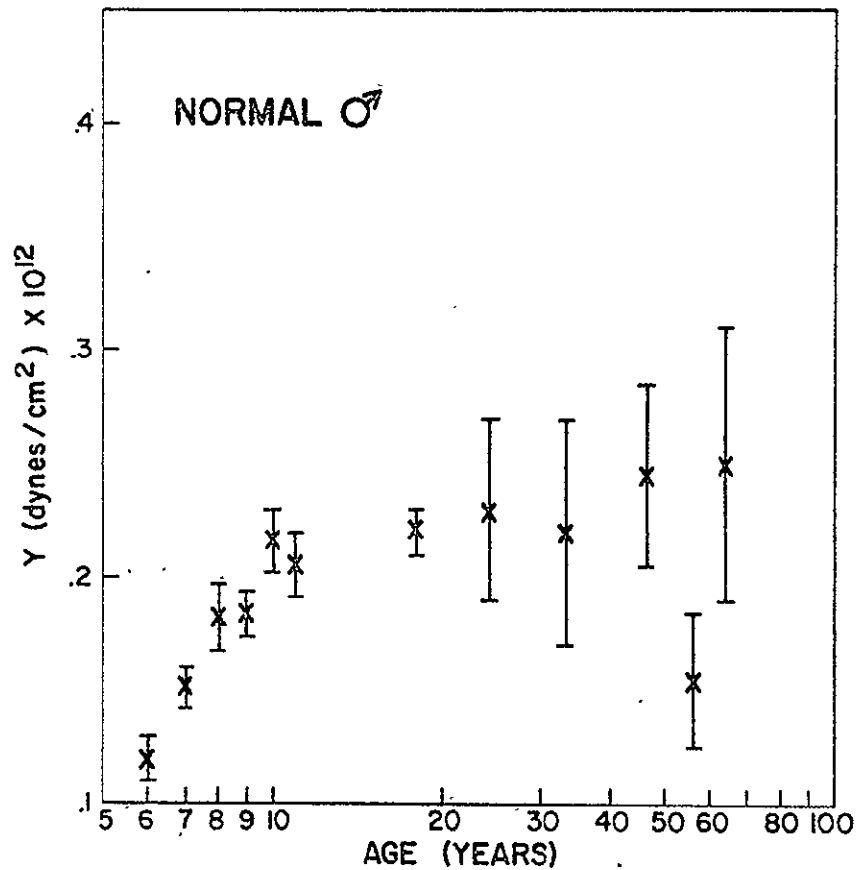


Fig 6: Y vs age for 91 normal male subjects. The range bars enclose  $\pm 1$  standard error of the mean.

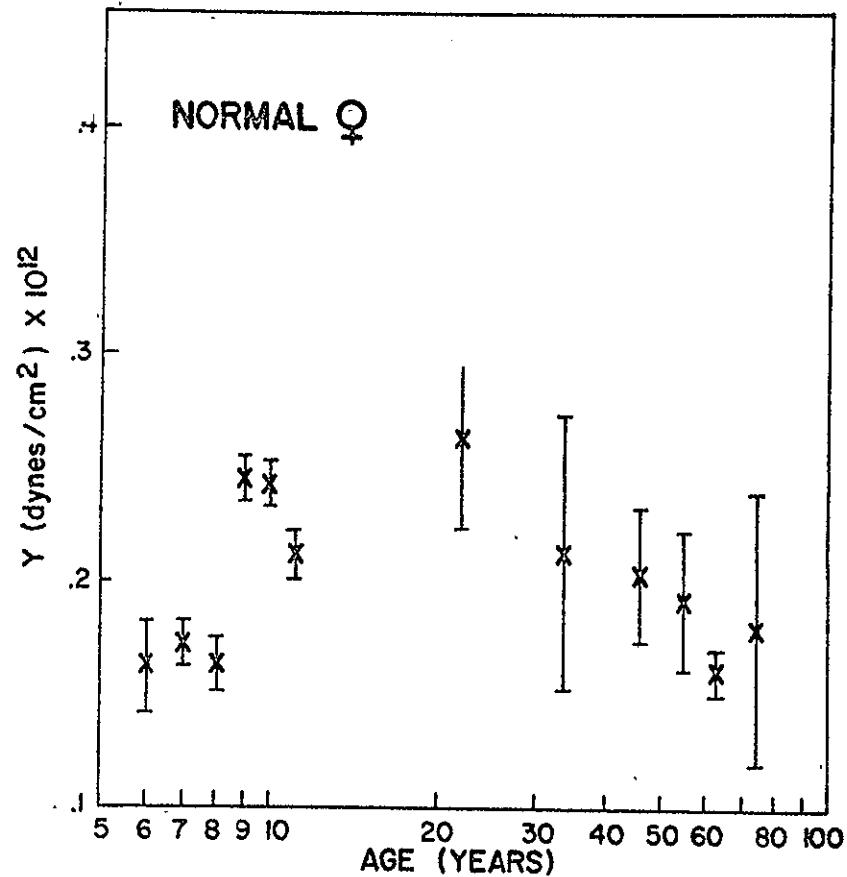


Fig 7: Y vs age for 97 normal female subjects.

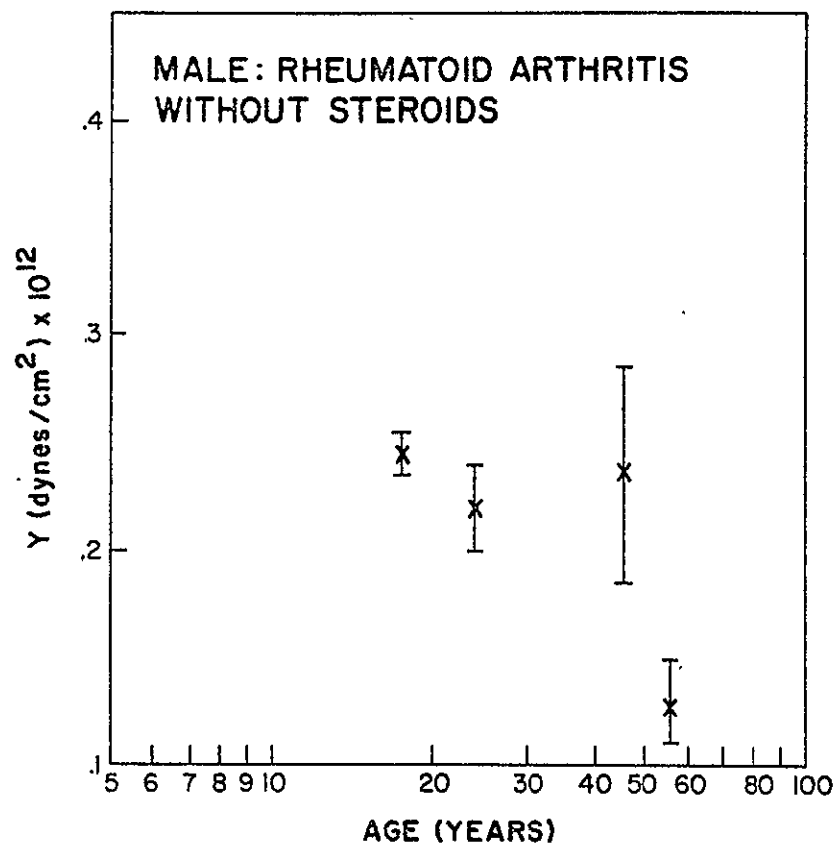


Fig 8: Y vs age for 17 males with rheumatoid arthritis and no history of corticosteroid therapy.

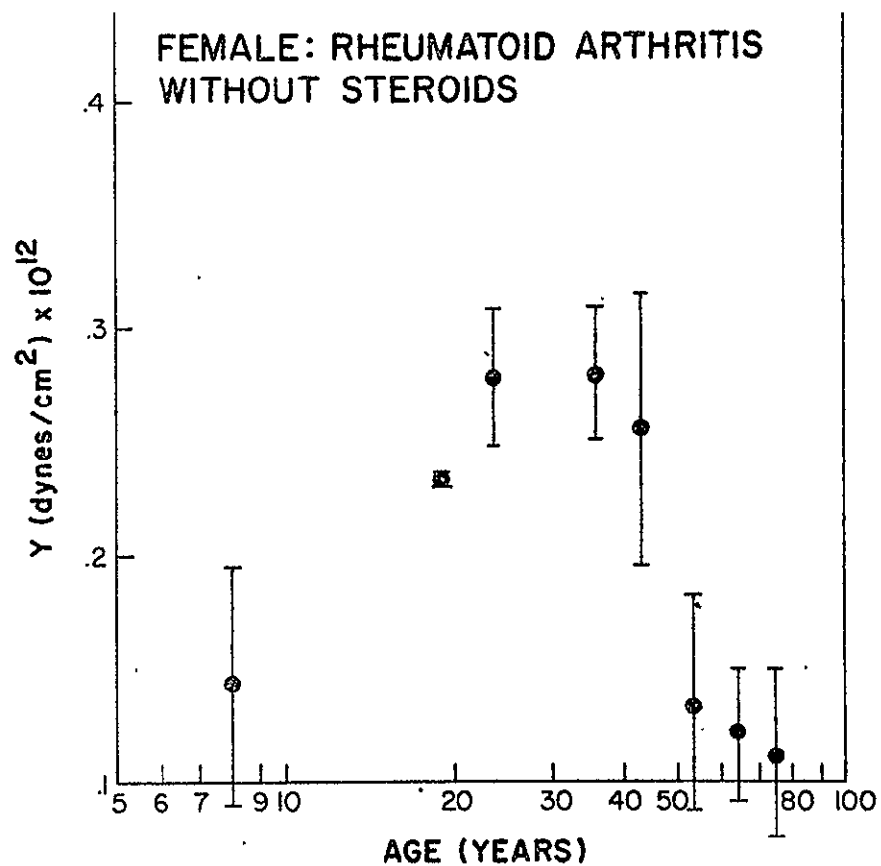


Fig 9: Y vs age for 39 rheumatoid females without steroid therapy.

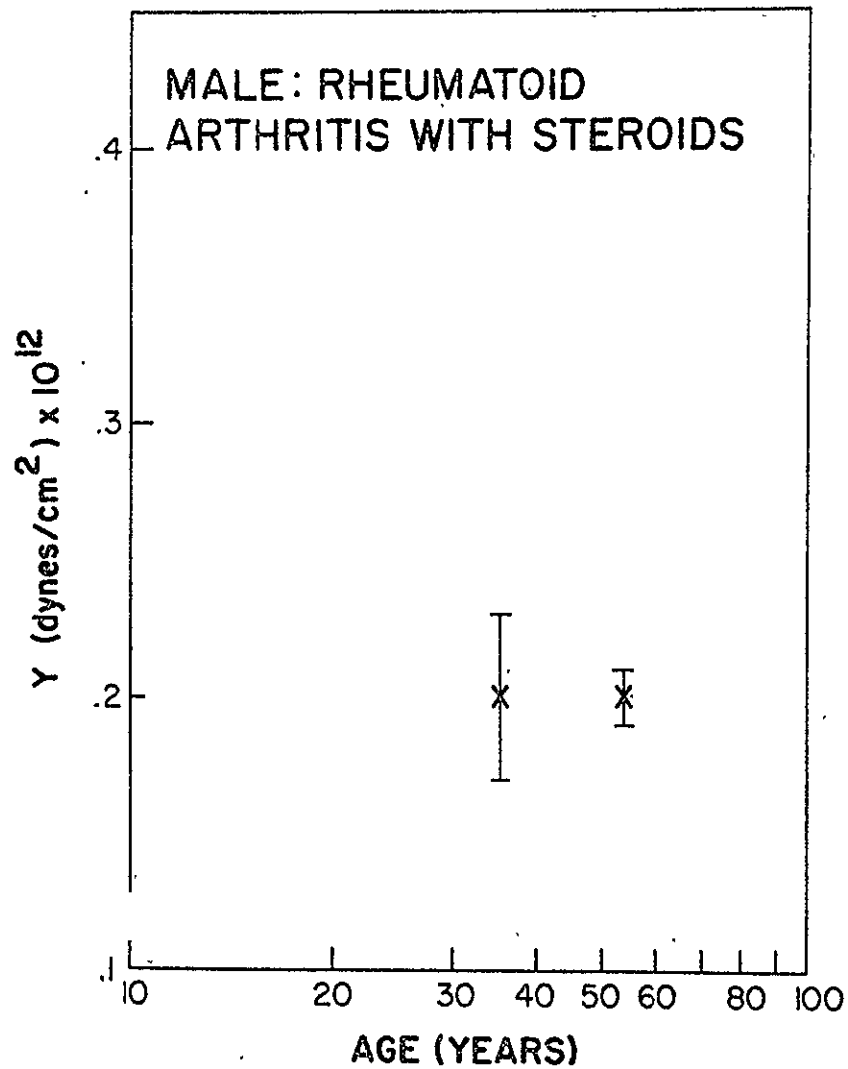


Fig 10: Y vs age for 11 rheumatoid males with a history of steroid therapy.

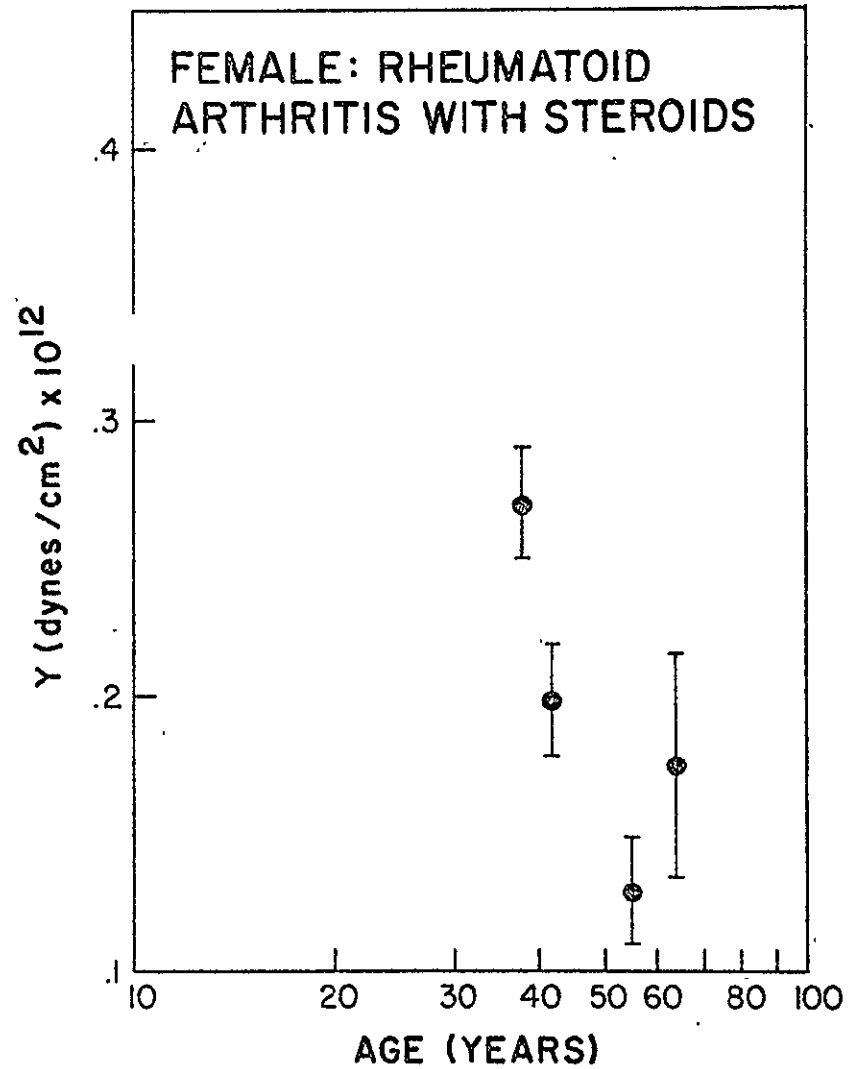


Fig 11: Y vs age for 34 rheumatoid females with a history of steroid therapy.

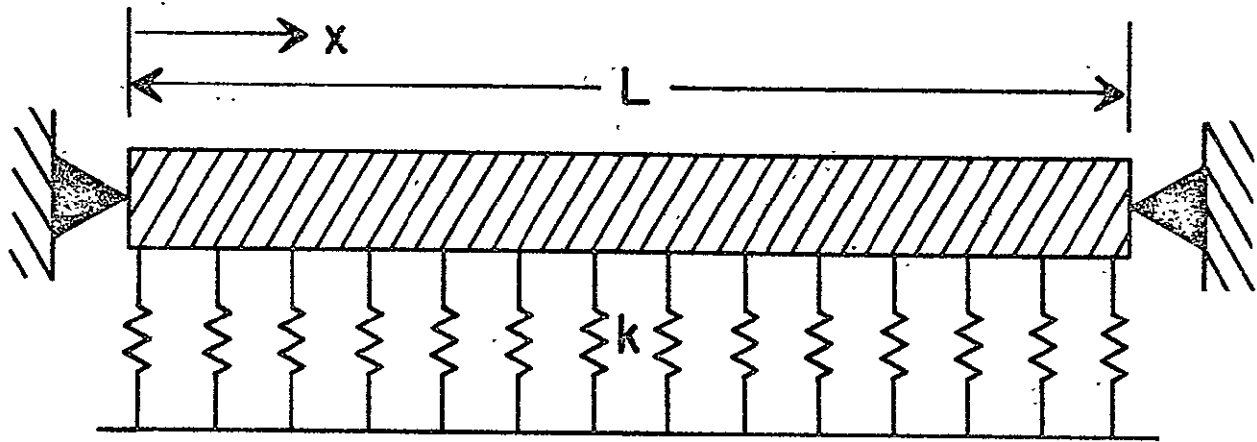


Fig 12: Model II boundary conditions.

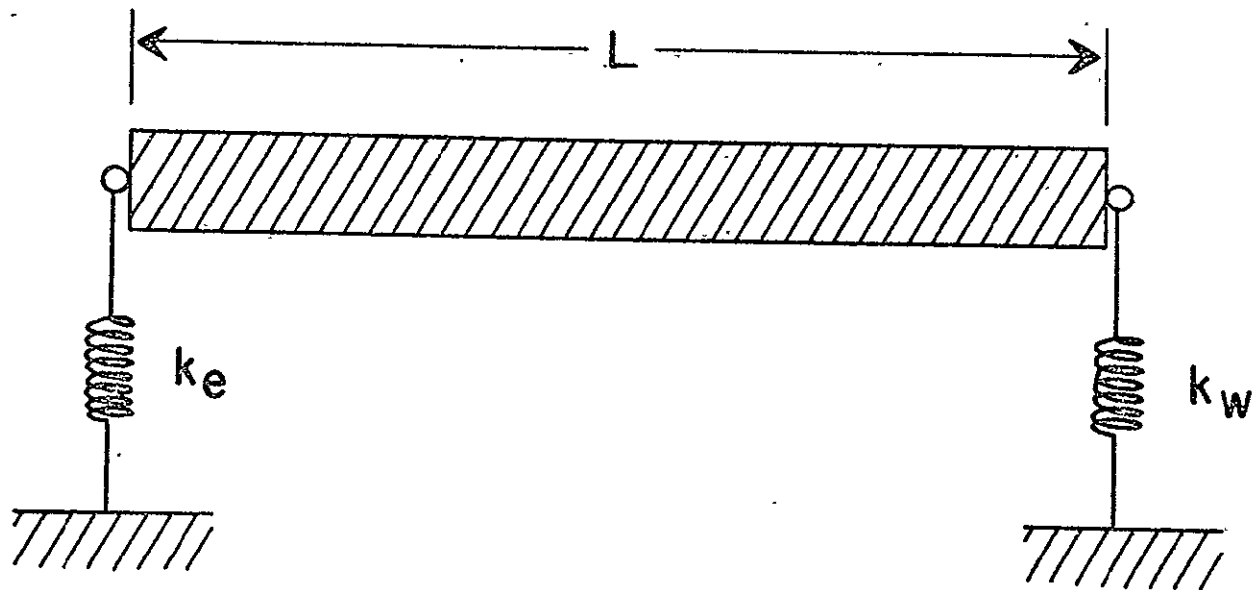


Fig 13: Model III boundary conditions.

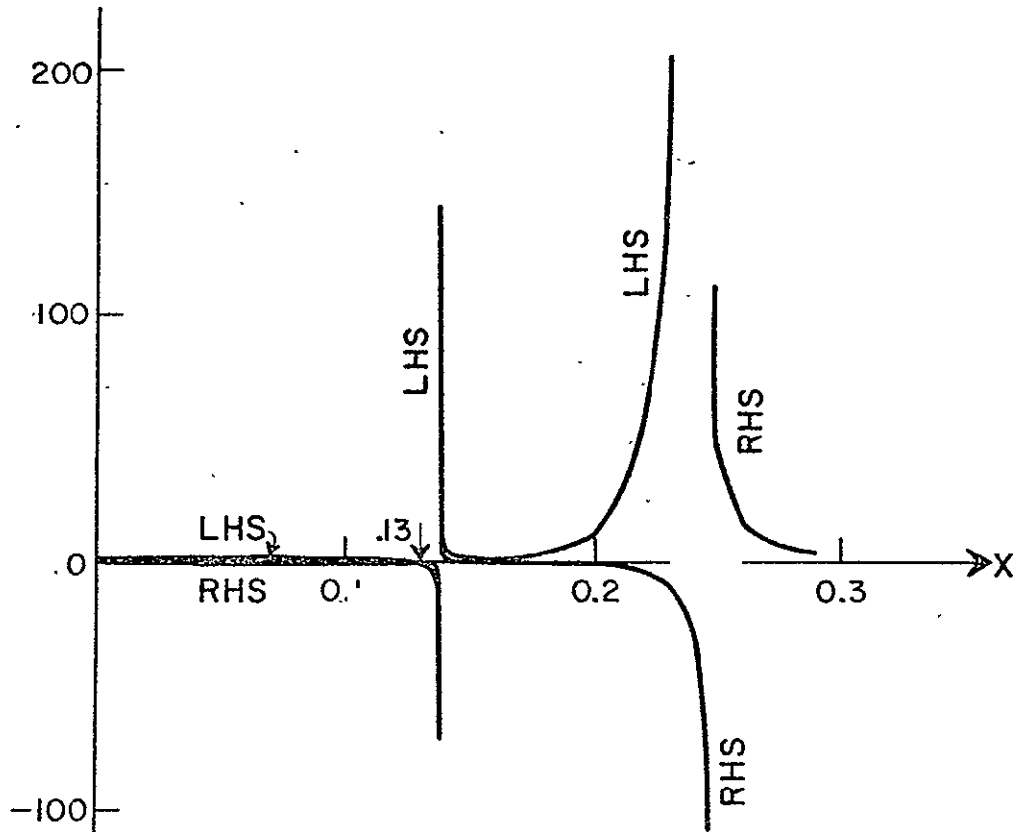


Fig 14: Typical plot of Equation 36. The fundamental resonance occurs at  $X \approx 0.13$ .

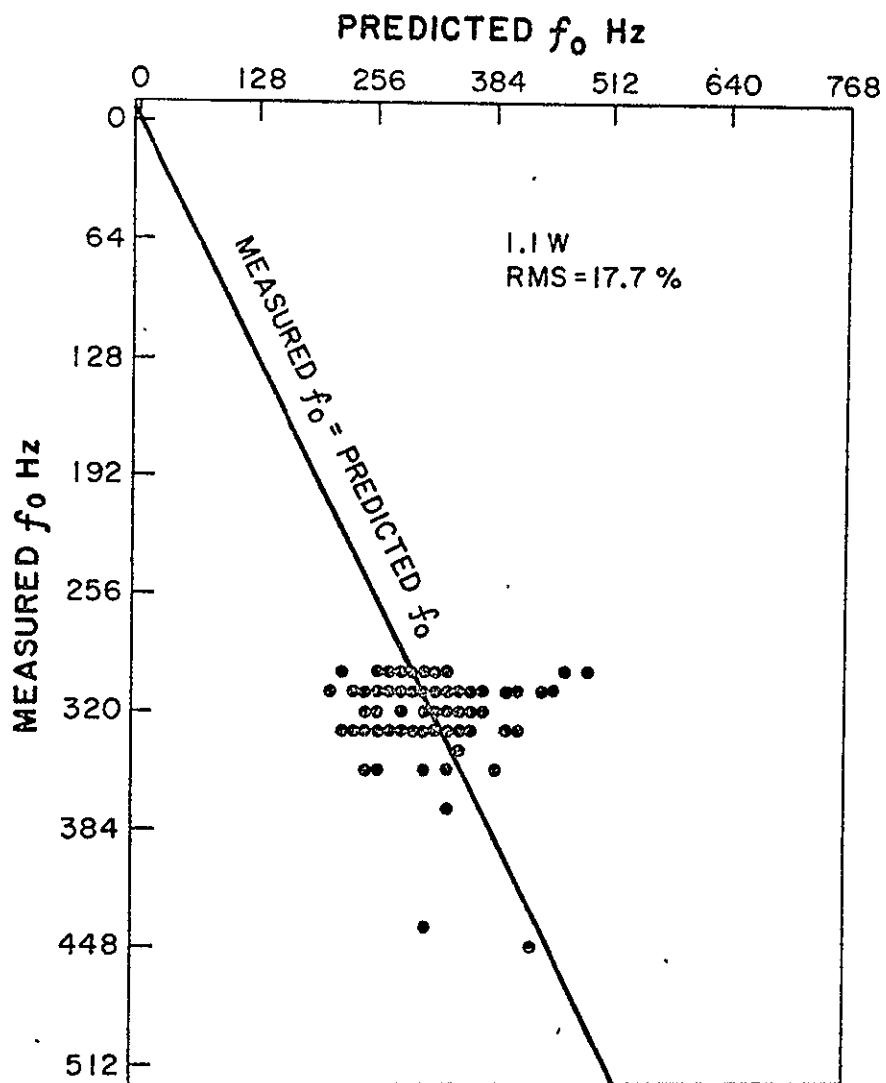


Fig 15: Predicted  $f_0$  vs measured  $f_0$  based on Model III for 118 schoolchildren. 1.1W was substituted for the measured value of W in Equation 36.

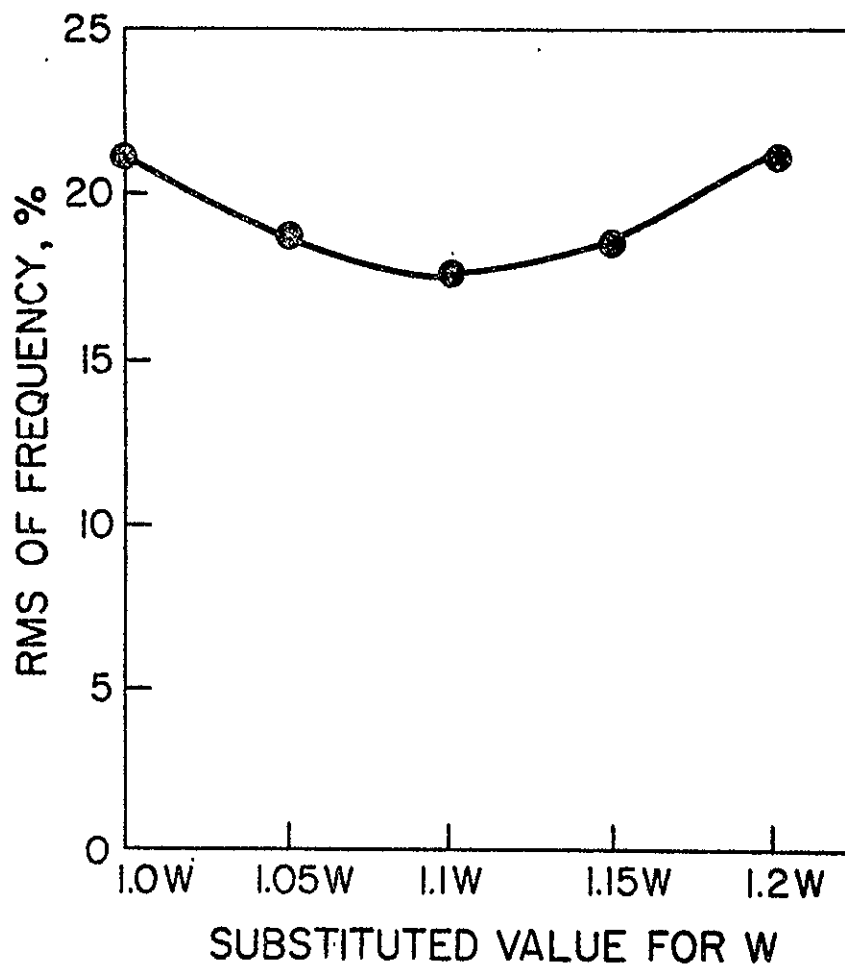


Fig 16: RMS vs substituted value for W in Equation 36 for 118 schoolchildren.

## EXPERIENCE WITH A COMPUTER BASED CLINICAL DATA RETRIEVAL SYSTEM

John Jurist and Kianpour Kianian

Previous reports [COO-1422-45, COO-1422-46] described a coding system used for recording clinical and normative data for various studies of skeletal status. This report describes experience with the coding system.

As of 23 February 1971, data from 433 subjects had been coded and stored in accordance with our system. (This represents a backlog of more than 250 subjects.) These data were recorded on 5,163 standard 80 column punch cards (an average of 11.9 cards/subject) and transcribed onto magnetic tape. Each card image requires 0.1 inch of tape (with 0.75 inch record gaps between card images) at a data density of 800 characters/inch. Hence, the 5,163 punch card images are stored on 365 feet of tape. At this data density, a reel of tape could hold data from approximately 2,850 subjects.

Of the 16 card types described in the previous reports, 3 have never been used (long bone impact data, skull and mandible data, and phase shift data).

A program was developed which translates the data on each patient into a format which can be conveniently used by the physician. A sample output from this program is included with this report. Note that, since the computer reads a blank or missing data as the number zero, some missing data (sitting height, for example) are assigned zero values.

A short program which identifies patients with specific diagnoses and therapeutic regimens was written. This program searched the data tape for the patient categories listed in the enclosed table. Execution of this program required 67 minutes on a Raytheon 440 computer and involved 10 passes through the magnetic data tape. Since the computer costs \$30/hour to operate, a data search costs approximately \$3.35/tape pass. In contrast, a manual search through the data would require about 4 man hours/pass.

We anticipate that this data recording and retrieval scheme will be useful in clinical studies of skeletal status.

Our next goal is to write a general purpose data searching program for identifying any patient with any specified diagnosis or therapeutic history.

ELEPHONE

WISC

BMID 2705 HOSPITAL ID 159097 LOCATION UW PATIENT  
MALF CAUCASIAN HANDEDNESS RIGHT BORN 12/ 5/ 1

REFERRAL BY ALLERGY

HISTORY OBTAINED 5/22/70

TRAUMATIC FRACTURE OF RIGHT 'WRIST'

TRAUMATIC FRACTURE OF LEFT SHOULDER

TRAUMATIC FRACTURE OF LEFT 'ANKLE'

NO SPONTANEOUS FRACTURES

NO FAMILY HISTORY OBTAINED

PHYSICAL DATA, DIAGNOSIS, AND THERAPY OBTAINED 5/22/70

INTERMEDIATE ACTIVITY

STANDING HEIGHT = 175 CM, SITTING HEIGHT = 0 CM, STANDING/SITTING HEIGHT = .00

TRICEPS SKINFOLD = MM, WEIGHT = 178 LBS

DIAGNOSIS -- BRONCHITIS

DIAGNOSIS -- SINUSITIS

LABORATORY DATA OBTAINED 5/19/70

SERUM TOTAL CALCIUM = 9.7 MGPCT, PHOSPHORUS = 2.1 MGPCT, TOTAL CA\*P = 20.4 MGPCT\*\*2

TOTAL PROTEIN = 7.5 GPCT, IONIC CALCIUM = 4.2 MGPCT, IONIC CA\*P = 8.8 MGPCT\*\*2

SERUM ALK PHOSPHATASE = 10.0 K+A UNITS, GGT = 0 UNITS, GPT = 0 UNITS, LDH = 0 UNITS

BONE MINERAL MEASURED 5/22/70

LEFT RADIUS, DISTAL 1/3

IODINE SOURCE AT 30 CM

BM = 1.41 G/CM, W = 1.66 CM, BM/W = .85 G/CM\*\*2, W/BM = 1.18 CM\*\*2/G

LEFT ULNA, DISTAL 1/3

IODINE SOURCE AT 30 CM

BM = 1.18 G/CM, W = 1.22 CM, BM/W = .97 G/CM\*\*2, W/BM = 1.04 CM\*\*2/G

LEFT RADIUS, 1.5-3 CM DISTAL

IODINE SOURCE AT 24 CM

BM = 1.32 G/CM, W = 2.63 CM, BM/W = .51 G/CM\*\*2, W/BM = 2.00 CM\*\*2/G

BONE MINERAL MEASURED 5/22/70

LEFT ULNA, 1.5-3 CM DISTAL

IODINE SOURCE AT 24 CM

BM = .70 G/CM, W = 1.11 CM, BM/W = .64 G/CM\*\*2, W/BM = 1.59 CM\*\*2/G

COMMENT DATED 5/22/70 LITTLE MILK, LITTLE DAIRY PRCD, SOME EXERCISE, BRONCHITIS 30  
YRS

END OF PATIENT RECORD

<u>SEX</u>	<u>GROUP</u>	<u>NUMBER OF PATIENTS IN GROUP</u>
F	Normal	41
F	Rheumatoid Arthritis (RA)	39
F	RA with cortisone	34
F	No RA with cortisone	9
F	Osteoporosis, no RA, no cortisone	6
M	Normal	29
M	RA	17
M	RA with cortisone	11
M	No RA with cortisone	4
M	Osteoporosis, no RA, no cortisone	1

MEASUREMENT OF TIBIAL RESONANT FREQUENCY:  
A PRELIMINARY REPORT

John W. Raasoch and John M. Jurist

Our laboratory is studying bone resonant frequency measurement as an indication of relative skeletal strength [1,2]. To date, we have used the ulna for resonant frequency studies -- driving the ulna at the olecranon process and measuring its response as a function of frequency with an accelerometer at the ulnar head. In hopes of improving the precision and usefulness of the resonant frequency measurement, we are evaluating the tibia. There are two reasons for employing the tibia: First, the tibia is less irregularly shaped than the ulna. Second, the tibia is a weight-bearing bone.

Our first consideration was whether the tibia should be horizontally or vertically oriented during the resonant frequency measurement. The horizontal position was chosen for several reasons. During resonant frequency studies, numerous specific modes of vibration have been detected. These different vibrational modes may be more readily excited by imperfect or inconsistent positioning relative to the irregularly shaped bone, variations in muscle tension, soft tissue edema, and other variable factors [3]. The excitation of inconsistent modes with repeated measurements occurs less frequently and is easier to detect with the tibia in the horizontal position than in the vertical position (Figure 1). In the horizontal position, two modes are often excited during a single recording, thus aiding in identification of these different modes. Another advantage of the horizontal position is the ability of a healthy subject to lay down, while a "cart patient" is not always able to sit up and hold his leg in a vertical position. The horizontal position is also convenient for the technician because of the relative ease of making the resonant frequency recording.

The next consideration was the positioning of driver and accelerometer on the tibia. Eight different combinations of accelerometer and driver position were investigated on eight tibiae (four subjects). The different locations are illustrated in Figure 2. As shown in Table I, position I is more desirable than positions II through VI because of a smaller probability of erroneously identifying inconsistent vibrational modes. A much "cleaner" record is also obtained with position I. It should be

noted that whenever the driver and the accelerometer are close together (positions III, VII, and VIII), two resonance peaks are commonly found on the same record. With the accelerometer at midshaft (positions VI, VII, and VIII), two peaks are also observed.

The ratio of the frequencies of the two different modes ( $F_B/F_A$ ) is essentially constant for positions I through VI. The  $F_B/F_A$  for positions VII and VIII, however, are markedly different. An elastic body filled with an incompressible fluid [4] exhibits vibrational modes which are approximately given by  $F_N = K_1 (K_2 + N)$ , where  $K_1$  and  $K_2$  are constants, and  $N$  is an integer. In order to obtain an  $F_B/F_A$  ratio of 1.33, it is assumed that  $K_2 + N_B = 4$  for mode B and  $K_2 + N_A = 3$  for mode A. The  $F_B/F_A$  ratio can be increased (as it was for positions VII and VIII), by decreasing the  $K_2 + N$  value, for example, to 2 for mode "A". Then,  $F_B/F_A = 1.50$ . However, if the second or higher mode (B) was suppressed, and the next higher mode was excited instead, the ratio of the two modes would be 1.67 ( $K_2 + N_C = 5$ ,  $K_2 + N_A = 3$ ) which approximates the 1.69 and 1.62 values obtained in positions VII and VIII. This latter possibility is also consistent with the increased difference between modal frequencies found in these positions (roughly twice the  $F_B - F_A$  values of positions I through VI). Therefore, it seems that mode B is suppressed or not excited and that a higher mode is excited in positions VII and VIII. In the equation  $F_N = K_1 (K_2 + N)$ , the value(s) of  $N$  can change with the positioning of the accelerometer and driver.  $K_1$  was also found to vary with these positional changes, presumably because of changes in boundary conditions. Positions I through III did not exhibit any significant shift in the value of  $K_1$ , while positions IV and VI exhibited  $K_1$  values about 20% larger than those of positions I through III. Positions V, VII, and VIII exhibited decreased values (10-20% less than the  $K_1$  of position I).

The "best" position for operational measurement of tibial resonant frequency becomes a choice between positions I, VII, and VIII. The lowest probability of erroneously identifying inconsistent vibrational modes was obtained with position VII (Table II). Subjectively, the "cleanest" resonance peak was obtained with

position I, and the largest resonance peak with position VIII. Therefore, no clear-cut choice between these three positions can be made, so position I will be used routinely because of the relative ease of measurement in this position.

Another consideration in measuring the tibia is whether to place the driver on the medio-anterior surface or on the anterior edge. Driving the tibia on the anterior edge is occasionally painful so the medio-anterior surface is used when pain is encountered. The amplitude of response is usually somewhat larger when the tibia is driven on the anterior edge.

Another finding in this study was the rather poor correlation between age and either tibial or ulnar resonant frequency. The ulnar resonant frequencies of children were significantly lower than previously reported [2] (Figures 3, 4, 5, and 6). However, these data were collected in the hospital, so some deviation from the findings for a "normal" population is not unreasonable.

Although we do not have sufficient data to prove this hypothesis, we believe that the resonant frequency versus age data shown in Figures 3 through 6 may represent "families" of curves corresponding to different vibrational modes.

The reproducibility of the tibial resonant frequency measurement ranged from 3% to 13% (RMS about the mean value). For 30  $F_A$  measurements made on one subject during one day, the RMS reproducibility was about 3%. The 13% reproducibility was obtained over several months of measurement (6 tibiae, 36  $F_A$  measurements) without correction for possible excitation of inconsistent modes. When different modes were identified, the RMS reproducibility about each individual mode was 6%. Without this modal identification, the RMS reproducibility of the ulnar  $F_A$  measurement was 10%. The standard deviation for the repeated ulnar resonant frequency measurement is about 32 Hz as contrasted to that for the tibia (about 42 Hz). However, the difference between adjacent vibrational modes for the tibia is about 37 Hz as compared to about 16 Hz for the ulna. A larger number of different modes can be excited in the ulna than in the tibia (Figure 7). However, the ulna still has a better reproducibility, especially when the measurements are corrected for vibrational mode. The technique of ulnar measurement involves the use of an arm support, while the preliminary tibial measurements were done with a hand-held driver. With some refinement of the tibial measurement technique, the large interval between adjacent resonance peaks in this bone suggests that

resonant frequency studies will improve in reliability by employing the tibia rather than the ulna. The relatively large interval between adjacent tibial resonance peaks will be especially useful during longitudinal studies of skeletal status by allowing identification of different vibrational modes.

In addition to being dependent on positioning, measured resonant frequency is also dependent on frequency sweep rate. It is necessary to use a constant frequency sweep because, at different sweep speeds, different modes may be preferentially excited. For example, our present apparatus has two frequency ranges: A "low" range (about 75 to 550 Hz), and a "high" range (about 150 to 1100 Hz). In the frequency interval in which the two ranges overlap (150 to 550 Hz), different frequency sweep rates are obtained, depending on which range the oscillator is set. We measured both ulnar and tibial resonant frequencies on four subjects (eight ulnae, eight tibiae) with both oscillator ranges. On six of the eight ulnae, the resonant frequencies measured on the two ranges were not equivalent. The resonant frequencies obtained with the oscillator set to the "high" range were higher than those with the oscillator set to the "low" range. On two of the ulnae (three vibrational modes), however, the resonant frequencies matched on both oscillator ranges (Table III). On three of the eight tibiae, resonant frequency values measured on the two ranges were not equivalent. On five of the tibiae (six modes), however, the resonant frequencies matched on both oscillator ranges (Table III). We interpret these findings as showing preferential suppression of lower vibrational modes at high frequency sweep rates such as obtained on the oscillator "high" frequency range. The other phases of this study were performed with the oscillator set on the "low" frequency range only. This problem warrants further investigation.

Age and skeletal condition reportedly affect ulnar resonant frequency [2]. Osteoporotics have been shown to have lower resonant frequencies -- possibly caused by preferential excitation of lower vibrational modes -- than normal subjects matched for age and sex. However, it is also possible that boundary conditions may be different in osteoporotics than in normal subjects because of systematic differences in muscle mass, joint impedance, etc.

Resonant frequency studies are ultimately aimed at distinguishing "osteoporotic" individuals from "normal" subjects. Ulnar resonant frequency studies have shown lower resonant frequencies for osteoporotic subjects [2] and preliminary (unpublished) tibial data support this. However, at present there is too much modal variation

between individuals to allow for an accurate diagnostic test. Positioning must be improved and specific vibrational modes and frequency intervals must be identified. "Good" or consistent positioning is also a function of the cooperation of the subject and thus indirectly of his health. Mode identification and subsequent correction of resonant frequency data increases reproducibility. With such correction, the tibia may prove more useful than the ulna. To this end, we will construct a tibia driver support, analogous to the ulna driver support described previously [1]. Figure 8 shows our design for such a driver.

#### References

1. Jurist, J. M.: In vivo determination of the elastic response of bone: I. Method of ulnar resonant frequency determination, Physics in Med. & Biol. 15:417-426, 1970.
2. Jurist, J. M.: In vivo determination of the elastic response of bone: II. Ulnar resonant frequency in osteoporotic, diabetic, and normal subjects, Physics in Med. & Biol. 15:427-434, 1970.
3. Jurist, J. M.; Dymond, A. M.: Reproducibility of ulnar resonant frequency measurement, Aerospace Med. 41:875-878, 1970.
4. Engin, A. E.; Liu, Y. K.: Axisymmetric response of a fluid-filled spherical shell in free vibrations, J. Biomechanics 3:11-22, 1970.

TABLE I

<u>POSITION</u>	<u>OCCURRENCES</u>		<u>PROBABILITY OF ERRONEOUS MODE IDENTIFICATION</u>	<u>MEAN FREQUENCIES</u>		$F_B/F_A$	$F_B - F_A$ (Hz)	$K_1$ (% of $K_1$ for Position I)
	<u>MODE A</u>	<u>MODE B</u>		$F_A$ (Hz)	$F_B$ (Hz)			
I	1/8	7/8	1/8	178	236	1.33	58	100
II	2/8	6/8	2/8	171	238	1.39	67	96
III	3/8	6/8	3/8	170	245	1.44	75	96
IV	5/8	3/8	3/8	211	260	1.23	49	119
V	6/8	2/8	2/8	158	206	1.30	48	89
VI	3/8	7/8	3/8	208	267	1.28	59	117
VII	8/8	8/8	0/8	147	249	1.69*	102	83
VIII	7/8	7/8	1/8	146	236	1.62*	90	82

\*For the first 6 positions, the mean value of  $F_B/F_A$  was 1.33 with a standard deviation of 0.08.

TABLE II

<u>POSITION</u>	<u>PROBABILITY OF ERRONEOUS MODE IDENTIFICATION</u>
I	1/8
VII	0/8
VIII	1/8

TABLE III

<u>BONE</u>	<u>RESONANT FREQUENCY VALUES (in Hz) OBTAINED FOR DIFFERENT OSCILLATOR FREQUENCY RANGES</u>			
	<u>LOW RANGE</u>		<u>HIGH RANGE</u>	
Ulna	202	207	201	205
	205	208		
Ulna	252		246	
Ulna	223	226	233	
	223	227		
	224	234		
Tibia	277		264	
Tibia	255		259	
Tibia	260		247	
Tibia	268	285	272	
	271			
Tibia	223	230	236	
	224	231		
	227	243		
	228			
Tibia	260	283	281	
	260	285		
	227	243		
	228			

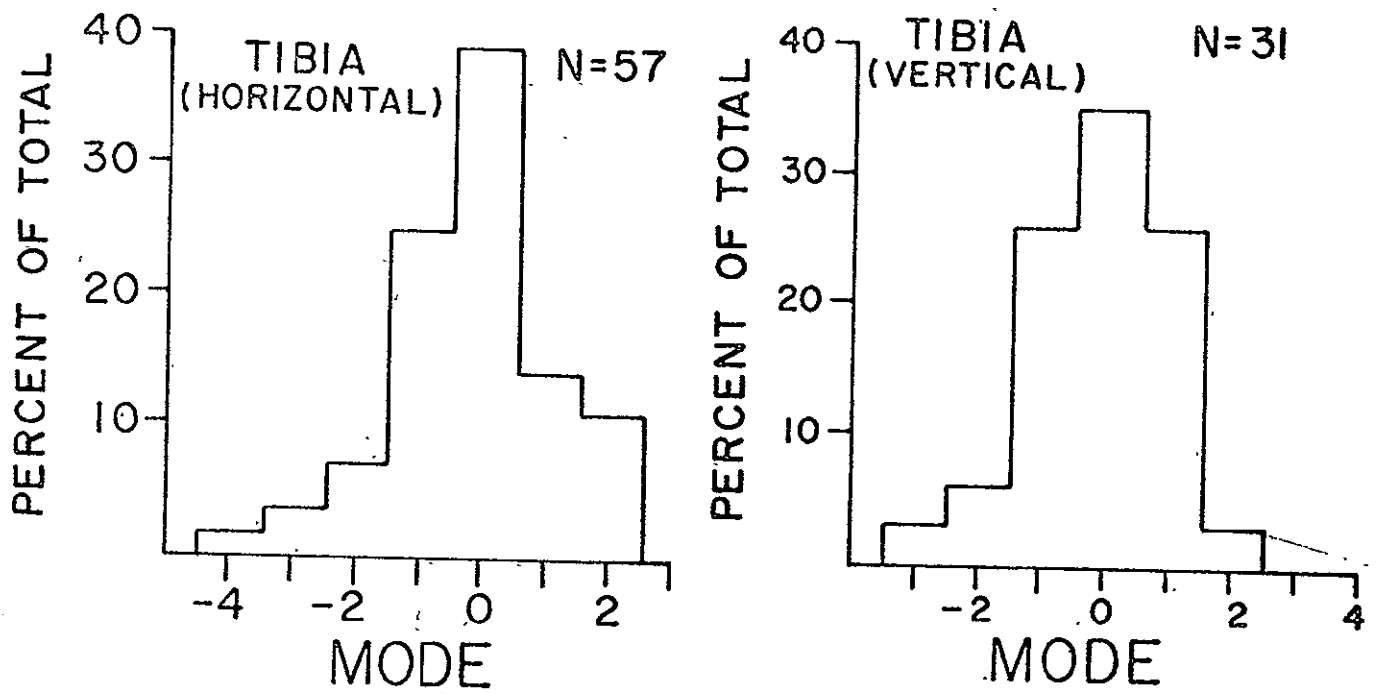


Fig. 1: Distribution of excitation of different vibrational modes in the human tibia as a function of orientation.

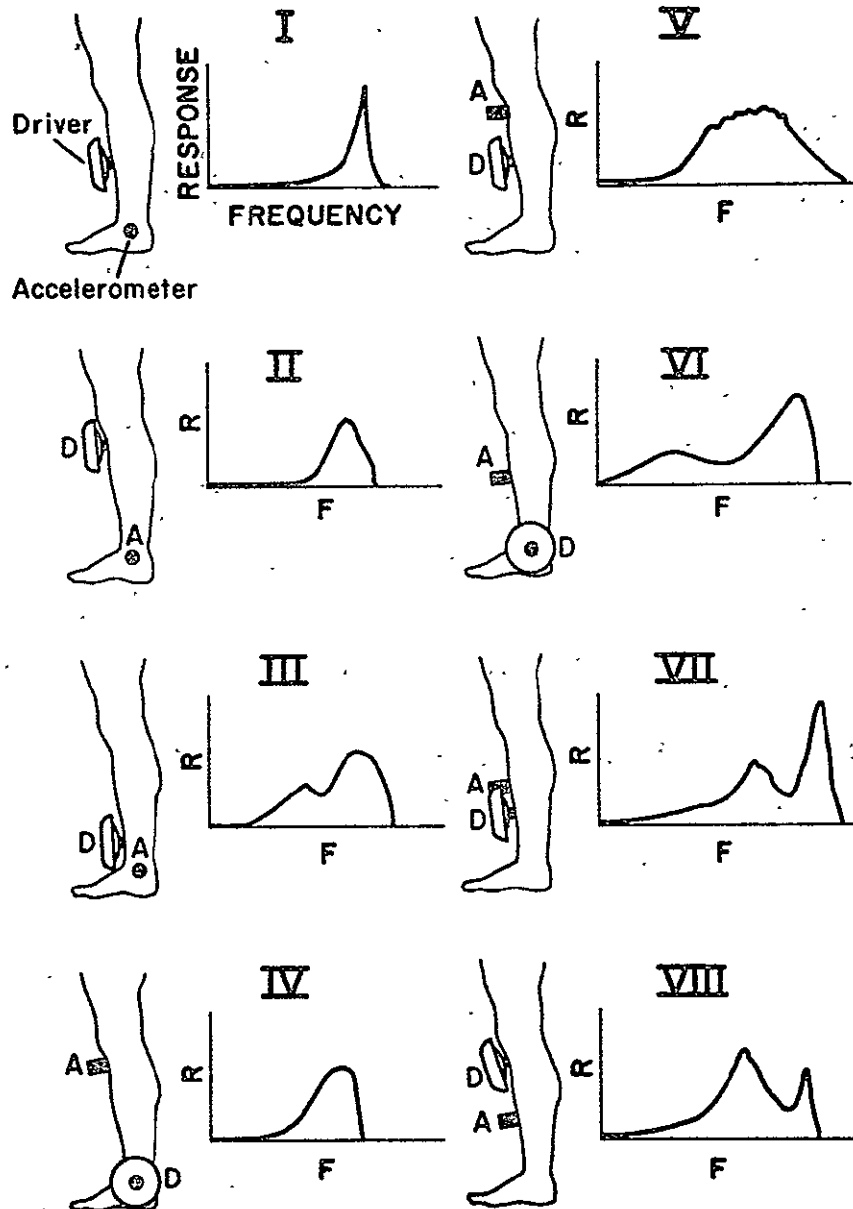


Fig. 2: Location of the driver and accelerometer on the leg for the 8 positions studied. The shape of a typical acceleration response vs driving frequency curve is illustrated for each position.

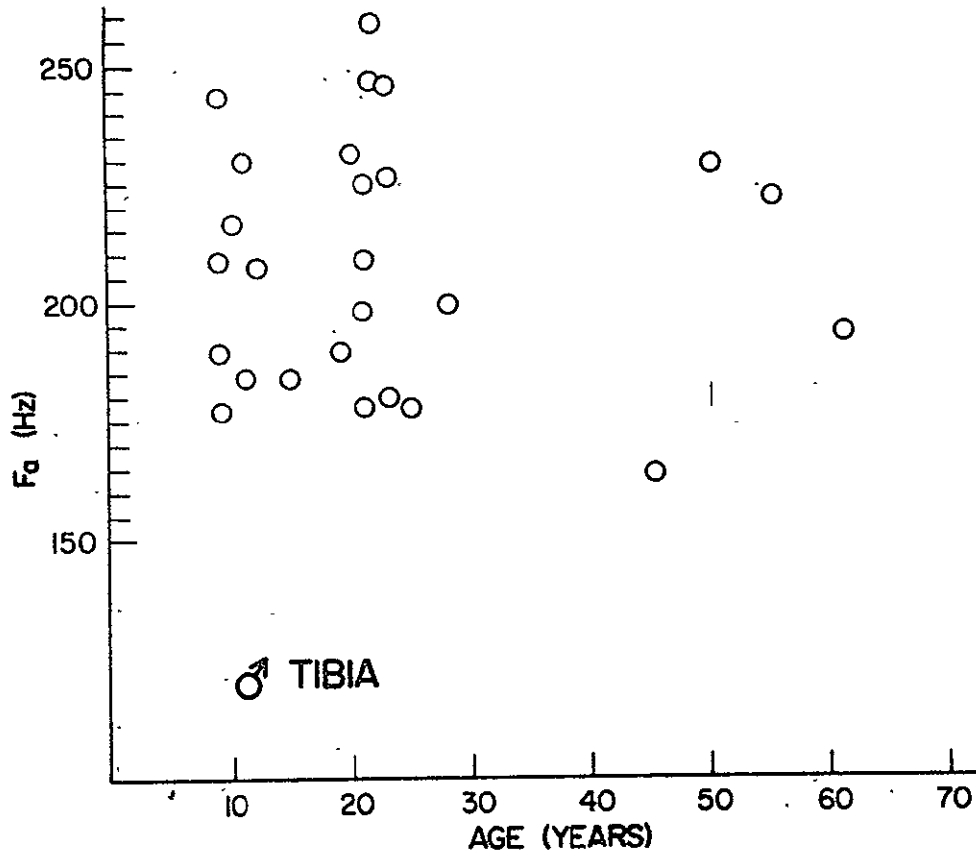


Fig. 3: Tibial resonant frequency vs age for 26 male patients.

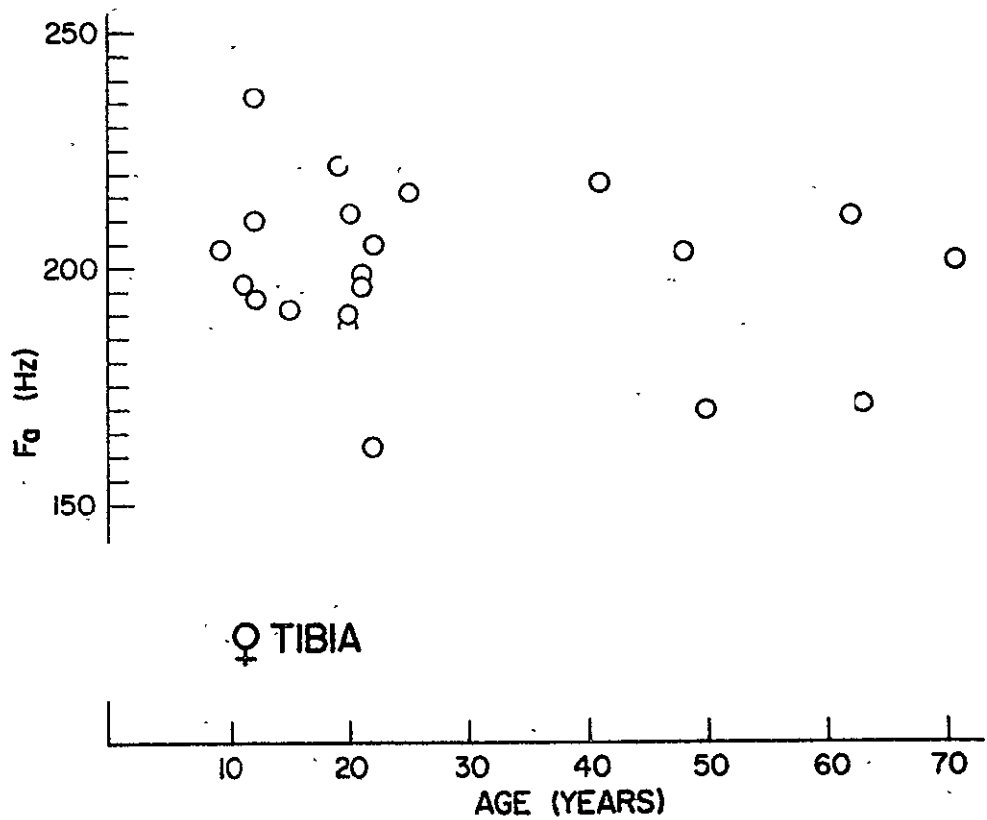


Fig. 4: Tibial resonant frequency vs age for 21 female patients.

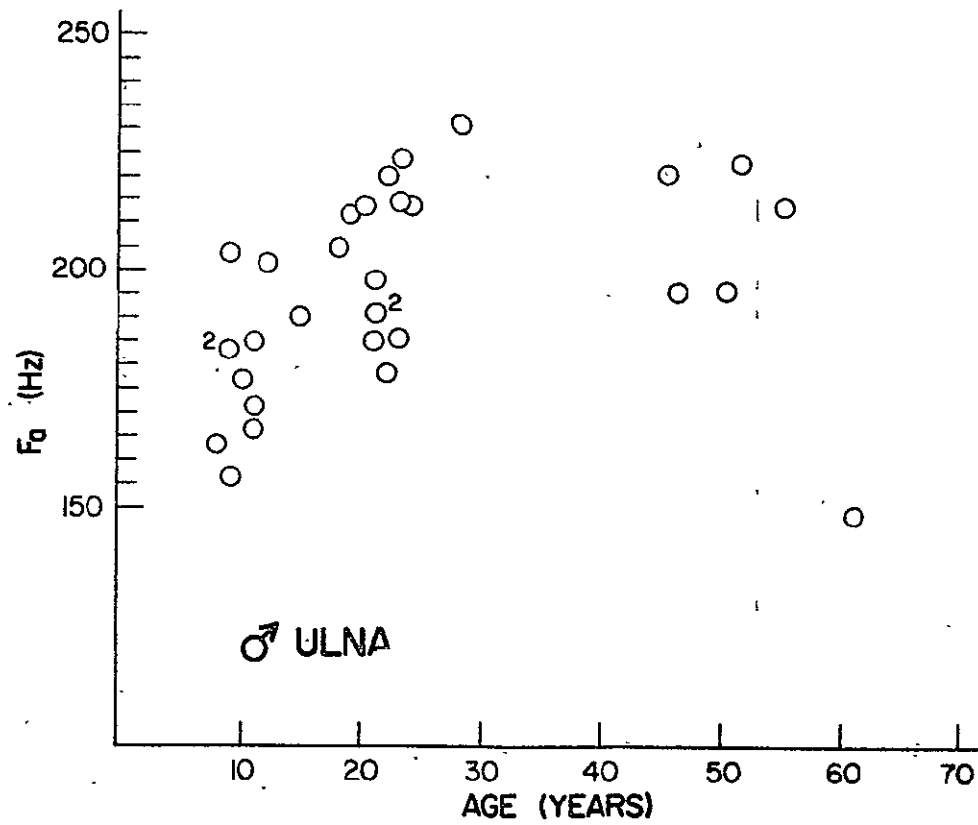


Fig. 5: Ulnar resonant frequency vs age for 31 male patients.

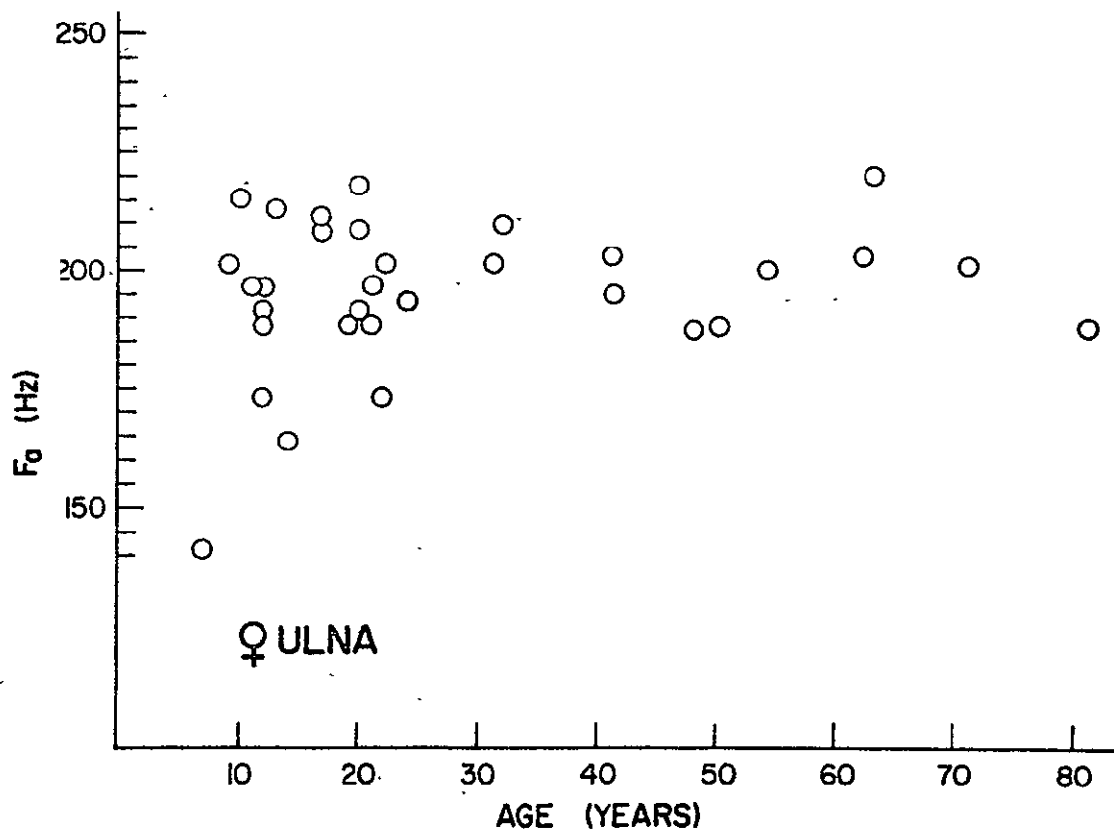


Fig. 6: Ulnar resonant frequency vs age for 32 female subjects.

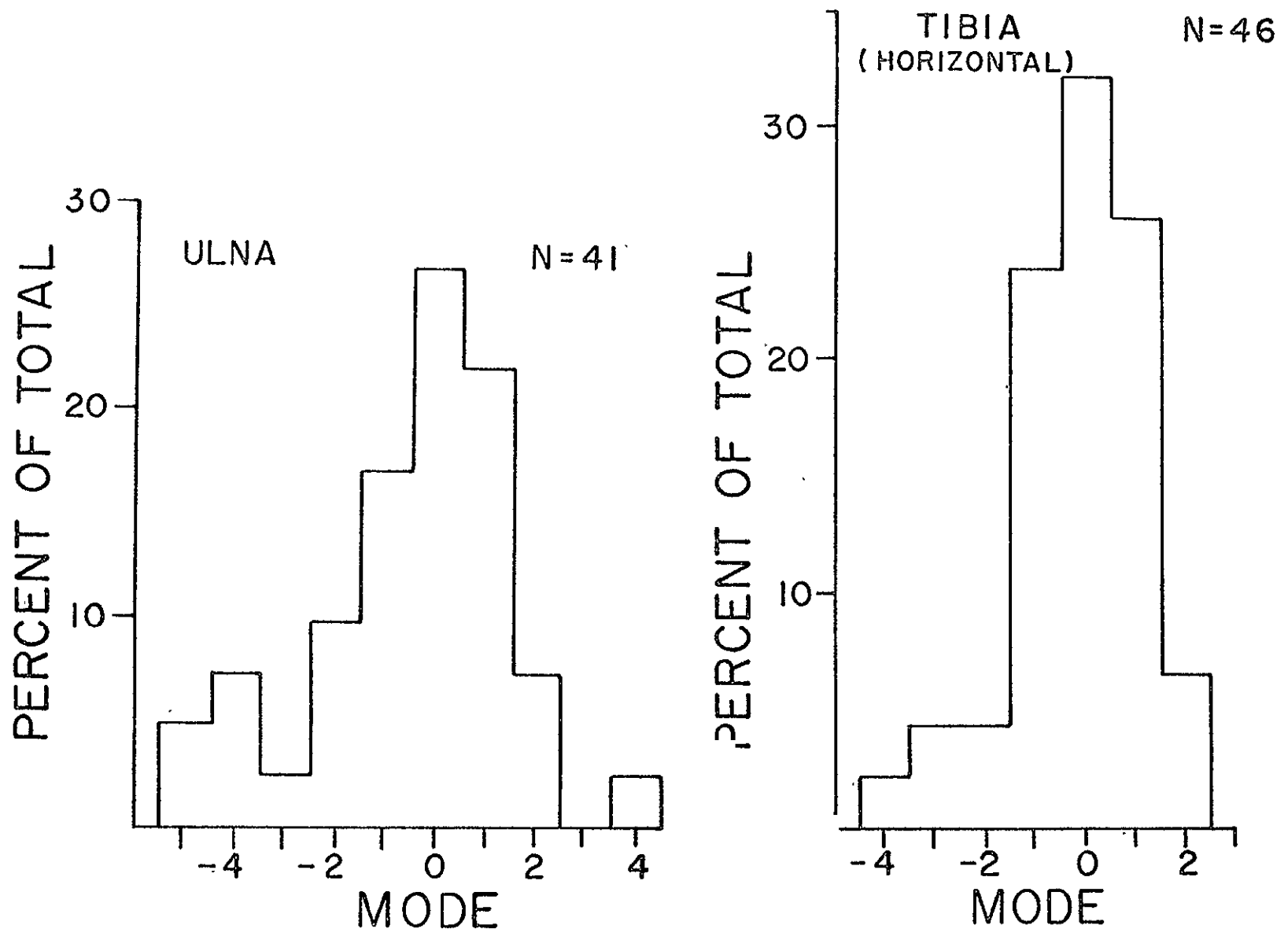


Fig. 7: Distribution of excitation of different vibrational modes in the ulna and in the tibia.

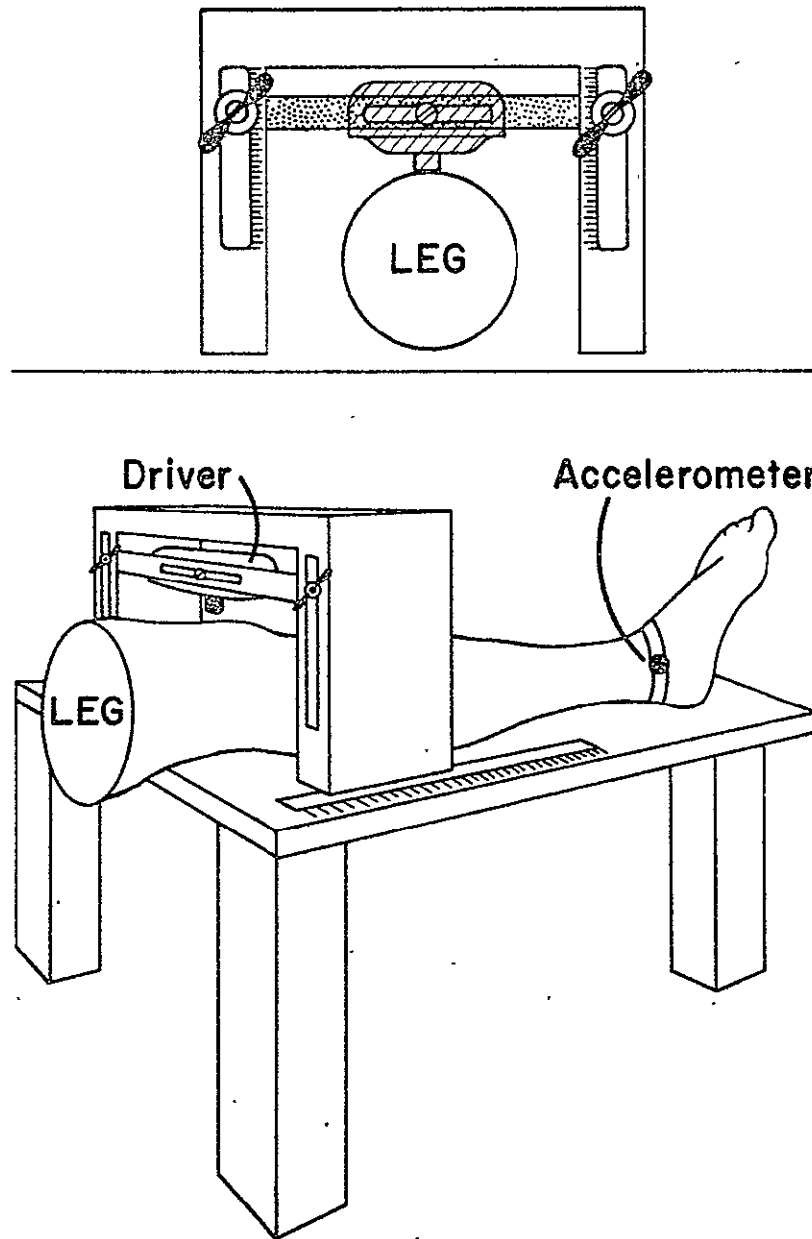


Fig. 8: Proposed support for tibial driver unit.

Femoral Trabecular Patterns and Bone Mineral Content<sup>\*⌘</sup>

BY DONALD H. KRANENDONK, M.D.<sup>⌘</sup> AND JOHN M. JURIST, PH.D.<sup>§</sup>,

MADISON, WISCONSIN

From the Division of Orthopedic Surgery, University  
of Wisconsin Medical Center, Madison

\* This investigation was supported by grants from the University of Wisconsin Division of Orthopedic Surgery, NASA (NGR50-002-051), and AEC (AT(11-1)1422).

⌘ Direct correspondence and reprint requests to Dr. Jurist.

⌘ 1015 Harlyn Ave., Rothchild, Wisconsin 54474.

§ 1300 University Ave., Madison, Wisconsin 53706.

### Introduction

We were intrigued by a recent article published by Singh and co-workers<sup>7</sup>. This article described a method of diagnosis and grading of the degree of osteoporosis in the proximal femur on the basis of trabecular pattern. The purpose of our study was to determine the relationship between the femoral rating system of Singh and the measured bone mineral content (BMC) of the radial midshaft in a series of women.

Cameron and co-workers at the University of Wisconsin have developed an accurate method of determining BMC by means of  $^{125}\text{I}$  photon absorptiometry<sup>3,9</sup>. This method is consistently reproducible at the 2% level<sup>2,6</sup>. The  $^{125}\text{I}$  photon absorptiometric method of measuring bone mineral content has demonstrated agreement with ash measurements of cadaver bones at the 3% level<sup>2,6</sup>. In addition, the usefulness of the radial midshaft BMC determination in assessing the degree of generalized osteoporosis has been established in our laboratory and in other laboratories using the same measurement site and technique<sup>4,5,8</sup>. Measurements of BMC made at the radial midshaft correlate well with measurements made at other sites on the appendicular skeleton including the humeral midshaft, ulnar midshaft, distal ulna and radius, distal femur, and tibial and

fibular midshaft. In addition, the radial BMC measurement correlates well with the grade of spinal osteoporosis as determined radiographically and with the vertebral and whole skeleton ash content as measured on cadavers. Detailed descriptions of the technique are available in the literature.

### Methods

Nineteen subjects were included in the study. They were females at least forty-eight years old who had no evidence of rheumatoid arthritis. These women had never received corticosteroid therapy. The group contained nine presumably nonosteoporotic controls and ten patients known to have symptomatic osteoporosis. We defined symptomatic osteoporosis to be the presence of vertebral collapse or femoral neck fractures associated with minimal trauma.

Anteroposterior radiographs of the proximal femora of these subjects were taken while their hips were internally rotated 20°. Three hips were not included in the study because of the presence of a femoral nail, an Austin-Moore prosthesis, and an ununited femoral neck fracture. Two orthopedic residents and three orthopedic staff members rated the hip films according to Singh's system.

### Results

Femoral trabecular patterns can be consistently scored by different individuals. The root-mean-square deviation about the mean score for each femur was 0.86 points on a scale of one to six. Over 90% of the scores were within 1.2 points of the mean for each femur. For the sixteen subjects in which bilateral hip films were used, there was good agreement between the scores for left and right femora (Fig. 1).

There was no significant correlation between the femoral trabecular score and the radial bone mineral content. In fact, there was a slight negative correlation ( $r = -0.130$ ) between these two parameters (Fig. 2). As osteoporosis develops, resorption of fine trabeculae makes a coarse trabecular pattern more apparent. This factor may be responsible for the negative correlation. An illustration of the negative correlation between the femoral score and BMC is provided by a forty-eight year old woman (M.S.) with known symptomatic osteoporosis. She had the second lowest BMC in our series (0.58 g/cm). The mean bone mineral content for women referred to our laboratory with spontaneous hip or vertebral fractures is  $0.62 \pm 0.12$  (standard deviation) g/cm. The upper limit of BMC for women with spontaneous fractures<sup>8</sup> is about

0.80 g/cm. The average bone mineral content for normal forty to forty-nine year old women<sup>1</sup> is  $0.98 \pm 0.10$  g/cm. Yet, the trabecular ratings for this woman averaged 5.6--the highest in our series (Fig. 3).

We then tested the relationship between the femoral score and the bone mineral content corrected for age. For this test, the difference ( $\Delta$ BM) between the BMC of each patient and the mean BMC of clinically normal women of the same age range was expressed as a function of femoral score. A statistically insignificant negative correlation ( $r = -0.242$ ) was obtained (Fig. 4). The normal values of BMC were obtained from a previously published report<sup>1</sup>.

It is our impression that the tensile trabeculae are relatively less prominent and often nearly absent in valgus hips (Fig. 5). We have also noted a poor association between femoral cortical thickness and scores based on trabecular patterns.

### Conclusion

On the basis of these observations, we conclude that the trabecular patterns of the proximal femur as described by Singh and co-workers are not correlated with bone mass. Thus, these trabecular patterns are of little or no help in establishing the

diagnosis or severity of osteoporosis.

#### Summary

Radiographs of thirty-five hips internally rotated by  $20^{\circ}$  in nineteen women at least forty-eight years old without rheumatoid arthritis were scored for the relative degree of osteoporosis according to criteria published by Singh and co-workers. Bone mineral content of the radial midshaft was measured in these women by the  $^{125}\text{I}$  photon absorptiometric method developed by Cameron and co-workers.

No significant correlation was found between these two parameters either directly or after correction of the bone mineral data for the ages of the subjects.

We conclude that the trabecular scoring method described by Singh and co-workers is of little or no help in establishing the diagnosis for severity of osteoporosis.

Note: We wish to acknowledge the assistance of Doctors Andrew McBeath, Rolf Lulloff, and Herman Wirka in scoring radiographs and providing helpful criticism.

References

1. CAMERON, J.: Summary of Data on the Bone Mineral of the Radius in Normals. AEC Contractor Report COO-1422-41, 1969.
2. CAMERON, J.; MAZESS, R.; and SORENSON, J.: Precision and Accuracy of Bone Mineral Determination by Direct Photon Absorptiometry. *Inv. Radiol.*, 3:141-150, 1968.
3. CAMERON, J.; and SORENSON, J.: Measurement of Bone Mineral in Vivo: An Improved Method. *Science*, 142:230-232, 1963.
4. GOLDSMITH, N.; JOHNSTON, J.; URY, H.; VOSE, G.; and COLBERT, C.: Bone-Mineral Estimation in Normal and Osteoporotic Women. *J. Bone and Joint Surg.*, 53-A:83-100, Jan. 1971.
5. JOHNSTON, C.; SMITH, D.; YU, P.; and DEISS, W.: In Vivo Measurement of Bone Mass in the Radius. *Metabolism*, 17:1140-1153, 1968.
6. MAZESS, R.; CAMERON, J.; O'CONNOR, R.; and KNUTZEN, D.: Accuracy of Bone Mineral Measurement. *Science*, 145:388-389, 1964.
7. SINGH, M.; NAGRATH, A.; and MAINI, P.: Changes in Trabecular Pattern of the Upper End of the Femur as an Index of Osteoporosis. *J. Bone and Joint Surg.*, 52-A:457-467, Apr. 1970.
8. SMITH, E.; JURIST, J.; BABCOCK, S.; and CAMERON, J.: Detection of Osteoporosis by Measurement of Monoenergetic Photon Absorption. In 8th International Congress of Gerontology, Proceedings-Volume II, p. 53. Washington, D.C., International Association of Gerontology, 1969.
9. SORENSON, J.; and CAMERON, J.: A Reliable in Vivo Measurement

of Bone-Mineral Content. J. Bone and Joint Surg., 49-A:481-497,  
Apr. 1967.

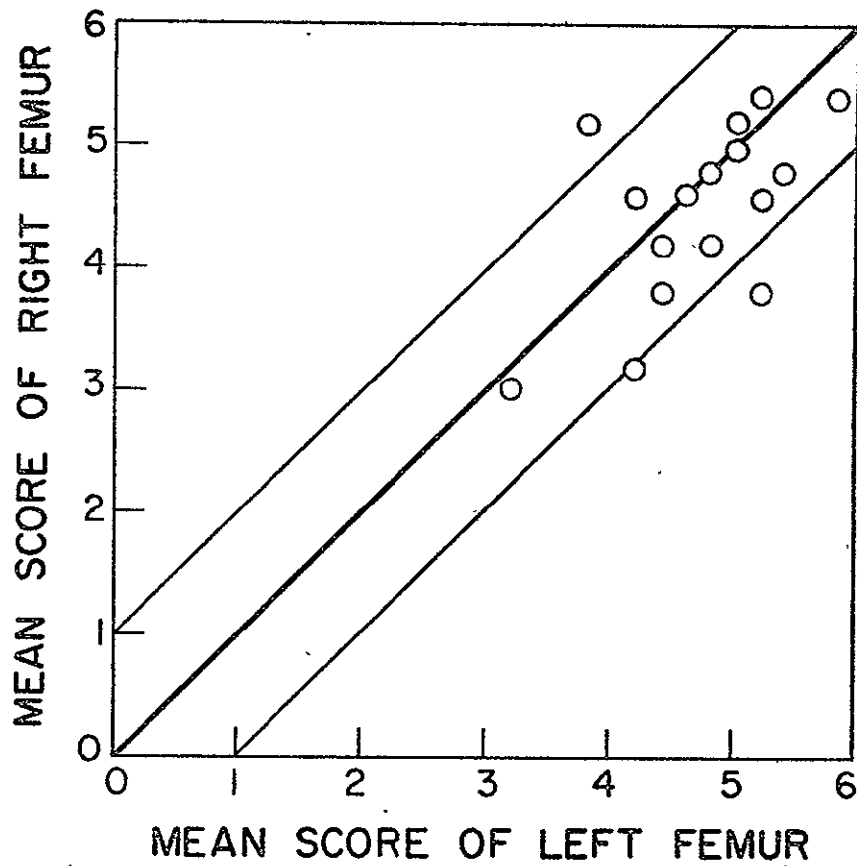


Fig. 1: Mean trabecular score of right femur versus mean score of left femur in sixteen women. Note that thirteen of the sixteen pairs of scores agree within one point.

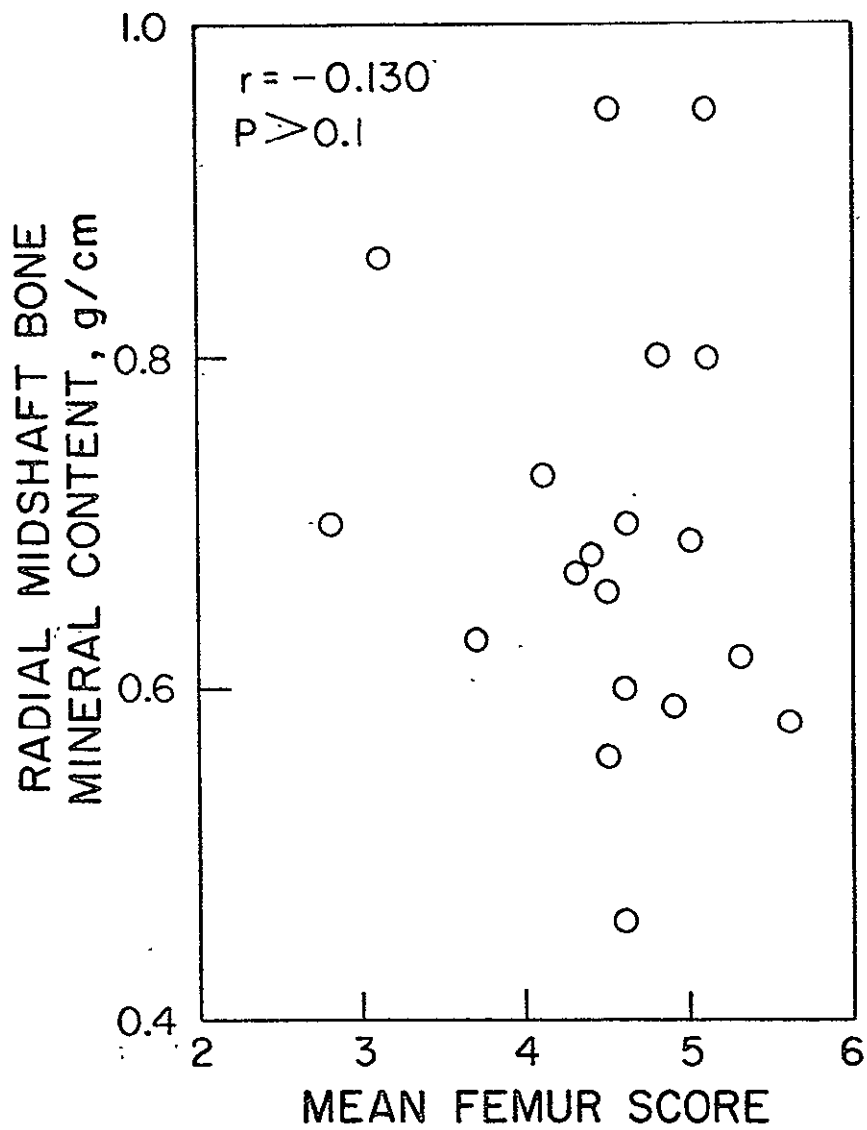


Fig. 2: Radial midshaft bone mineral content (BMC) versus mean femoral score. Note the lack of significant correlation between these two parameters.

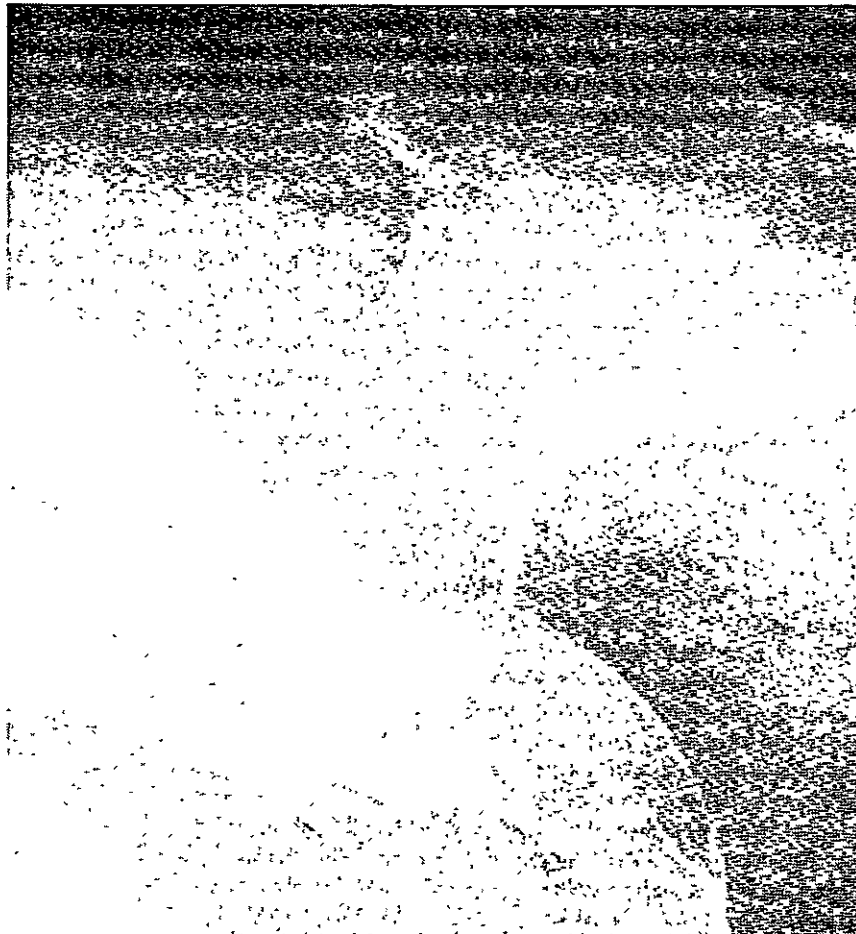


Fig. 3: Left femur with a mean score of 5.8. The score of the right femur of this patient was 5.4. The bilateral average score of 5.6 was the highest in our series although the BMC of 0.58 g/cm was the second lowest in our series.

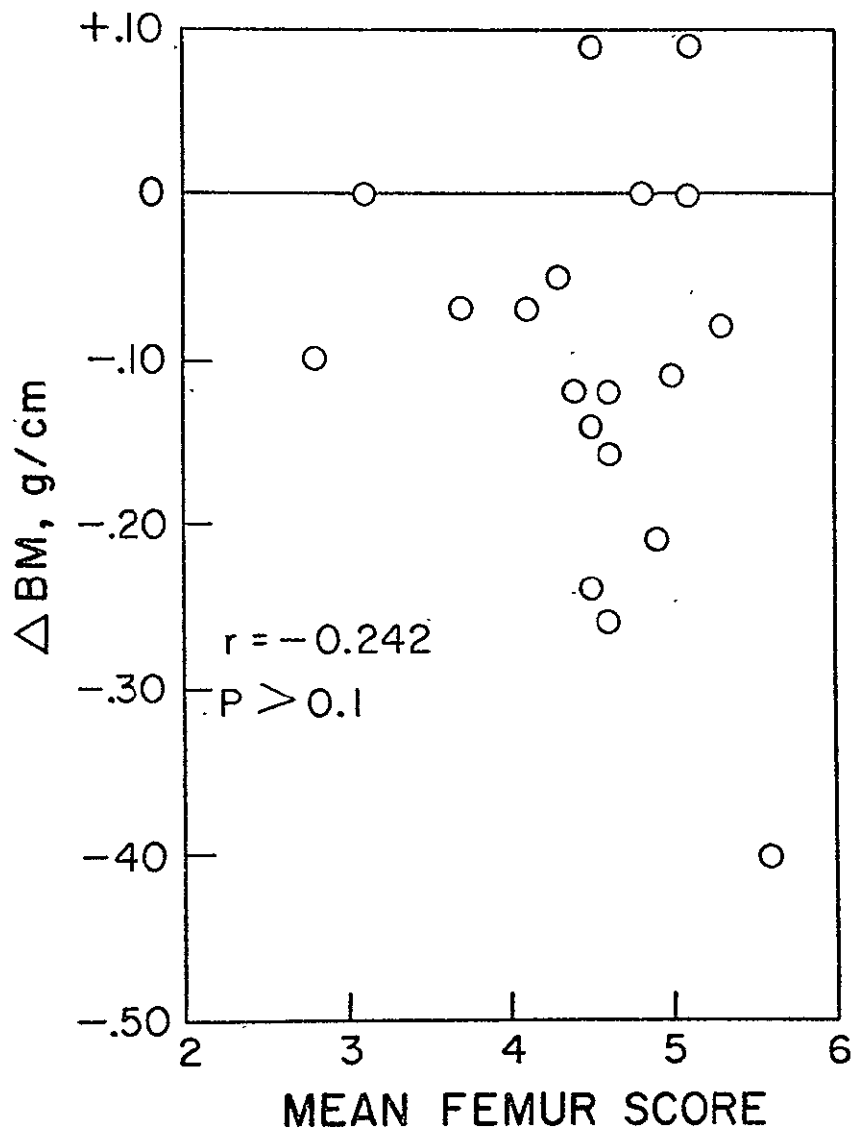


Fig. 4: Radial midshaft BMC corrected for age versus mean femoral score. Negative values signify below normal BMC. There is no significant correlation.

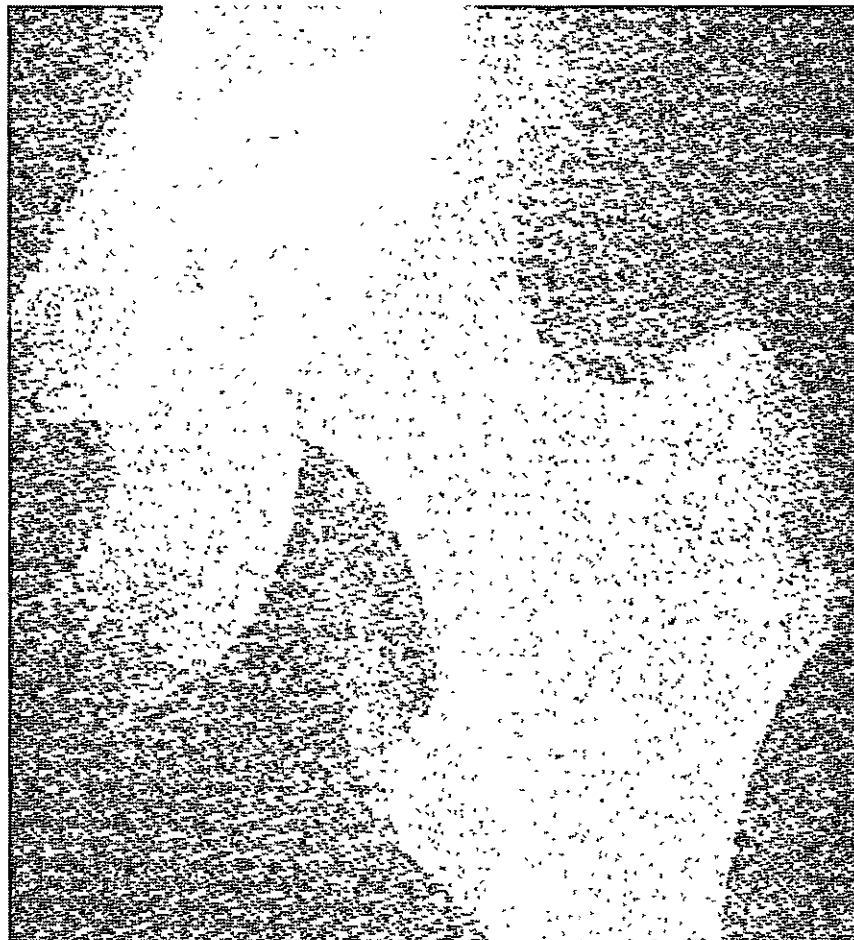


Fig. 5: Valgus hip. Note the relative absence of the principal tensile trabeculae. The absence of these trabeculae was a common finding in valgus hips. The mean score for this femur was 3.0, yet the BMC of this patient was 0.86 g/cm--a normal value. In fact, this woman had the third highest BMC in our series. Note that the femoral cortex is relatively thick even though the trabecular score of 3.0 was the second lowest in our series.

**Skeletal Status in Rheumatoid Arthritis:**

**A Preliminary Report**

**Mark N. Mueller and John M. Jurist**

From the University of Wisconsin Medical Center, 1300 University Avenue, Madison, Wisconsin 53706.

MARK N. MUELLER, MD: Assistant Professor, Department of Medicine. JOHN M. JURIST, PhD: Assistant Professor, Division of Orthopedic Surgery.

### SYNOPSIS

Twenty-six women with ARA classic or definite rheumatoid arthritis age-matched with controls were evaluated for bone mineral content and rigidity. Significant bone loss occurred in arthritics treated with corticosteroids. Bone losses at diaphyseal and metaphyseal sites were of similar magnitude -- suggesting no preferential loss of trabecular bone. A significant decrease in relative ulnar rigidity was observed in rheumatoids not receiving corticosteroids. An even larger decrease was noted in subjects receiving steroids.

### INTRODUCTION

Osteoporosis is commonly held to be associated with rheumatoid arthritis (1-9). Radiographic descriptions of rheumatoid arthritis frequently cite juxta-articular and generalized bone loss as being characteristic of this disease (10-12). The etiology of the bone loss is not understood, but is attributed to multiple factors such as local inflammation, immobilization, generalized catabolic processes secondary to the disease itself, poor nutrition, and the nature and duration of therapy with corticosteroids or other anti-inflammatory agents. The specific role of each factor is

poorly defined at present -- partly because of the lack of sensitive quantitative techniques of evaluating changes in mass or structural properties of the skeleton.

For the past 10 years, the Bone Measurement Laboratory at the University of Wisconsin has been developing a technique for the precise determination in vivo of bone mineral content by monoenergetic photon absorptiometry (13,14). Recently, we extended our interest in the physical evaluation of skeletal status to include measurement of bone resonant frequency (15,16). This paper reports the mineral content and resonant frequency of bone in patients with rheumatoid arthritis.

## METHODS

### Subjects

All patients attending the University of Wisconsin Arthritis Clinic are evaluated for bone mineral and resonant frequency on a routine basis. Twenty-six women with classic or definite rheumatoid arthritis by American Rheumatism Association criteria (17) were sequentially selected from the Clinic and matched for age with equal numbers of female control subjects who were free of any identifiable arthritis or other diagnosis commonly associated with osteoporosis.

The control subjects were selected from University of Wisconsin staff, visitors, and local women's groups and were not University of Wisconsin Hospital or Clinic patients.

#### Monoenergetic Photon Absorptiometry

Traditional roentgenographic or densitometric techniques are unsatisfactory for objective evaluation of bone mass because of large systematic errors and poor reproducibility. The monoenergetic photon absorptiometric technique was developed to eliminate the major sources of error associated with radiographic photodensitometry.

The photon absorptiometric technique measures attenuation of a photon beam (usually the 27.4 keV photon of  $^{125}\text{I}$ ) passing through the bone of interest (Fig 1). The bone mineral mass ( $M_B$ ) at any point in the path of the photon beam is proportional to  $\ln(I_0^*/I)$  when the total "tissue" thickness is constant both above and at the sides of the bone. The measured quantities are the intensity of the beam through the soft tissue adjacent to the bone ( $I_0^*$ ) and through a point of the bone ( $I$ ). The proportionality constant relating  $M_B$  and  $\ln(I_0^*/I)$  may be determined empirically or may be obtained from tabulated absorption coefficients since a single, well-defined photon energy is used. The photon absorptiometric technique has been described in detail elsewhere (18,19).

### Measurement of Vibratory Properties

The measurement of relative bone rigidity is of interest because of the reported correlations between bone strength, mineral content, geometry, and elastic moduli as measured in vitro (20,21). Thus, if reliable in vivo estimation of rigidity can be made, it will ultimately be possible to predict the bone strength of patients with disorders affecting the skeleton.

The speed of sound in a material is related to both elasticity and density (22,23). Hence, measurement of the speed of sound propagation in bone affords a possible way of estimating the elasticity and therefore strength of this material. We are studying measurement in vivo of the speed of sound in the ulna, tibia, and pelvis. Our most effective approach has been to determine resonant frequency of a long bone such as the ulna from a recording of the response of the bone to mechanical vibration as a function of frequency (Fig 2).

The resonance of the ulna (or any other long bone) may be described by  $F_a L = KC$ , where  $F_a$  and  $L$  are the measured ulnar resonant frequency and length,  $C$  is the speed of sound in the ulna, and  $K$  is a proportionality constant dependent on the mode of vibration, boundary conditions, and geometrical factors. Since  $Y = \rho C^2$ , where  $Y$  is Young's elastic modulus of bone and  $\rho$  is its density,  $Y$  is

proportional to  $(F_a L)^2$ . Thus, the measured value of  $F_a L$  may be used as an indication of relative bone rigidity or elasticity.

### Measurements

The bone mineral content (BM) and width (W) of the left radial diaphysis was measured at a distance of 30% of the ulnar length proximal to the ulnar head in 26 women with ARA classic or definite rheumatoid arthritis. Measurement at this site provides an index of compact bone mass. In addition, BM and W were measured near the distal end of the left radius in these women (at a site 2 cm proximal to the ulnar head) in order to obtain an index of the mass of trabecular bone. These two measurement sites are termed diaphyseal and metaphyseal sites, respectively.

The product of ulnar resonant frequency and length ( $F_a L$ ) was measured on both left and right ulnae of 23 women with classic or definite rheumatoid arthritis. The left and right  $F_a L$  values of each woman were averaged.

### RESULTS

A summary of our findings is presented in Figs 3-5. Bone mineral/width ratios (BM/W) for rheumatoid subjects without prior corticosteroid treatment are not significantly different from those

of their age and sex-matched controls. Resonant frequency measurements ( $F_a$ ) were approximately 20% less than those of control subjects.

Corticosteroid-treated rheumatoid women demonstrate significant differences in mineral content at both diaphyseal and metaphyseal sites of the radius relative to their controls. Resonant frequency differences between the steroid-treated rheumatoids and their controls are more marked than for the rheumatoids not treated with steroids.

The mean metaphyseal-diaphyseal ratio of BM/W in control subjects is 0.71. The corresponding ratios for nonsteroid and steroid-treated rheumatoids are not significantly different.

#### DISCUSSION

Although any conclusions to be drawn from this preliminary study are necessarily limited by the small number of subjects involved, some generalizations may be made. In noncorticosteroid-treated subjects, no apparent difference in bone mineral content was observed at the metaphyseal or diaphyseal site. With larger numbers of patients, significant differences may become apparent, particularly when the variables of disease duration and severity are considered.

The differences between rheumatoids and controls at both sites

of the radius are significant in corticosteroid-treated patients. Whether these differences are a result of corticosteroid administration or are related to a possible selective process in women for whom cortisone is prescribed is not clear. Further studies to resolve this question by matching rheumatoids on cortisone with those not on cortisone for disease duration and severity are in progress.

The apparent loss of skeletal mass in corticosteroid-treated rheumatoids is of similar magnitude at the diaphyseal and metaphyseal sites of the radius. This finding does not support the hypothesis that a preferential loss of bone occurs at the metaphyseal site, as would be implied from radiographic descriptions of "juxta-articular" osteoporosis.

The  $F L_a$  determination provides an index of the relative rigidity of bone. Rigidity of any long object is a function of mass, the spatial distribution of material about the long axis of the object, and the mechanical quality or elasticity of the material. A decrease in bone mass would therefore produce a consequent decrease in  $F L_a$ . However, in our observations, a relatively small percentage change in bone mineral (or bone mass) apparently leads to a large change in  $F L_a$ . This suggests that the structural or mechanical quality of the long bone as well as its mass may be altered by corticosteroid therapy.

### ACKNOWLEDGMENTS

This research was supported by grants and awards from the following agencies: The Arthritis Foundation of Wisconsin, the Wisconsin Alumni Research Foundation, the University of Wisconsin Surgical Associates, the National Aeronautics and Space Administration (Grant NGR50-002-051), and the Atomic Energy Commission (Grant AT(11-1)1422).

The authors are indebted to Drs. John Cameron and Andrew McBeath for their advice and support. Mrs. Joyce Fischer and Mrs. Susan Kennedy aided substantially in the collection and reduction of data.

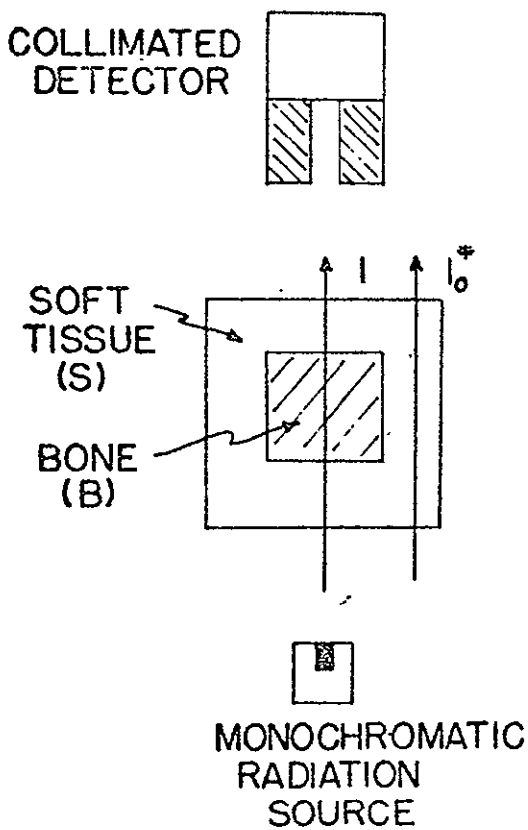
### REFERENCES

1. Soila P: Roentgen manifestations of adult rheumatoid arthritis. Acta Rheum Scand, supplement 1, 1958
2. Bywaters E: The early radiological signs of rheumatoid arthritis. Bull Rheum Dis 11:231-234, 1960
3. Bjelle A, Nilsson B: Osteoporosis in rheumatoid arthritis. Calcif Tissue Res 5:327-332, 1970
4. McConkey B, Fraser G, Bligh A: Transparent skin and osteoporosis - a study in patients with rheumatoid disease.

- Ann Rheum Dis 24:210-223, 1965
5. Castillo B, ElSallab R, Scott J: Physical activity, cystic erosions, and osteoporosis in rheumatoid arthritis. Ann Rheum Dis 24:522-526, 1965
  6. Duncan H, Frost H, et al: The osteoporosis of rheumatoid arthritis. Arthritis Rheum 8:943-954, 1965
  7. Saville P, Karmosh O: Osteoporosis of rheumatoid arthritis. Influence of age, sex, and corticosteroids. Arthritis Rheum 10:423-430, 1967
  8. O'Brien W, Samuels B, et al: The role of corticosteroids in causing osteoporosis in rheumatoid arthritis. Arthritis Rheum 11:501, 1968
  9. Martel W: Radiologic manifestations of rheumatoid arthritis with particular reference to the hand, wrist, and foot. Med Clin N Amer 52:655-665, 1968
  10. Berens P, Lockie L, et al: Roentgen changes in early rheumatoid arthritis. Radiology 82:645-654, 1964
  11. Soila P: The causal relations of rheumatoid disintegration of juxta-articular bone trabeculae. Acta Rheum Scand 9:231-236, 1963

12. Collins D: Pathology of Bone. London, Butterworths, 1966, pp 120-128
13. Sorenson J, Cameron J: A reliable in vivo measurement of bone mineral content. J Bone Joint Surg 49A:481-497, 1967
14. Cameron J, Sorenson J: Measurement of bone mineral in vivo. Science 142:230-232, 1963
15. Jurist J: In vivo determination of the elastic response of bone: I. Method of ulnar resonant frequency determination. Phys Med Biol 15:417-426, 1970
16. Jurist J: In vivo determination of the elastic response of bone: II. Ulnar resonant frequency in osteoporotic, diabetic, and normal subjects. Phys Med Biol 15:427-434, 1970
17. Ropes M, Bennett G, et al: Diagnostic criteria for rheumatoid arthritis - 1958 revision. Ann Rheum Dis 18:49-53, 1959
18. Cameron J, Mazess R, Sorenson J: Precision and accuracy of bone mineral determination by direct photon absorptiometry. Invest Radiol 3:141-150, 1968
19. Mazess R, Cameron J, et al: Accuracy of bone mineral measurement. Science 145:388-389, 1964
20. Mather B: Comparison of two formulae for in vivo prediction

- of strength of the femur. Aerospace Med 38:1270-1272, 1967
21. Currey J: The mechanical consequences of variation in the mineral content of bone. J Biomech 2:1-11, 1969
  22. Kinsler L, Frey A: Fundamentals of Acoustics. New York, Wiley, 1950, p 68
  23. Abendschein W, Hyatt G: Ultrasonics and selected physical properties of bone. Clin Orthop 69:294-301, 1970



$$M_B = \frac{\rho_B \ln(I_0^*/I)}{(\mu_B \rho_B - \mu_S \rho_S)}$$

= BONE MINERAL MASS  
PER UNIT AREA IN  
RADIATION BEAM PATH  
(GM/CM<sup>2</sup>)

$\mu$  = MASS ABSORPTION  
COEFFICIENT (CM<sup>2</sup>/GM)

$\rho$  = MICROSCOPIC  
DENSITY (GM/CM<sup>3</sup>)

Fig 1: Schematic diagram illustrating the basic principles used in measuring bone mineral mass with a monoenergetic photon source. The bone mineral mass per unit area in the beam path is given by the equation.

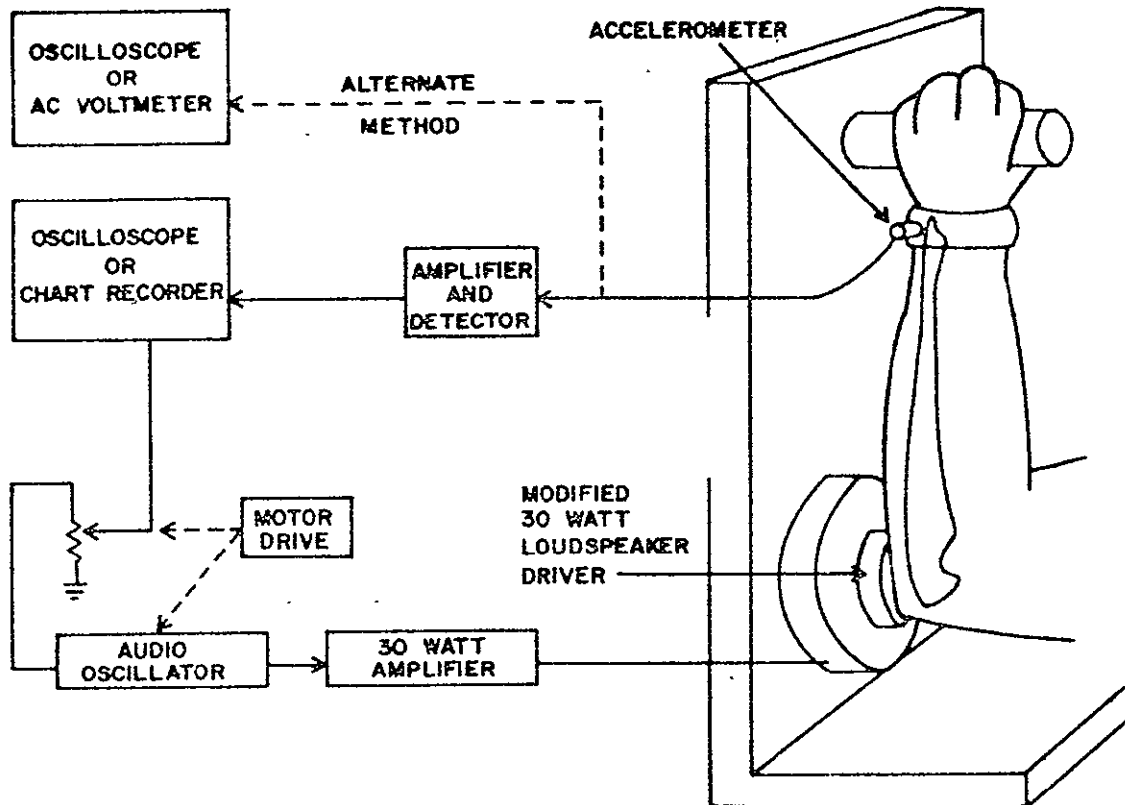


Fig 2: Method of measuring ulnar resonant frequency. Resonant frequency is determined from a recording of the acceleration response as a function of driving frequency.

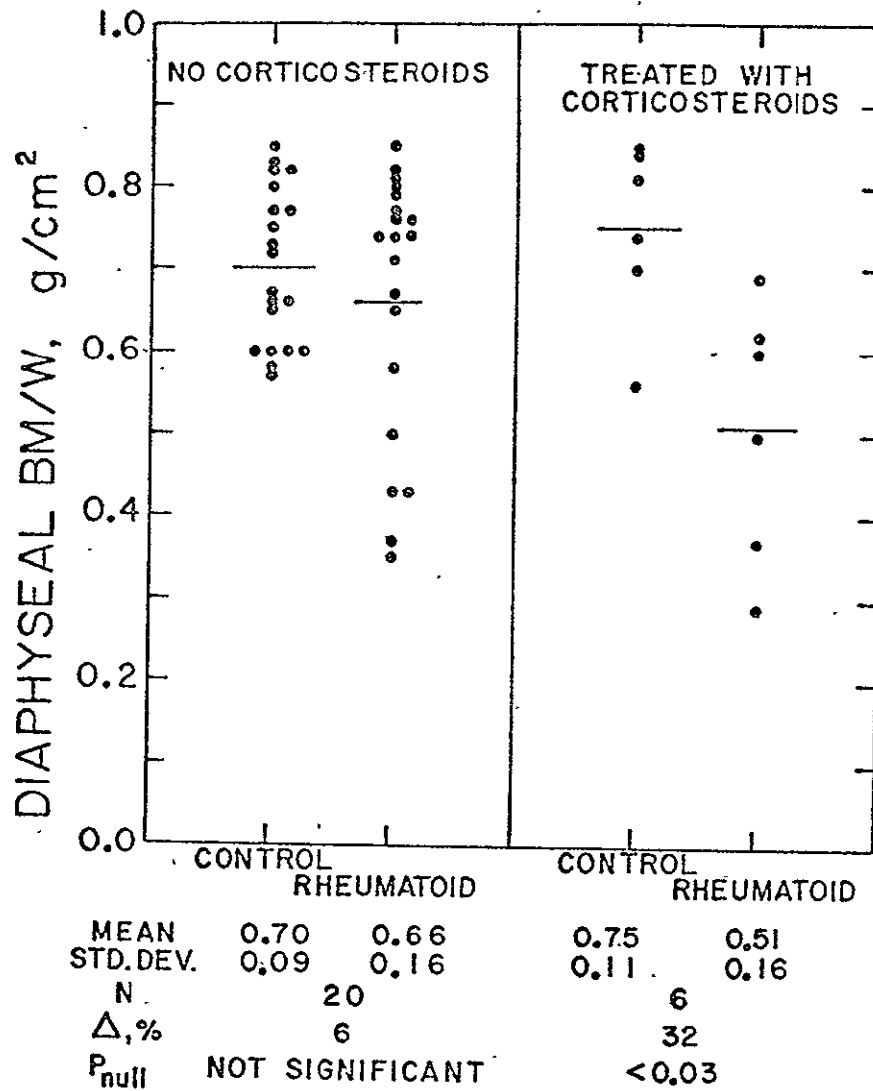


Fig 3: Diaphyseal BM/W for rheumatoids and their age-matched controls. The difference ( $\Delta$ ) between the mean BM/W of the rheumatoid and control groups is expressed as a percentage of the mean control value for the N pairs of subjects.

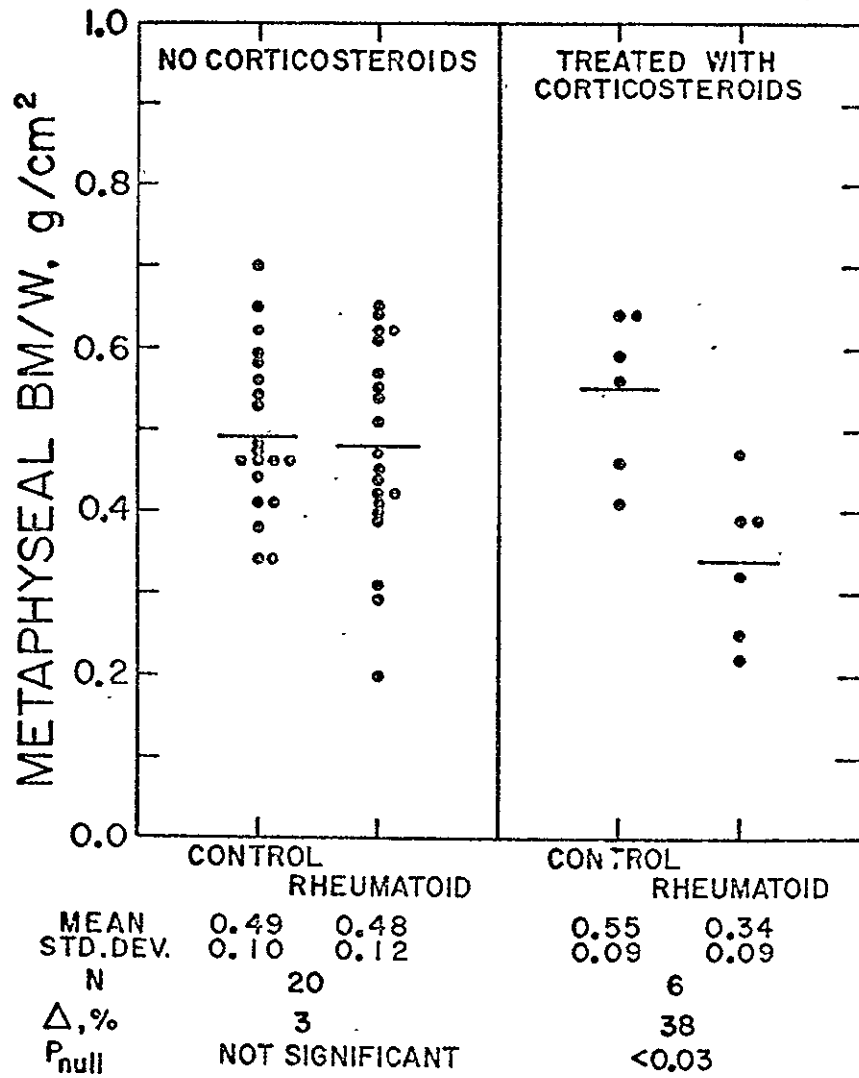


Fig 4: Metaphyseal BM/W for rheumatoids and their age-matched controls.

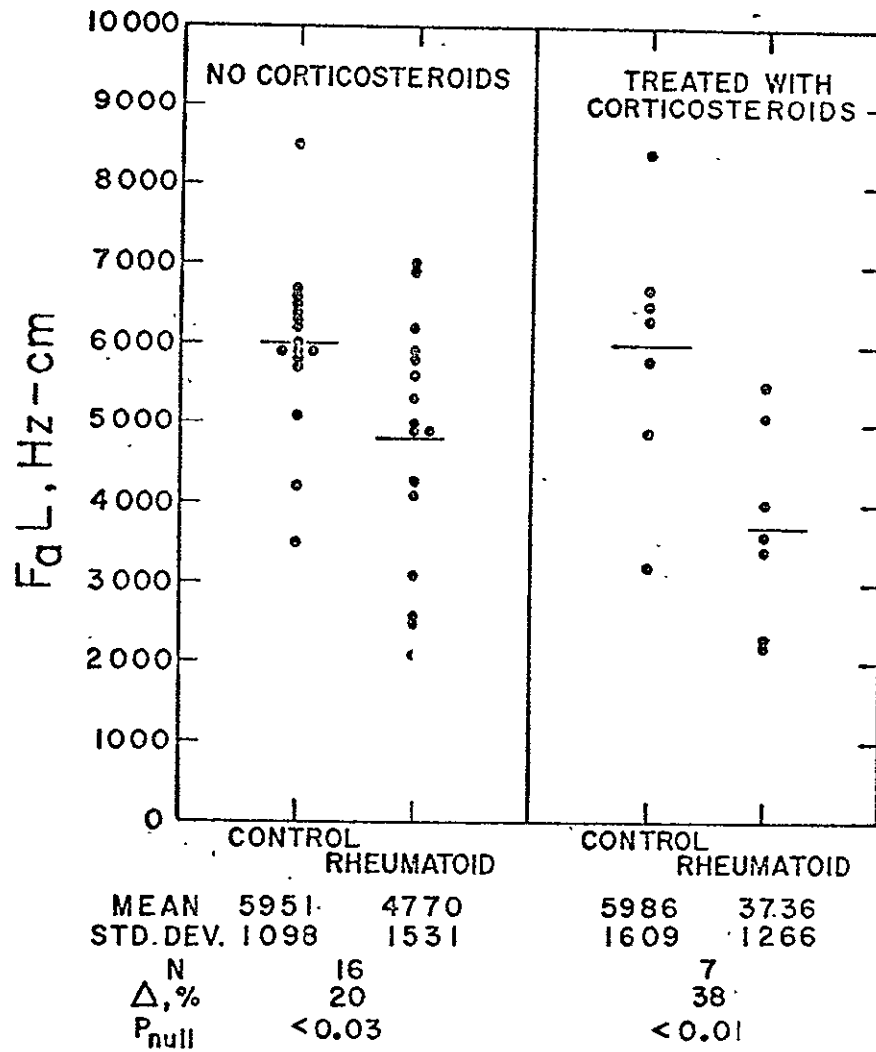


Fig 5: Ulnar F<sub>a</sub> L for rheumatoids and their age-matched controls.

## EFFECTS OF SODIUM FLUORIDE ON ULNAR RESONANT FREQUENCY IN ELDERLY WOMEN

John M. Jurist and C. Hugh Hickey

The subjects were nuns from the Notre Dame convent in Elm Grove, Wisconsin. These women ranged in age from 58 to 99 years with a mean age of 78.4 years. The use of nuns simplified the study for several reasons. First, all subjects were nulliparous -- thus eliminating a potential source of variation. Second, they all received a uniform diet and had similar activity patterns. The subjects were all of similar heredity and cultural (North European) background. Finally, they were motivated and cooperative.

The 114 subjects who completed a 2 month baseline study (described later) were randomly separated into control and experimental groups. Fifty-five subjects served as controls. Fifty-nine subjects were selected to receive 50 mg of sodium fluoride, 500 units of Vitamin D<sub>2</sub>, and 1 gm of calcium daily by means of enteric coated capsules.

Fifty-four of the 55 controls completed the experimental period of 8 months. Thirty-three of the 59 subjects in the experimental group discontinued their fluorides and were dropped. Thirteen discontinued because of nausea, 3 because of diarrhea, 1 was constipated, 1 developed a gastric ulcer, 2 developed cataracts, 5 declined to continue the experiment, 1 was discontinued because of senility (she was chewing her capsules), 5 discontinued for unknown reasons, and 2 died.

During the 2 month baseline period, a medical and therapeutic history with special emphasis on fractures, rheumatoid arthritis, and anti-inflammatory therapy was obtained from each subject. Serum calcium, phosphorus, and alkaline phosphatase determinations were performed. In addition, 24 hour urinary excretion of creatinine and hydroxyproline was measured. Hand-wrist, AP hip, and lateral thoracolumbar spine X-rays were taken for each subject. At the beginning and end of the baseline interval, the ulnar resonant frequencies were measured bilaterally as an index of relative rigidity of this bone.

Since we performed sequential measurements of our subjects,

relative changes of resonant frequency with time independent of ulnar length were studied. During the 2 month baseline interval, the average resonant frequency was 229 Hz. In contrast, the mean ulnar resonant frequency for 20 clinically normal 70-79 year old women measured in our laboratory was  $191 \pm 10$  (standard error) Hz. The overall resonant frequency reproducibility over 10 months was 36 Hz or approximately 16 percent of the mean value. The rate of change of resonant frequency during the 2 month baseline period was  $1.21 \pm 3.36$  Hz/month.

After the 2 baseline measurements, all control and experimental subjects were remeasured 3 months after initiation of sodium fluoride therapy, and then 8 months after initiation of therapy.

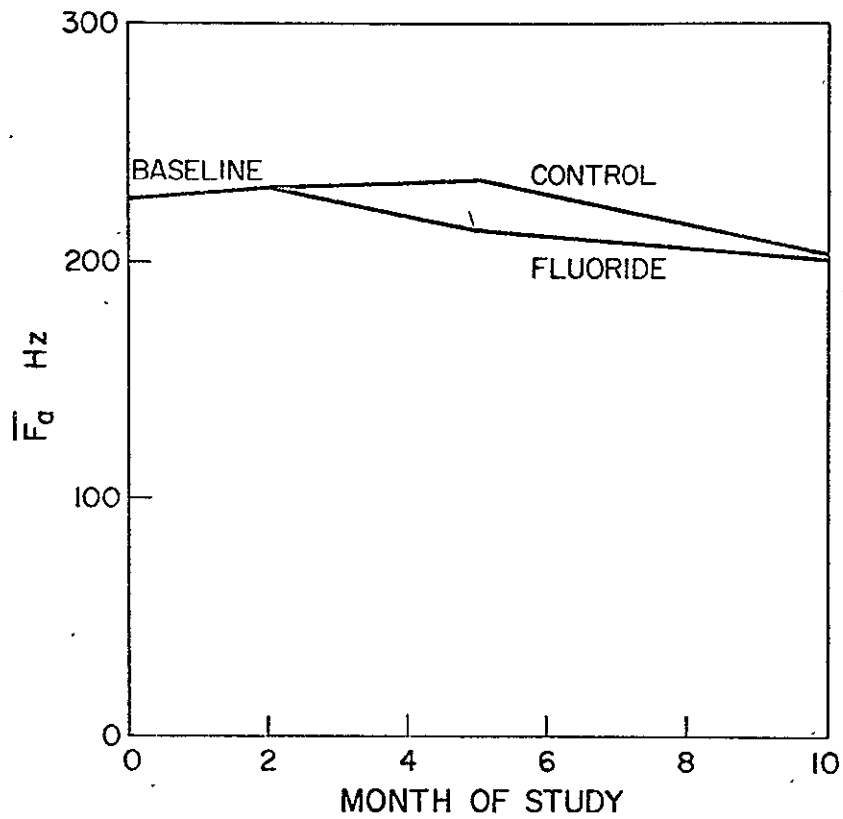
During the first 3 months of sodium fluoride therapy, the women who were receiving fluorides experienced a rapid decline in resonant frequency in comparison to the controls. This difference cannot be regarded as definitive since the t test showed significance only at the 2-5% level. During the second treatment interval of approximately 5 months, the women receiving fluorides declined in resonant frequency at a somewhat lower rate than did the controls. This difference was not statistically significant. These data are summarized in the table attached to this report. As shown in the enclosed figure, there was no significant overall change in resonant frequency over the entire 8 month period of treatment. Since the study was controlled, we cannot attribute the lack of effect of sodium fluoride on compensatory changes or drift in calibration of our equipment with time.

In summary, a control group of 55 subjects and an experimental group of 59 subjects were evaluated for ulnar resonant frequency for a baseline period of 2 months. They were then followed for an experimental period of 8 months during which time the experimental subjects received 50 mg of sodium fluoride daily along with calcium and Vitamin D supplements. Twenty-six of the 59 subjects receiving the fluorides completed the study -- 33 discontinued their medication and were dropped. Eighteen of the 33 dropouts discontinued for reasons directly related to gastrointestinal upset.

Our experiment failed to show significant changes in the resonant frequencies of the bones of the experimental subjects when compared to their controls. This suggests that sodium fluoride therapy in our therapeutic regimen did not have a significant effect on skeletal status over the 8 month period of study.

TREATMENT INTERVAL	$\frac{d}{dt} \bar{F}_a$ (Hz/MONTH)		SIGNIFICANCE	
	FLUORIDES	CONTROLS	t	P <sub>null</sub>
1 <sup>st</sup> 3 MONTHS	$-5.88 \pm 2.52^*$	$+1.01 \pm 1.68$	2.22	0.02-0.05
2 <sup>nd</sup> 5 MONTHS	$-2.47 \pm 1.86$	$-6.12 \pm 1.02$	1.88	0.05-0.10

\* STANDARD ERROR



QUANTITATION OF RADIOACTIVITY IN VIVO  
BY EXTERNAL COUNTING MEASUREMENTS \*

by

James A. Sorenson  
Department of Radiology  
University of Wisconsin Medical Center  
Madison, Wisconsin 53706

## ABSTRACT

A mathematical analysis of quantitative measurements of radioactivity, in vivo, by external  $\gamma$ -ray counting, is presented. The effects of subject thickness, and the depth, thickness and homogeneity of the source distribution are analyzed. It is concluded that variable subject thickness and source depth are major sources of error in quantitative in vivo measurements. This error is minimized by using the geometric mean of conjugate emission counts, corrected for subject thickness. The latter correction requires an independent measurement of subject thickness, e.g., by transmission techniques. The effects of source thickness and homogeneity are of lesser importance, but may also be accounted for by modification of the thickness correction factor.

## INTRODUCTION

External counting measurements are used for estimating radioactive content, in vivo, in several important areas of Nuclear Medicine. Well known examples are thyroid uptake studies and whole body counting. Recently there has also been increased interest in quantitating data from rectilinear scanners and scintillation cameras, and a number of computerized data collection systems have become commercially available for this purpose. The basic function of these systems is to obtain, store, and analyze data in a digital format. Implicit in the use of quantitative digital techniques is the belief that it will lead to a more accurate and objective determination of patient status. This is a reasonable expectation since most nuclear medicine tests are based on the fact that there are quantitative differences in the distribution, metabolism, or clearance rate of radioactive tracer substances between normal and abnormal tissues.

Digitization, however, is not equivalent to quantitation. It is an important first step, but does not eliminate the serious error or uncertainty that can arise in a quantitative measurement if the depth and distribution of the radioactivity within the patient are not known. Corrective methods must be used to account for these factors before accurate quantitation can be achieved.

Several authors have used the geometric mean,  $\sqrt{N_1 N_2}$ , of conjugate counting measurements (supine-prone or anterior-posterior) to minimize

---

\* Submitted for publication.

counting variations with source depth (1, 2). Under certain conditions (discussed below) the geometric mean of conjugate counting measurements is independent of source depth, but it is not independent of patient thickness. If patient thickness is known one may correct for its effects on the geometric mean of external counting measurements. Combined emission-transmission counting measurements were introduced for this purpose by Evans to accurately estimate the radioactive content of patients who had ingested radium (3). More recently, Cohn, et al, have applied this method to measurements in a whole body counter (4). Alfrey, et al, also used estimates of patient thickness to correct linear profile scan data obtained from patients injected with Fe-59 (5). However they did not describe their method for estimating patient thickness.

In each of the above cases, patient thickness corrections were derived using the inaccurate assumption that the radioactivity was a point source within the patient and no consideration was given to the effects of source distribution, e.g. source thickness and homogeneity. The effects of source thickness were discussed by Genna (1), but his discussion did not account for the effects of patient thickness or distribution inhomogeneities.

The purpose of this paper is to provide a more complete and general analysis of these factors in quantitative measurements. The analysis is applicable to several different subject-detector geometries, and to measurements with stationary or scanning detectors.

## MATHEMATICAL ANALYSIS

### A. Conjugate Counting Measurements

Consider the homogeneous volume source of radioactivity located in a patient of total thickness  $T$  (Figure 1). The source occupies a fraction  $f$  of the total thickness and thus has thickness  $fT$ . Consider first a counting measurement with the collimated detector positioned at a fixed distance  $c$  below the support table. The counts recorded from the source in the patient,  $N_s$ , must be related to the counts  $N_o$ , which would be obtained from the same amount of activity concentrated as a point source in air at some reference point. This will be taken as the top of the support table (marked  $x$  in the figure). The source activity ( $\mu Ci$ ) and the counts  $N_o$  can be related through factors involving collimator-detector sensitivity, disintegration constants, etc. We will not be concerned with this relationship, and hereafter the terms "source activity" and  $N_o$  will be used interchangeably.

The counts  $dN_s$ , recorded from a thin slab at a depth  $x$  are determined by the amount of activity in the slab;  $(N_o dx/fT)$ , by the distance  $(x+c)$ , and attenuation by the tissue thickness  $x$ . Thus:

$$dN_s \sim (N_o dx/fT) \exp(-\mu x) G(x+c) \quad (1)$$

where  $\mu$  is the linear attenuation coefficient of tissue (water) and  $G(x+c)$  is a geometric function accounting for the effects of changing

distance from the detector. In this discussion we will assume that "off-axis" geometric variations are negligible, i.e., "flat-field" collimation or some sort of scanning technique is used for the measurement. Only variations in distance ( $x+c$ ) will be considered.

The nature of the geometric function  $G(x+c)$  depends on the type of collimation and on the type of measurement. For example, with straight-bore collimation and static detector positioning, it is approximately an inverse-square law. For linear scanning (profile scanning) it is approximately an inverse-first power law, since the time during which the source is seen by the detector increases linearly with distance ( $x+c$ ). Finally, if total counts are recorded during a rectilinear scan, with any sort of collimation, the time during which the source is seen increases as the square of source-detector separation and  $G(x+c) \sim 1$ . This fact was noted by Sharma (6) and also by Arimizu and Morris (7) in their work on quantification of rectilinear scan data. Geometric invariance with distance also applies to measurements with camera-type instruments, provided counts are summed over the entire area of the crystal viewing the radioactive distribution.

In each of these cases, it is possible to obtain an exponential approximation for  $G(x+c)$ . This is shown by Figure 2 for the inverse-square and inverse-first power laws. The error is less than 10% for  $x \lesssim c$ . Thus we may write  $G(x+c) \sim \exp(-gx)$ , where  $g$  depends on the distance from the detector to the reference point and on the method of the measurement, as indicated in Figure 2. This also applies to rectilinear scanning with  $g \sim 0$ . With this approximation equation (1) may be rewritten:

$$dN_s \sim (N_0 dx / FT) \exp(-\gamma x) \quad (2)$$

where  $\gamma = g + \mu$ . The accuracy of this approximation for a particular counting system may be tested experimentally. Values for  $\gamma$  can be obtained by measuring point sources immersed at different depths in a water phantom.

Given that equation (2) is valid, the total counts recorded from the volume source may be obtained by integration with the result:

$$N_s \sim N_0 \exp(-\gamma d) \sinh(f\gamma T/2) / (f\gamma T/2) \quad (3)$$

where  $d$  is the mean source depth. The counts  $N_p$  recorded from the same subject measured in the prone position are given by the same equation, with  $d$  replaced by  $(T-d)$ . Taking the geometric mean of supine and prone counts and transposing terms one obtains:

$$N_0 \sim \sqrt{N_s N_p} \exp(\gamma T/2) (f\gamma T/2) / \sinh(f\gamma T/2) \quad (4)$$

Thus the activity  $N_0$  of a homogeneous volume source of radioactivity may be obtained from the geometric mean of supine and prone emission counting measurements, and a correction factor:

$$C_u = \exp(\gamma T/2) (f\gamma T/2) / \sinh(f\gamma T/2) \quad (5)$$

which can be calculated using assumed or measured values of  $f$ ,  $\gamma$ , and  $T$ . The relative importance of these three parameters on the accuracy of this calculation is indicated by Figure 3, showing  $C_u$  vs.  $f$ , for typical values of the product ( $\gamma T$ ). A 25% error or uncertainty in ( $\gamma T$ ) leads to a 25% error in  $C_u$  for all values of  $f$ . On the other hand, if ( $\gamma T$ ) is accurately known, and  $f = 2/3$  is assumed, then  $C_u$  varies by at most  $\pm 10\%$  as  $f$  ranges between the extremes of zero and one. If  $f = 0$  (point source model) is assumed, the possible error is larger (20%). In any case, it can be concluded that accurate knowledge of the parameters  $\gamma$  and  $T$  is required, but only a reasonable approximation is needed for  $f$ .

The mean source depth is obtained by taking the ratio rather than the product of supine and prone counts:

$$d \sim T/2 - (1/2\gamma) \ln(N_s N_p) \quad (6)$$

Note that the depth determination is independent of source thickness. Equations (4-6) are similar to results obtained by Gemma (1), except that he did not account for the effects of patient thickness.

A similar analysis can be carried out for the detector positioned above the patient support table (Figure 1). Again the top of the table will be taken as the reference point. Primed notation will be used for parameters associated with the upper detector.

For measurements with the subject supine, the counts from the thin slab  $dx$  are given by:

$$dN'_s \sim (N'_0 dx / FT) \exp(g'x) \exp[-\mu'(T-x)] \quad (7)$$

$$\sim (N'_0 dx / FT) \exp(-\mu't) \exp(\gamma'x) \quad (8)$$

where  $\gamma' = \mu' + g'$ , and  $N'_0$  are the counts that would be obtained with the volume source concentrated as a point source, in air, at the reference point. The parameter  $g'$  is again determined by the type of measurement and by the distance  $c'$ . The approximations given in Figure 2 may be used with  $c$  replaced by  $(c'/2)$ , since  $x = 0$  (reference point) represents maximum rather than the minimum distance from the source to the detector.

Equation (8) may be integrated to obtain the total counts recorded from the volume source:

$$N'_s \sim N'_0 \exp(-\mu'T + \gamma'd) \sinh(f\gamma'T/2) / (f\gamma'T/2) \quad (9)$$

For measurements with the subject prone,  $d$  is replaced by  $(T-d)$ . Taking the geometric mean and transposing terms, one obtains:

$$N'_0 \sim \sqrt{N'_s N'_p} \exp[(\mu' - g')T/2] (f\gamma'T/2) / \sinh(f\gamma'T/2) \quad (10)$$

Again there is no dependence on source depth  $d$ . The effects of subject thickness  $T$  are less with the detector above rather than below the support

table, since the difference ( $\mu' - g'$ ) rather than the sum ( $\mu + g$ ) is involved in the thickness term. Essentially this is because the effects of distance and attenuation are partially compensating in this geometry with thicker patients being nearer the detector. The effects of fractional source thickness  $f$  are exactly the same as with the detector below the table, and Figure 3 may be used for reference with  $\gamma$  replacing  $\gamma'$ . Mean source depth  $d$  can be obtained from the ratio of supine to prone counts:

$$d \sim (T/2) + (1/2 \gamma') \ln(N'_s/N'_p) \quad (11)$$

It is possible, at least in theory, to eliminate the exponential thickness term by making  $\mu' = g'$ , e.g., by adjusting the distance  $c'$ , or devising a collimator with exponential depth dependence for measurements in a static geometry. This condition would exist over only a certain range of photon energies, since  $\mu'$  is energy dependent. Thickness independence could not be obtained in rectilinear scan measurements, since  $g' = 0$  for all types of collimation.

A final possibility for conjugate counting is to use detectors above and below the patient support table. Equations (3) and (9) are applicable. Taking the geometric mean and transposing terms one obtains:

$$\sqrt{N'_o N'_o} \sim \sqrt{N'_s N'_s} \exp(\mu' T/2) \exp[(\gamma - \gamma') d/2] \\ \times (f \bar{\gamma} T/2) / \sinh(f \bar{\gamma} T/2) \quad (12)$$

where  $\bar{\gamma} = (\gamma + \gamma')/2$ . The use of  $\bar{\gamma}$  in the terms involving source thickness does not lead to a significant error, i.e., less than 2% error, so long as  $\gamma$  and  $\gamma'$  are the same within about a factor of two. The source thickness term is exactly the same as for the supine-prone geometries, and Figure 3 may be used for reference. It can be concluded that none of these counting geometries provide measurements that are totally independent of source distribution. Errors of 10-20% are possible, depending on whether one has started with the assumption of a point or a volume source.

Unlike the supine-prone counting measurements, the geometric mean of anterior and posterior counts is not independent of source depth, unless  $\gamma' = \gamma$ . The condition  $\gamma = \gamma'$  is likely to be obtained in measurements by rectilinear scanning or with a camera-type instrument since  $g \sim 0$  and  $\mu \sim \mu'$  in these measurements. It might also be obtained with fixed detectors or in profile scanning if the distances  $c$  and  $c'/2$  are about the same ( $g \sim g'$ ). However, there is a significant dependence on source depth with only small differences in  $\gamma$  and  $\gamma'$ . For example, if  $(\gamma - \gamma') \sim 0.1 \text{ cm}^{-1}$  there is a 5% change in the geometric mean per cm change in source depth. The possibility that  $\gamma$  and  $\gamma'$  may be different must be examined experimentally in any anterior-posterior counting geometry before depth-independent counting can be assumed.

If  $\gamma = \gamma'$ , then there is an important advantage to measurements carried out with opposed detectors over supine-prone measurements,

namely that "source-shifting is eliminated. This problem can be particularly troublesome if the source is free to move within the patient, e.g., radioactive urine in the bladder or a capsule in the stomach. If source depth changes by an amount  $\pm \Delta d$  when the subject is moved from the supine to the prone position, then  $d$  in equation (8) for measurements with the detector below the patient support table is replaced by  $(T-d \pm \Delta d)$  for the prone measurement. Taking the geometric mean and transposing terms one obtains:

$$N_o \sim \sqrt{N_s N_p} C_u \exp(\pm \gamma \Delta d / 2) \quad (13)$$

where  $C_u$  is as given by equation (5). Typical values for  $\gamma$  are in the range  $0.1 - 0.2 \text{ cm}^{-1}$ . Thus there is an error of 5-10% per cm of source shifting. This is not a trivial error and must be carefully considered in a supine-prone counting technique where source depth can change by more than a cm or two when the subject changes position.

#### B. Effects of Distribution Inhomogeneities

The uniform volume source model must also be modified to account for possible inhomogeneities within the source. A model for analyzing these effects is shown in Figure 4. Here the distribution is assumed to consist of a pair of uniform volume sources symmetrically positioned relative to a mean depth  $d$ . The two sources are each of thickness  $(fT)$ , which is variable, and are contained within a thickness  $(f_o T)$ , which is fixed.

For  $0 < f < f_o/2$ , the distribution consists of a separated pair of volume sources (Figure 4a). This source pair might represent, for example, the distribution of radioactive iron in the spine sternum. For  $f_o/2 < f < f_o$ , the volume sources overlap, and the radioactivity is more concentrated near the center of the distribution (Figure 4c). Overlapping distributions might be found, for example, in the distribution of radioactive colloid in the liver and spleen. Organs with an approximately circular cross-section, where the profile of organ mass vs. depth is more concentrated near the center, might also be approximated by this distribution. Finally, for  $f = f_o/2$  or  $f = f_o$ , the distribution is equivalent to a single uniform source of thickness  $(f_o T)$ .

We will consider measurements carried out with the detector beneath the table. Applying equation (3) for measurements on this two-source configuration one obtains:

$$N_s \sim (N_o/2) (2/f\gamma T) \sinh(f\gamma T/2) \left[ \exp(-\gamma d_1) + \exp(-\gamma d_2) \right] \quad (14)$$

$(N_o/2)$  is the activity of each member of the source pair.  $d_1$  and  $d_2$  are the depths of the two sources, which may be written in terms of the mean depth  $d$ , and  $f_o$ :

$$d_1 = d + (f_o - f)T/2 \quad (15)$$

$$d_2 = d - (f_o - f)T/2 \quad (16)$$

Substituting in (14) one obtains:

$$N_s \sim N_o \exp(-\gamma d) (2/f\gamma T) \sinh(f\gamma T/2) \left[ \cosh(f_o - f)\gamma T/2 \right] \quad (17)$$

Substituting  $(T-d)$  for the prone measurement, taking the geometric mean and transposing terms:

$$N_o \sim \sqrt{N_s N_p} C_u(f_o) / \cosh \left[ (f_o - f)\gamma T/2 \right] \quad (18)$$

where  $C_u(f_o)$  is as given in equation (5), with  $f = f_o$ .

The effects of source inhomogeneities are illustrated in Figure 5 showing the variation in the "correction factor" for the non-uniform source distribution:

$$C_n = C_u(f_o) / \cosh \left[ (f_o - f)\gamma T/2 \right] \quad (19)$$

as  $f$  ranges from 0 -  $f_o$ , for  $f_o = 2/3$ , and three values of the product  $(\gamma T)$ . Note that  $C_n = C_u(f_o)$  at  $f = f_o$ .

From this graph, it can be concluded that the effects of overlapping sources are quite small.  $C_n$  differs from  $C_u$  by only 2-3%, when  $f_o/2 < f < f_o$ . The split source configuration leads to a larger difference, with the worst possible case (15-20%) occurring when two "point" sources are present ( $f = 0$ ). True "point" sources are seldom found in vivo, however, so this is probably an overestimate of errors that actually occur when  $C_u$  is used as the correction factor in the presence of non-uniform distributions. It is likely that errors caused by source inhomogeneities are less than 10% for distributions in human subjects which are usually some combination of volume sources. On the other hand, uncertainty in  $(\gamma T)$  again leads to a larger error, as was observed earlier for the uniform source distribution.

This analysis of source distribution effects indicates that refined techniques for determining source distribution with depth (e.g. tomography) would not contribute as much to quantitative counting accuracy as the use of conjugate counting measurements and accurate determinations of the parameter  $\gamma$  and subject thickness  $T$ . The effects of source distribution can be accounted for with reasonable accuracy using the correction factor for uniform volume sources with an assumed fractional source thickness  $f \sim 2/3$ .  $f$  could also be adjusted in different studies. Variations in the source thickness and homogeneity within reasonable limits would not lead to errors of greater than about 10%.

### C. Measurement of Subject Thickness

Quantitation of source depth and activity by any of the conjugate counting methods described requires an accurate measurement of subject thickness. A simple and accurate determination of this quantity can be made from a transmission measurement with an external photon beam. If  $I_o$  and  $I$  are the unattenuated and transmitted beam intensities, respectively, then:

$$T = (1/\mu_t) \ln(I_o/I) \quad (20)$$

where  $\mu_t$  is the linear attenuation coefficient of the subject for the

transmission beam. For photon energies above about 100 keV, human tissues can be assumed to be water-equivalent, and  $\mu_t$  can be determined from measurements on water phantoms.

Substituting this expression for subject thickness into equation (4) for supine and prone measurements with the detector below the patient support table, with  $f = 0$  (point source) one obtains:

$$N_o \sim \sqrt{N_s N_p} \quad (I_o/I) (\gamma/2 \mu_t) \quad (21)$$

As a matter of convenience for calculation, it would be useful to have  $\gamma = \mu_t$ . This cannot be obtained, however, simply by using the same radionuclide source for the transmission and emission measurements, since  $\gamma$  involves geometric effects as well as attenuation. Also, one would not expect either of the attenuation coefficients  $\mu$  and  $\mu'$  for internal sources to be equal to  $\mu_t$ , even for the same radionuclide, since the measuring conditions are quite different. The effects of scattered radiation are more significant in the case of an internal source, and in general, one would expect both  $\mu$  and  $\mu' < \mu_t$ . Because of these differences, there is no particular advantage to using the same radionuclide source for the transmission and emission measurements. Separate and accurate determination of each of the various exponential coefficients is required.

Subject thickness could also be measured by morphometric means, e.g., with a pair of calipers. However, the transmission measurement has an important advantage over these types of measurements, namely that it also reflects internal changes in subject composition or density. Changes which occur near bony structures and air-filled spaces such as the lungs, lead to variations in the attenuation properties of the subject. Bone is the lesser problem, especially in the trunk of the body where bone density and thickness are low. The fact that bones of the axial skeleton cannot be seen in transmission scan images obtained at  $\gamma$ -ray energies above about 100 keV suggests that the overall effect of bone on the attenuation coefficients  $\mu$  and  $\mu'$  is negligible (8).

More serious changes can occur in lungs, which may have a density less than one-half that of muscle or water. However, compensating changes occur in  $\gamma$  and in  $\mu_t$ , such that the important ratio,  $(\gamma/\mu_t)$ , of equation (21) tends to remain constant. The compensation is not complete, since the geometric component of  $\gamma$  is not affected by changes in attenuation properties of the patient. Nevertheless, the partial compensation that is obtained is an important advantage of transmission techniques over other types of thickness measurements.

## CONCLUSIONS

Figure 6 summarizes the results of the analysis presented above regarding the relative importance of source depth, subject thickness, and source volume or thickness in quantitative counting measurements. The curves apply to measurements made with the detector beneath the support table with  $\gamma \sim 0.1 \text{ cm}^{-1}$ . The effects of source depth are the most severe, with a variation in counts recorded with only one subject position (e.g. supine) of about 10% per cm. Depth effects may be

eliminated by taking the geometric mean of conjugate counting measurements, in which case subject thickness is the important variable. There is about a 5% change in the geometric mean per cm change in subject thickness under the conditions described. The effects of subject thickness can be accounted for with a thickness correction factor, based on an accurate determination of subject thickness, such as by transmission measurement. The final concern is then source distribution. Source thickness has a relatively minor effect as indicated by the graph. Source inhomogeneities are also of a lesser concern according to the previous discussion.

## REFERENCES

1. Genna, S., Analytical Methods in Whole Body Counting, Clinical Uses of Whole Body Counting, IAEA Symposium, 1965.
2. Ben Haim, A., and Dudley, R.A., Calibration Problems in Whole Body Counting with NaI(Tl) Detectors, Clinical Uses of Whole Body Counting, IAEA Symposium, 1965.
3. Evans, R.C., Radium Poisoning II, The Quantitative Determination of the Radium Content and Radium Elimination Rate in Living Persons. Am. J. Roentg. 37: 368 (1937).
4. Cohn, S.H., Dombrowski, C.S., Pate, H.R., and Robertson, J.S., A Whole Body Counter with Invariant Response to Radionuclide Distribution. Phys. Med. Biol. 14: 645 (1969).
5. Alfrey, C.P., Cook, V., and Pittman, J.P., The Design and Use of a Linear Scanner. J. Nucl. Med. 8: 859 (1967).
6. Sharma, R.R., Depth Independence in Quantitative Radioisotope Imaging. Br. J. Radiol. 41: 949 (1968).
7. Arimizu, N., and Morris, A.C., Quantitative Measurement of Radioactivity in Internal Organs by Area Scanning. J. Nucl. Med. 10: 265 (1969).
8. Sorenson, J.A., Evaluation of Radionuclide Sources for Transmission Scanning. Invest. Radiol. 5: 92 (1970).

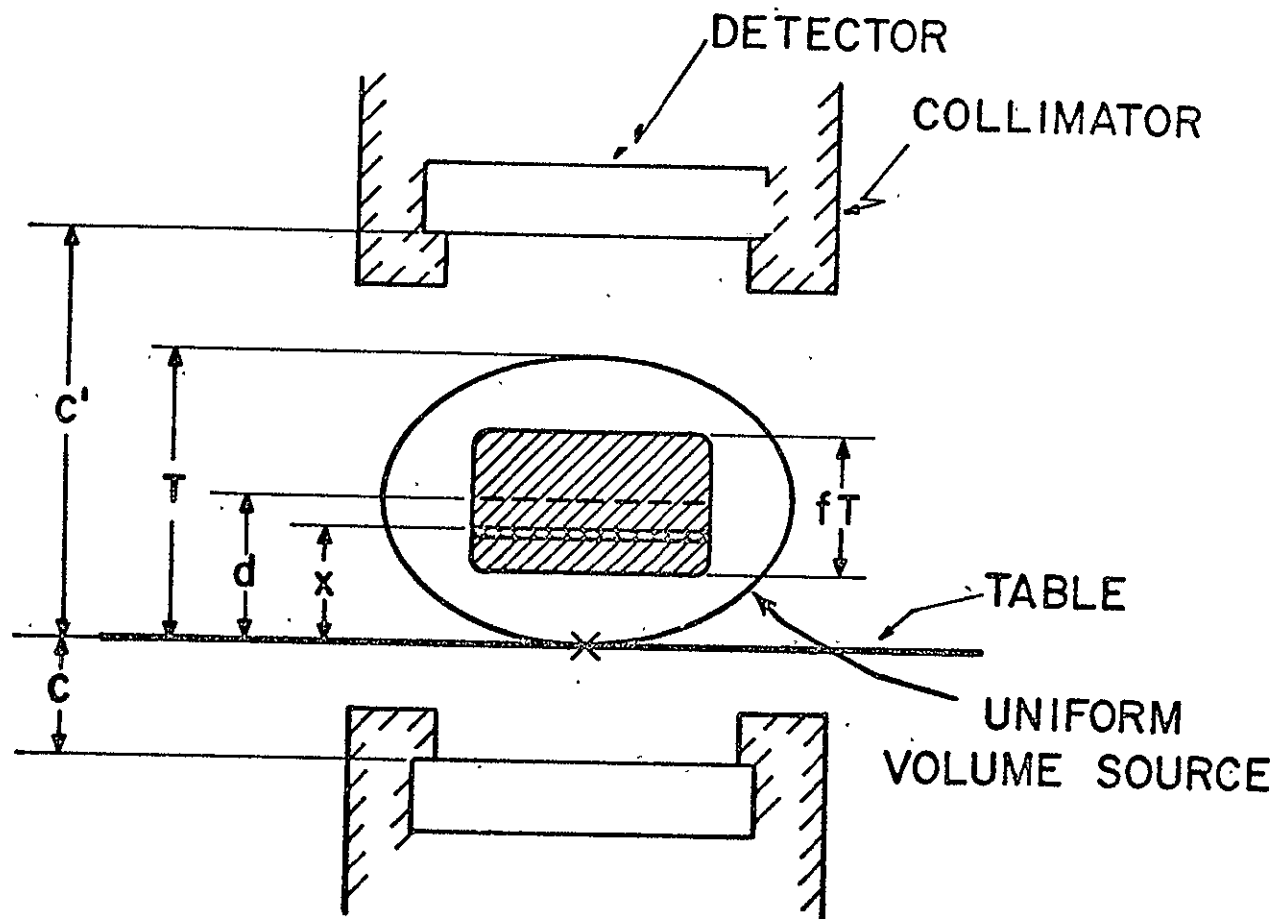


Figure 1. Uniform source of radioactivity in a patient. Midline source depth is  $d$ , and source thickness is a fraction  $f$  of total patient thickness,  $T$ .

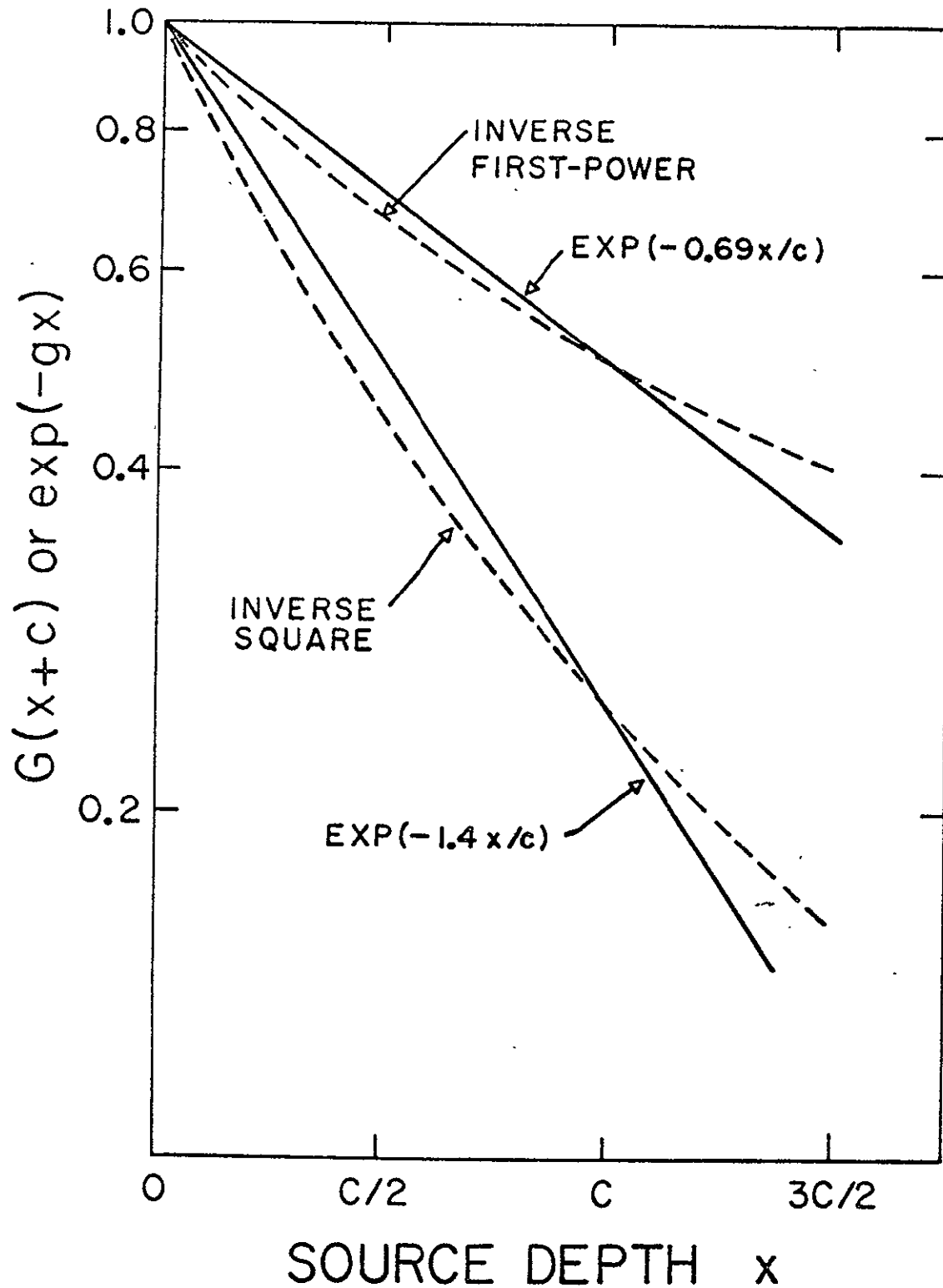


Figure 2. Exponential approximations for two possible distance-dependent geometric functions. Errors are  $< 10\%$  for  $x \lesssim c$ .

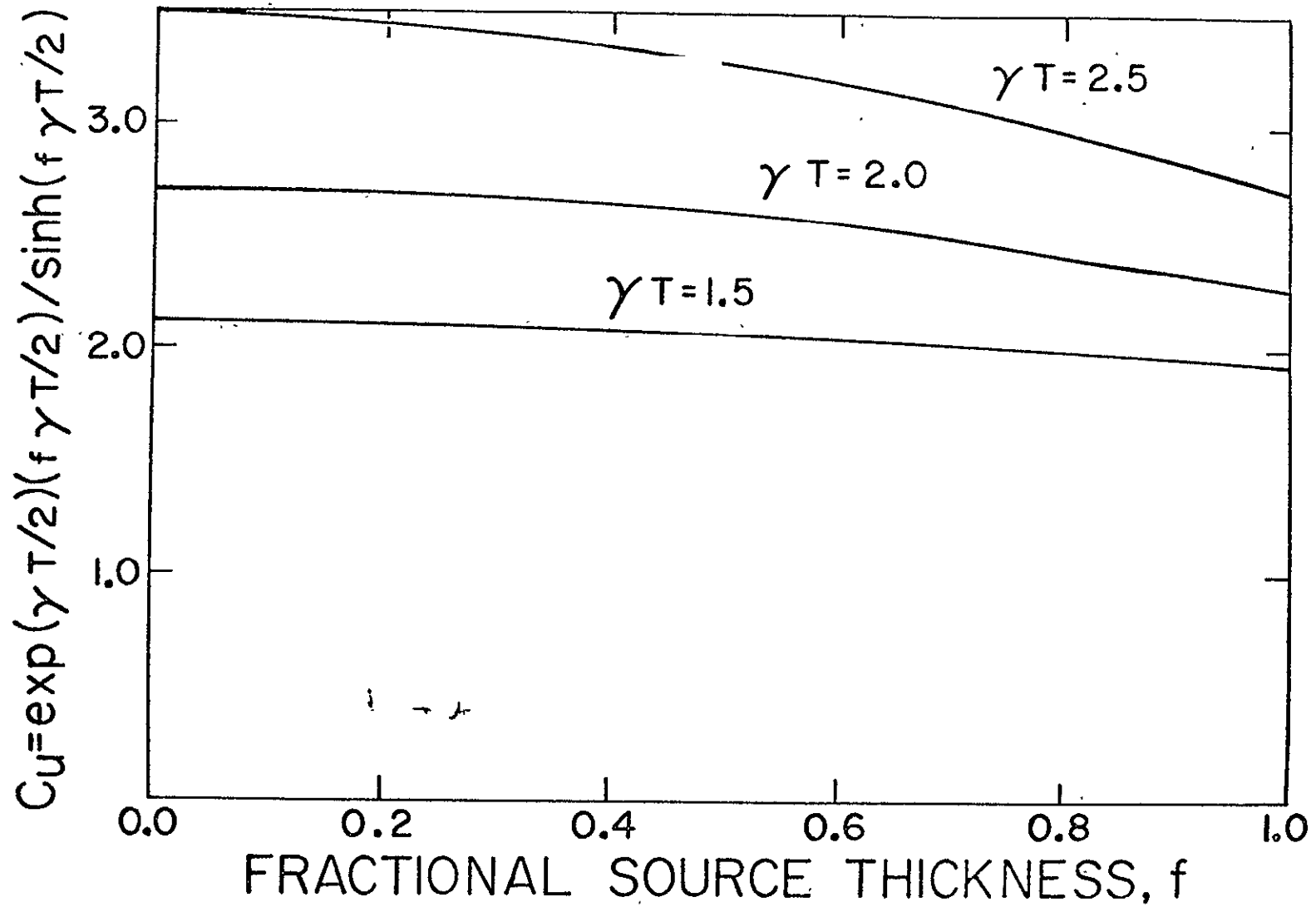


Figure 3. Variations in the correction factor for a uniform volume source  $C_u$  with fractional source thickness  $f$ , for three values of the product  $(\gamma T)$ . Variations in  $(\gamma T)$  cause greater errors in  $C_u$  than variations in  $f$ .

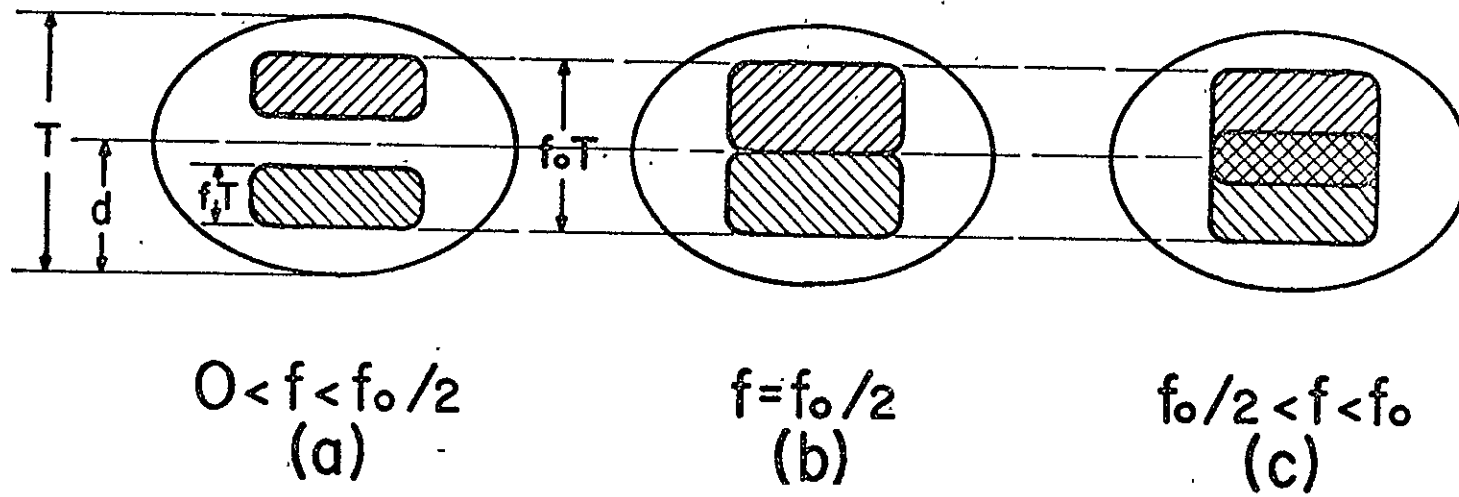


Figure 4. Non-uniform distributions obtained by varying the thickness ( $fT$ ) of a pair of uniform sources, symmetric with respect to a midline depth  $d$ , and contained within a fixed total thickness  $f_0T$ .

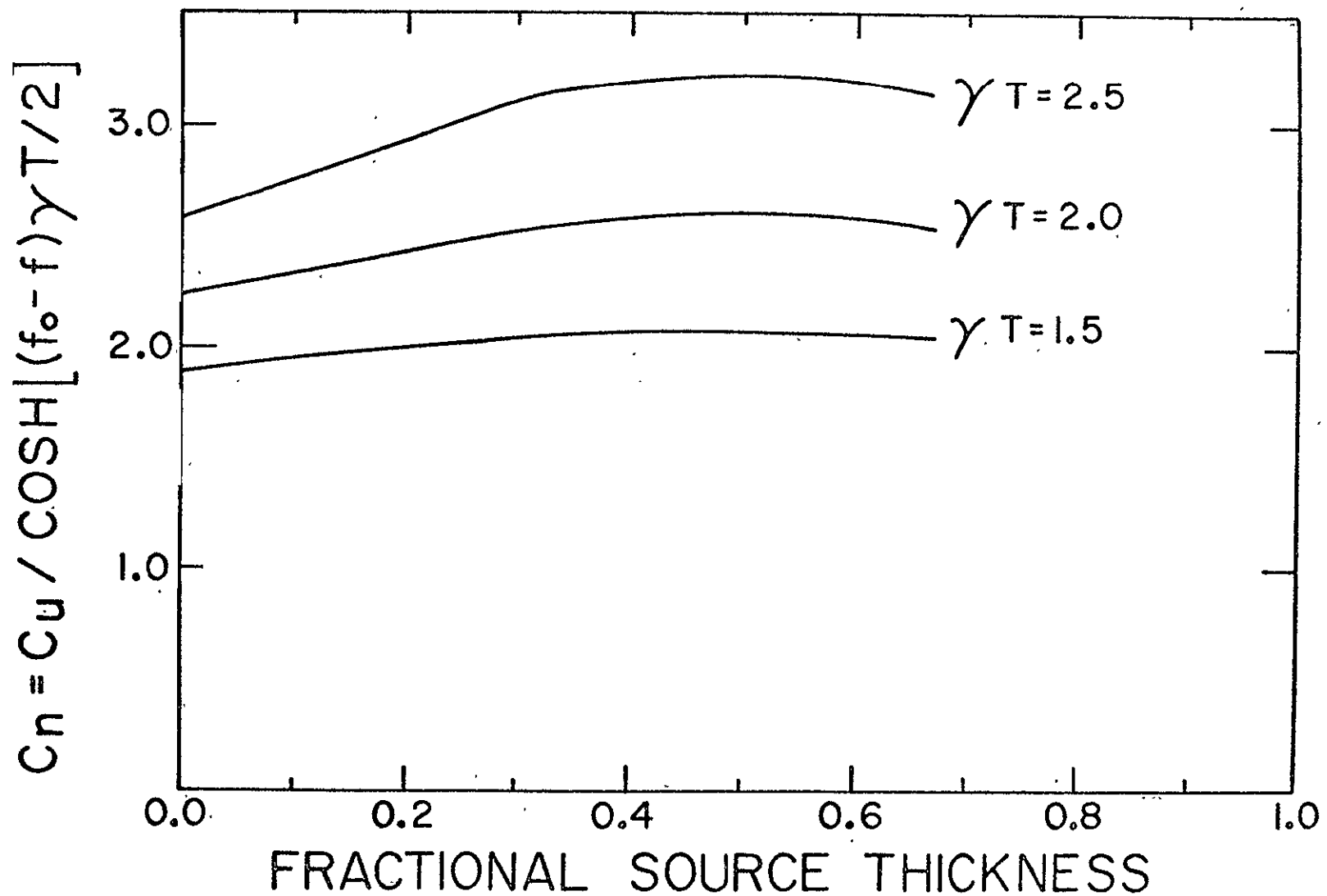


Figure 5. Effects of source inhomogeneities on the correction factor  $C_n$  for the source pair shown in Figure 4. Marked variations are obtained when the distribution approaches a pair of point sources, but very small errors (2-3%) are obtained with overlapping sources.

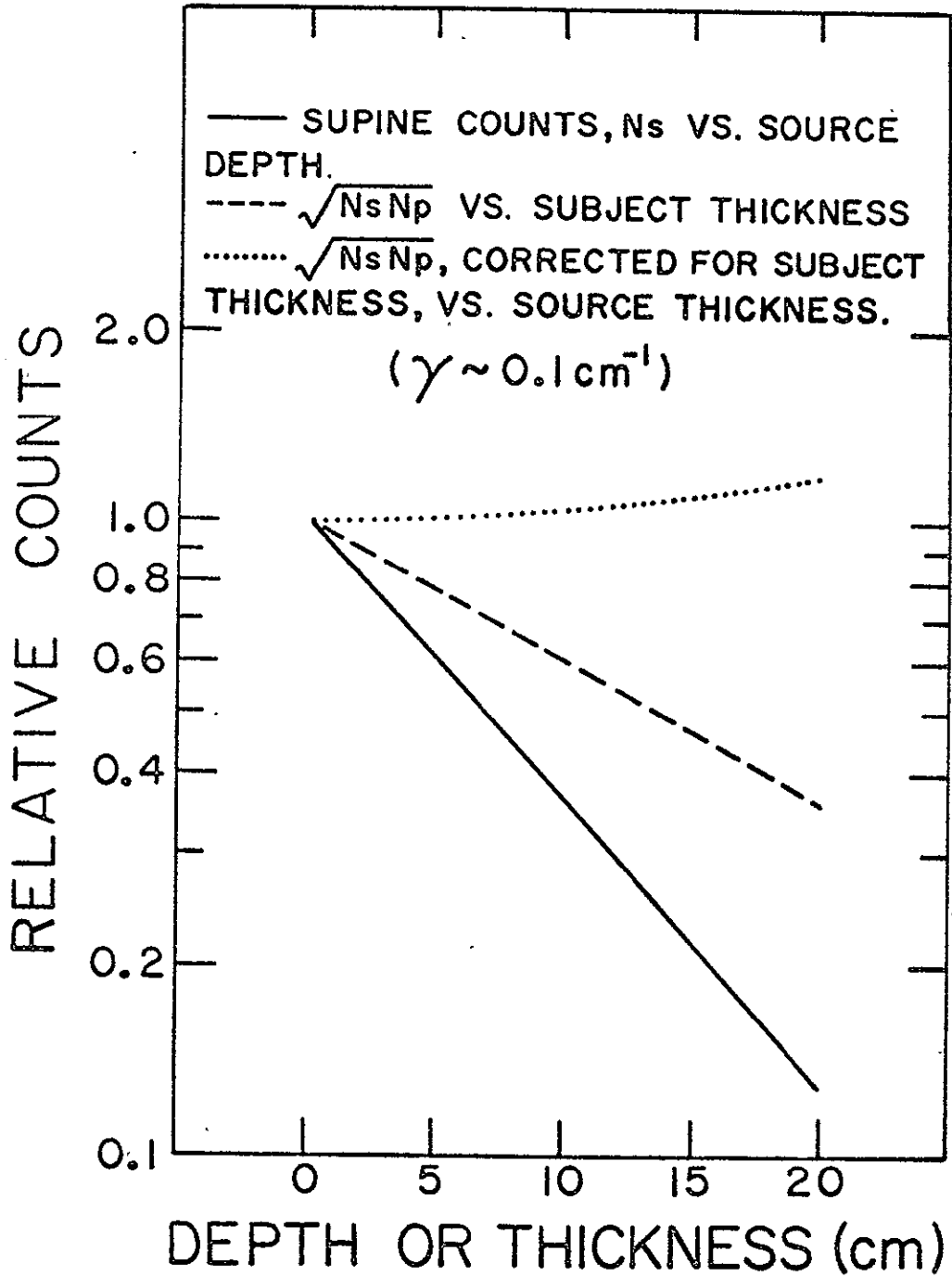


Figure 6. Summary of the relative effects of source depth, patient thickness, and source thickness on quantitative counting measurements.